# GNSS Ionosphere: How and Why
# (*brief visual discovery*)

**Manuel Hernandez Pajares(1,2)**

(1) UPC-IonSAT, Barcelona, Spain; (2) IEEC, Barcelona, Spain.

contact e-mail: manuel.hernandez@upc.edu

*Eastern Africa Capacity Building Workshop on Space Weather and Low-latitude, Ionosphere*
Malindi, Kenya, 03 October 2023 to 12 October 2023

UNIVERSITAT POLITÈCNICA DE CATALUNYA BARCELONATECH

# What is this?

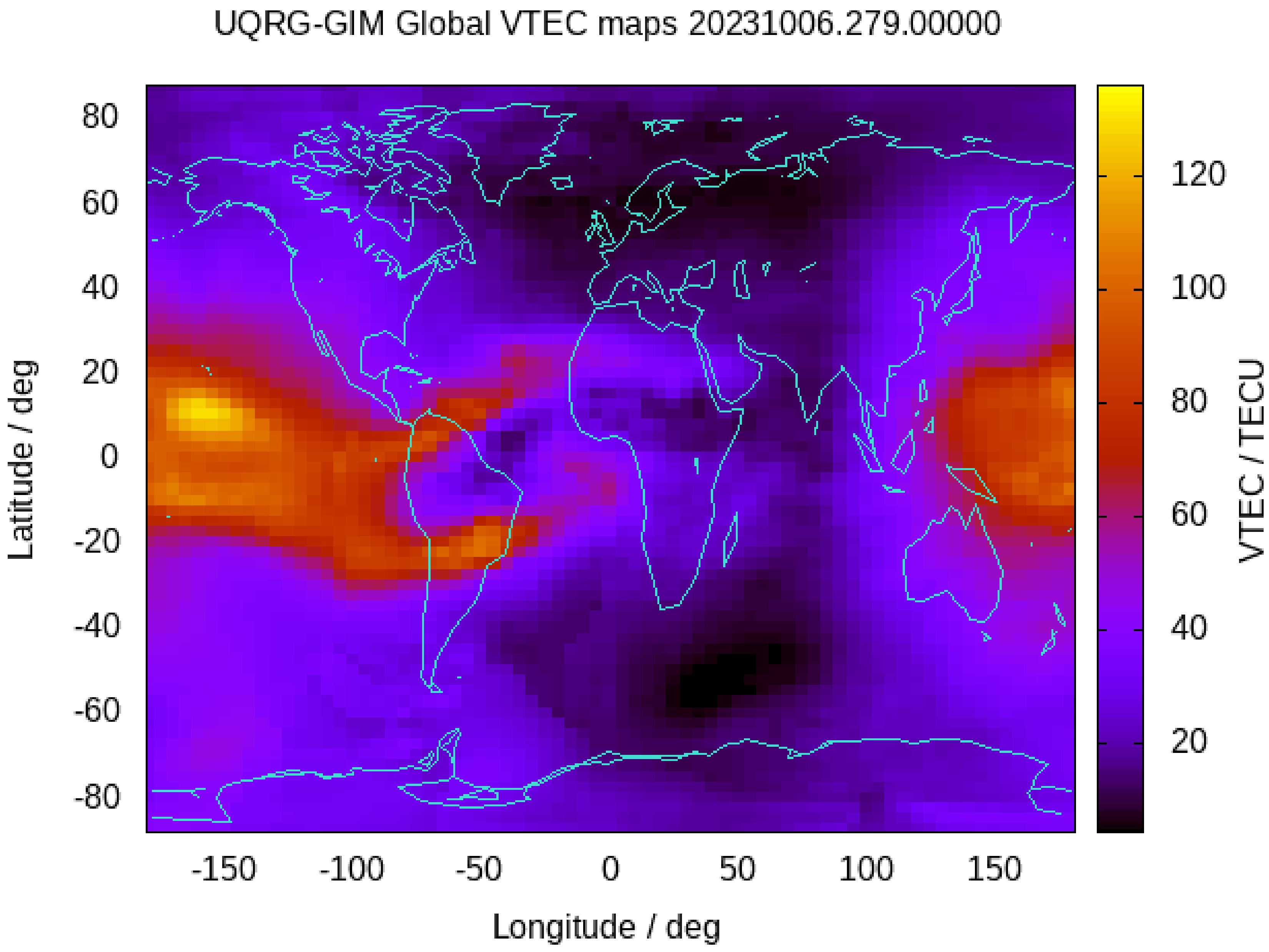
UQRG-GIM Global VTEC maps 20231006.279.00000
Latitude / deg
80
60
40
20
0
-20
-40
-60
-80
-150
-100
-50
0
50
100
150
Longitude / deg
120
100
80
60
40
20
VTEC / TECU

# What is this?

Movie of the vertically integrated electron number density (AKA Vertical Total Electron Content, VTEC) of the partially ionized part of the Earth atmosphere (ionosphere) obtained from worldwide Global Navigation Satellite System (GNSS) multifrequency measurements

Do you wish to check the present global VTEC, from RT UPC-IonSAT GIMs? If yes:

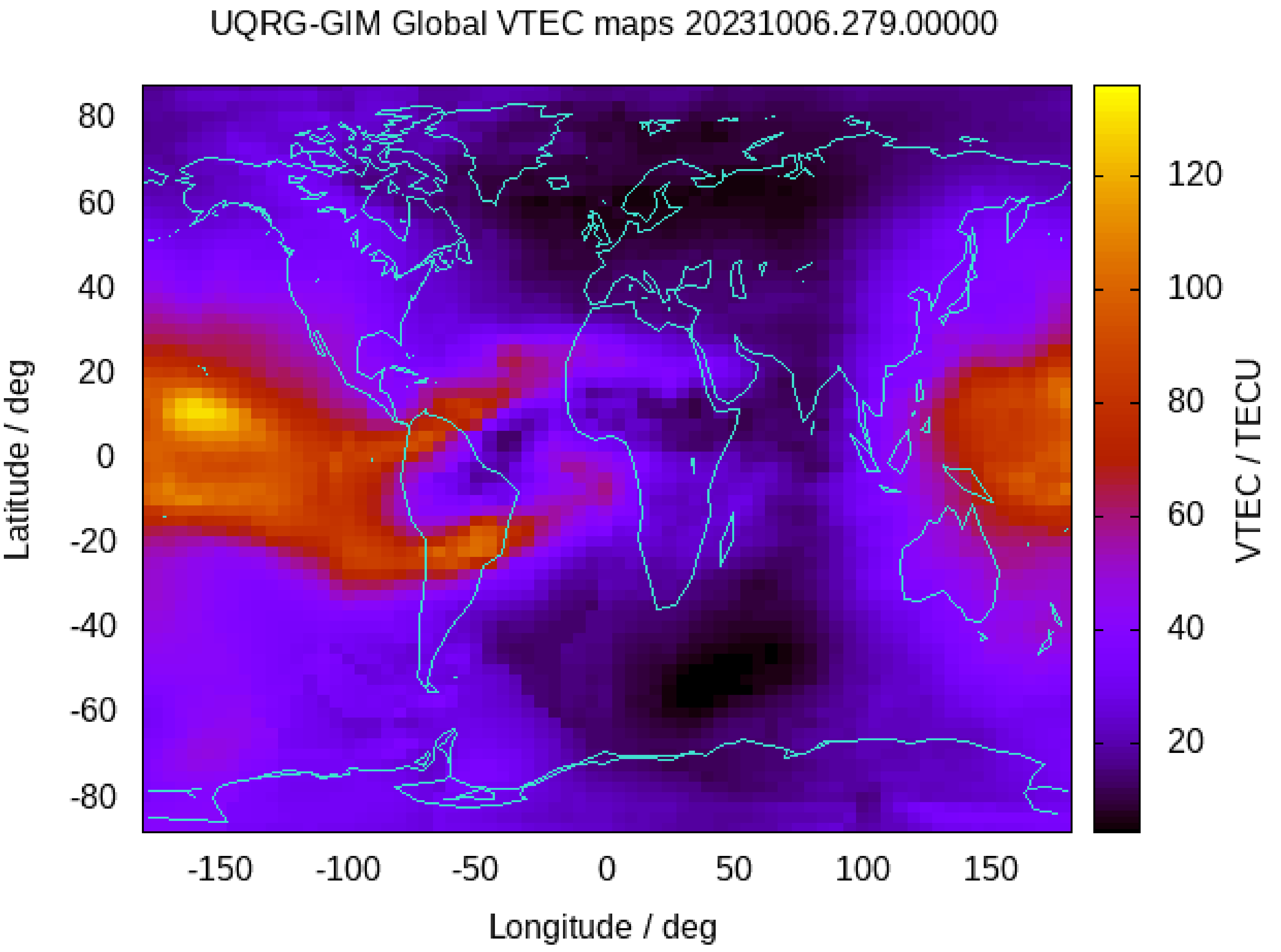


***http://chapman.upc.es/tomion/real-time/quick/last_results.uadg/RT-DAILY-VTEC-MOVIE.gif***

UNIVERSITAT POLITÈCNICA DE CATALUNYA BARCELONATECH

IonSAT

# Why there are free electrons within the Earth atmosphere?

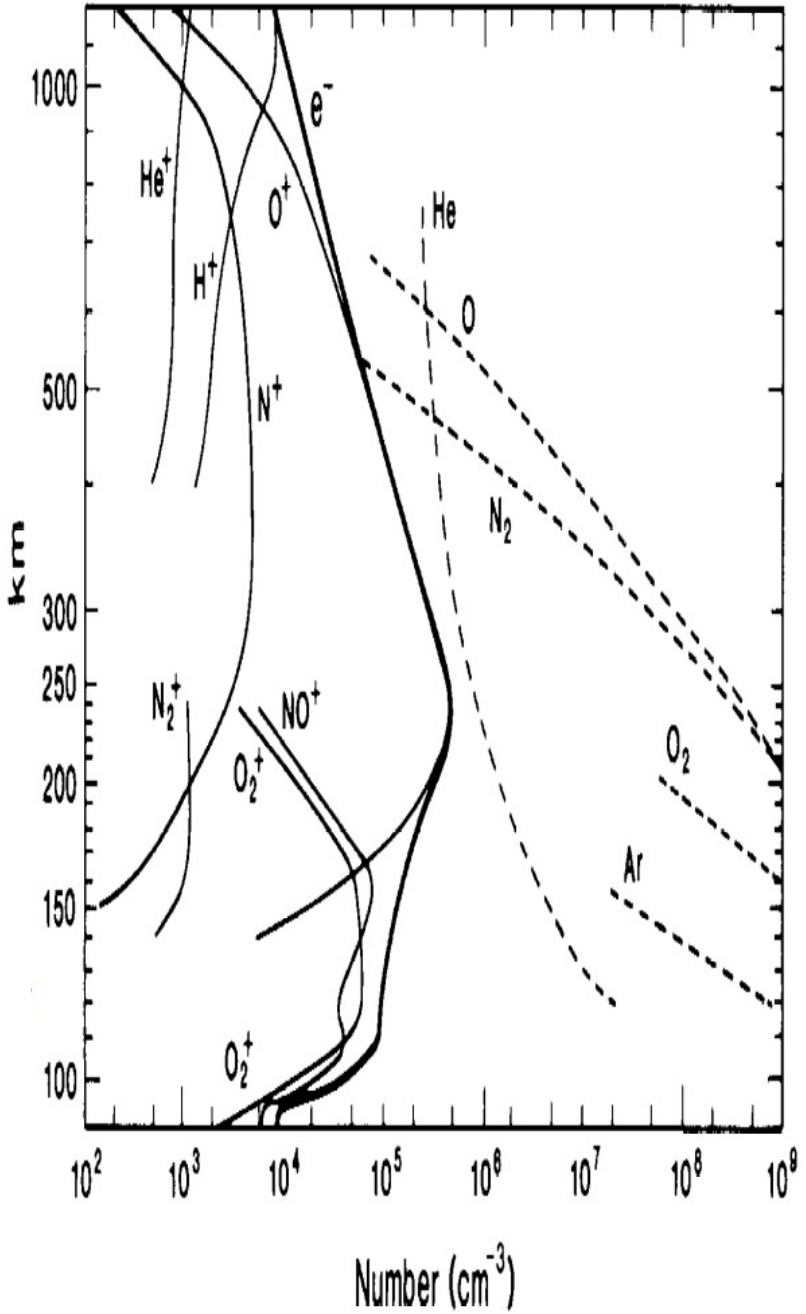

# Why there are free electrons within the Earth atmosphere?

The chemical reactions on the Earth atmosphere of dissociation of different molecules at different heights by solar photons (mostly in EUV and X-ray bands).

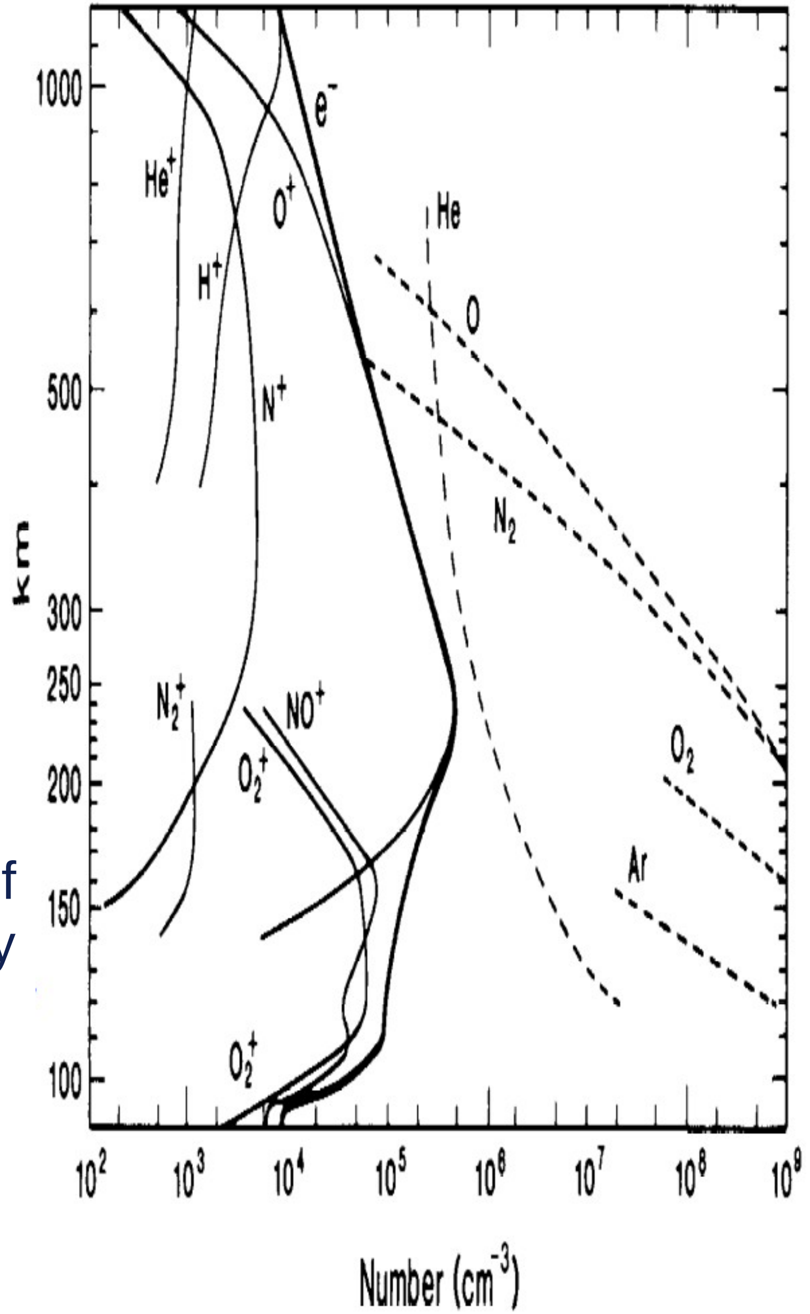

# How can the VTEC distribution be explained?

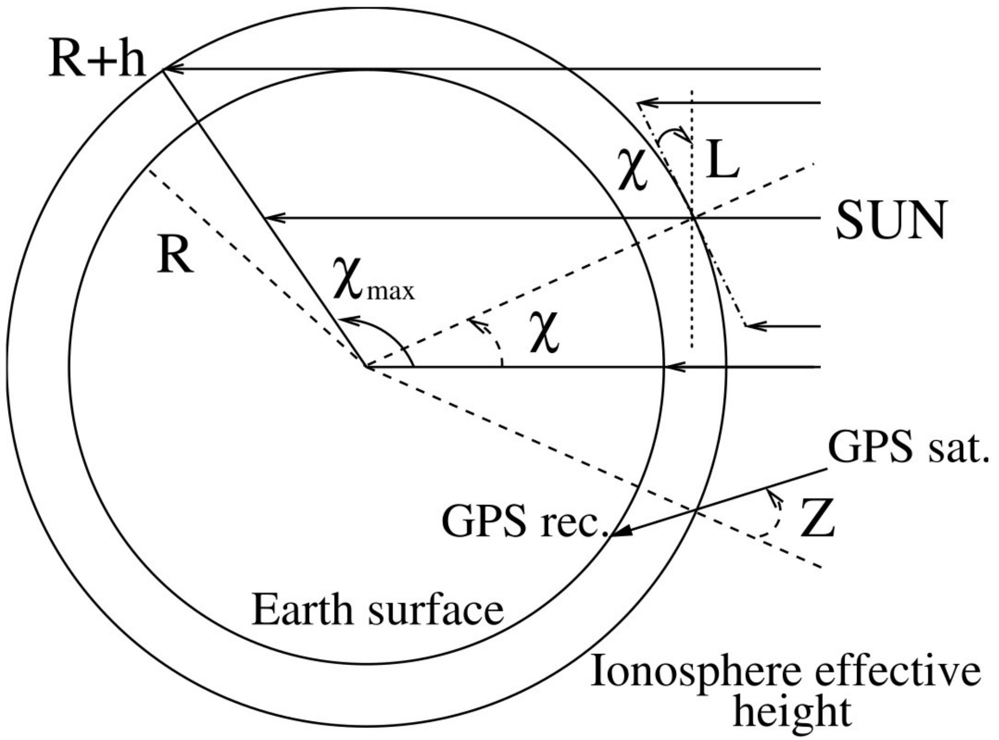


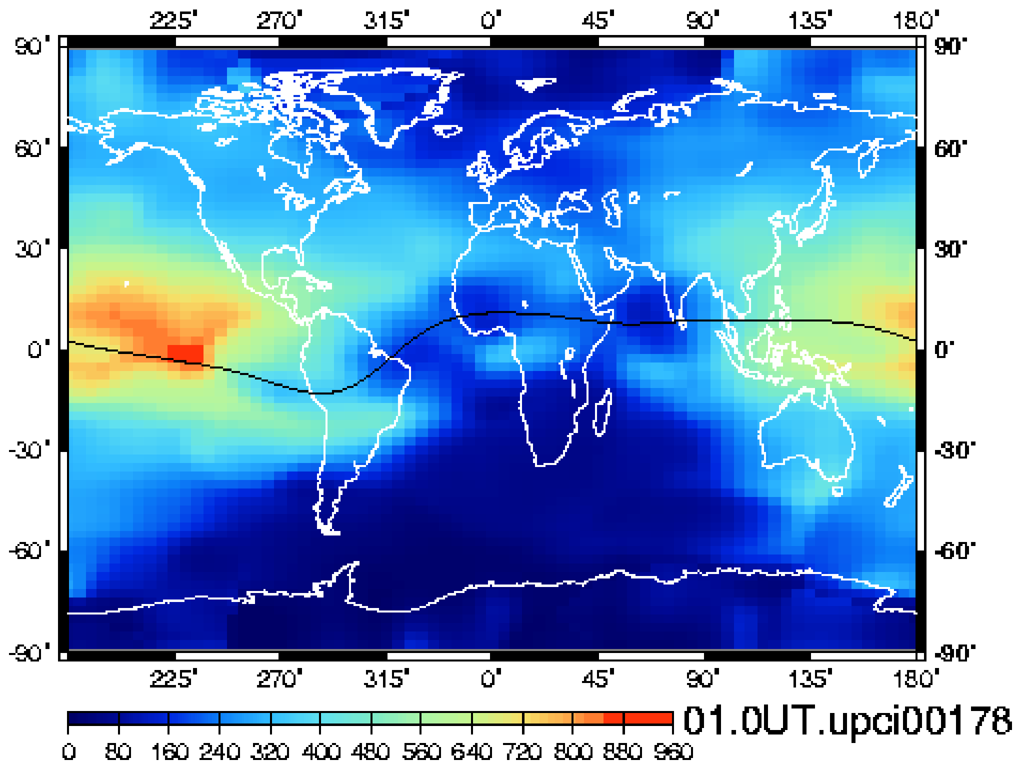

# How can the VTEC distribution be explained?

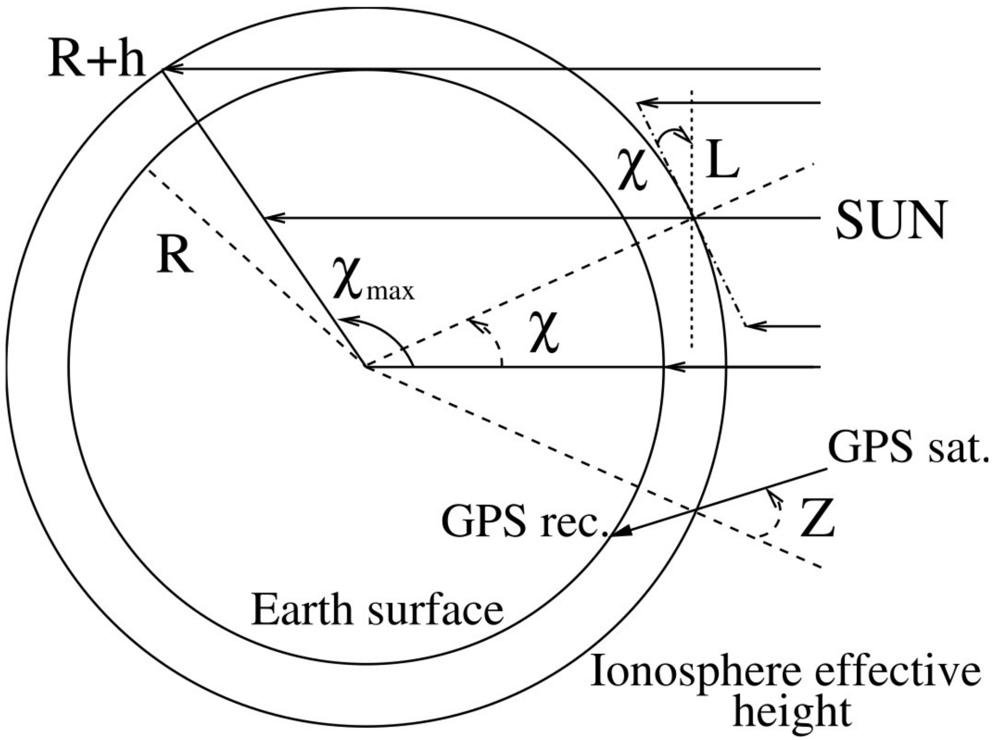


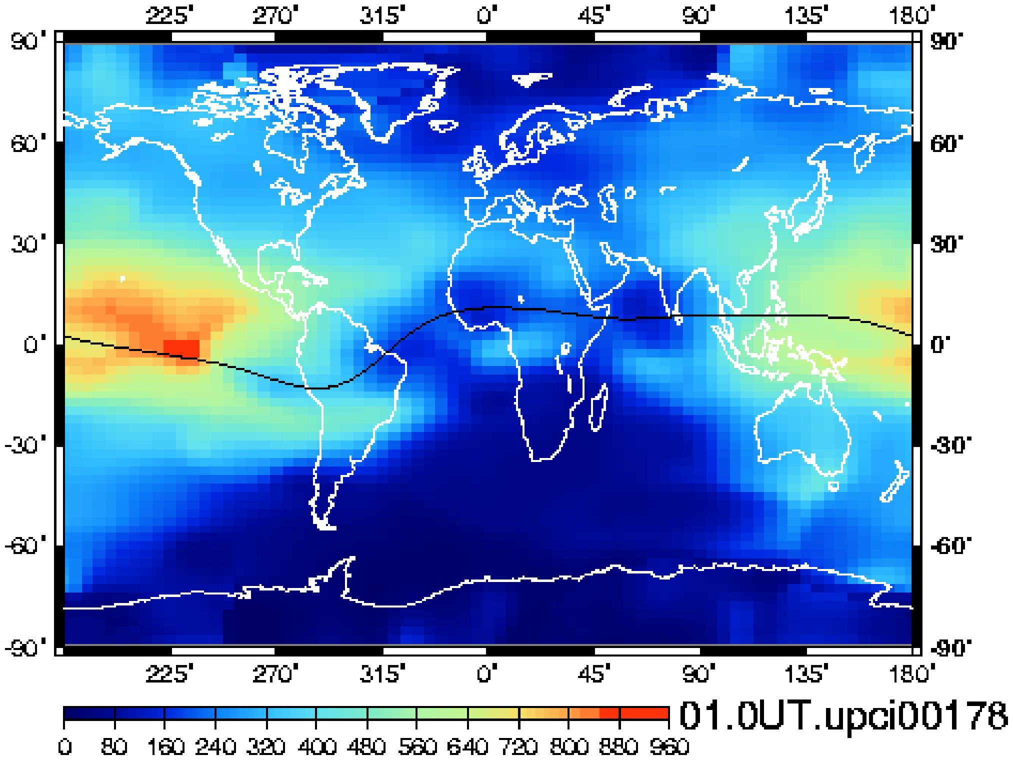


- In principle, taking into account with different solar irradiance in function of the latitude

- (And the Earth rotation!)

# Anything else to be explained? What about the double VTEC peak (equatorial anomaly)?

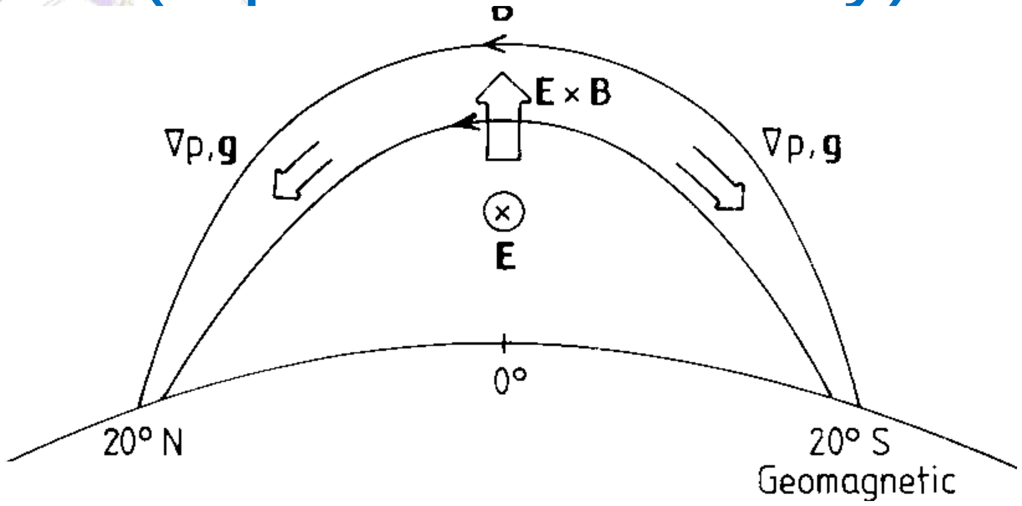


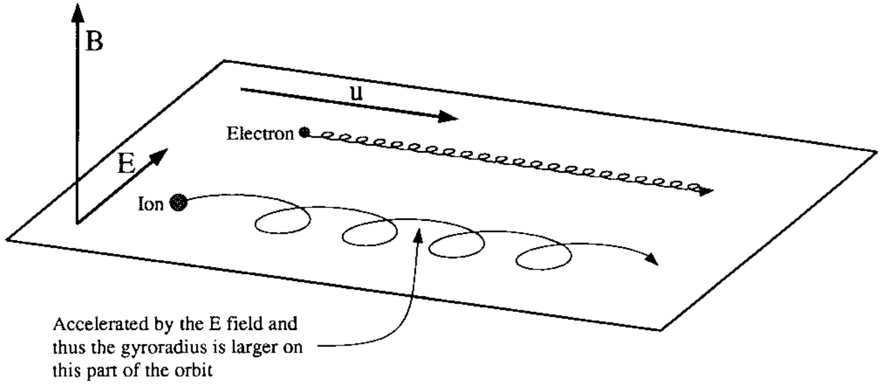


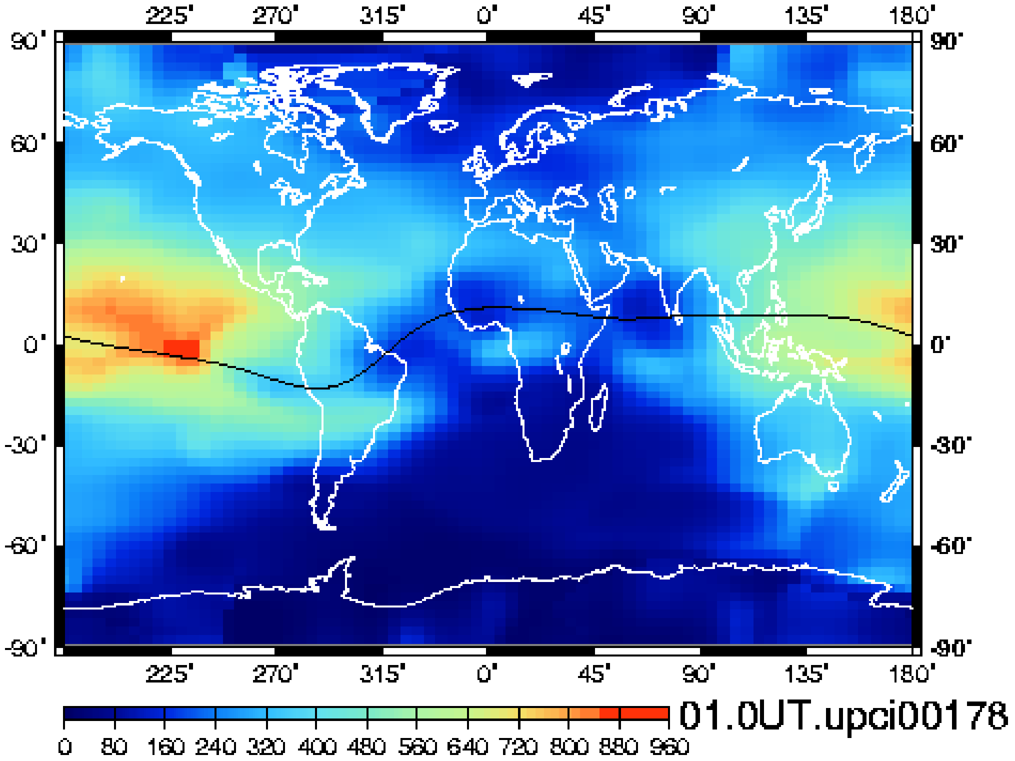

# Anything else to be explained? What about the double VTEC peak (equatorial anomaly)?

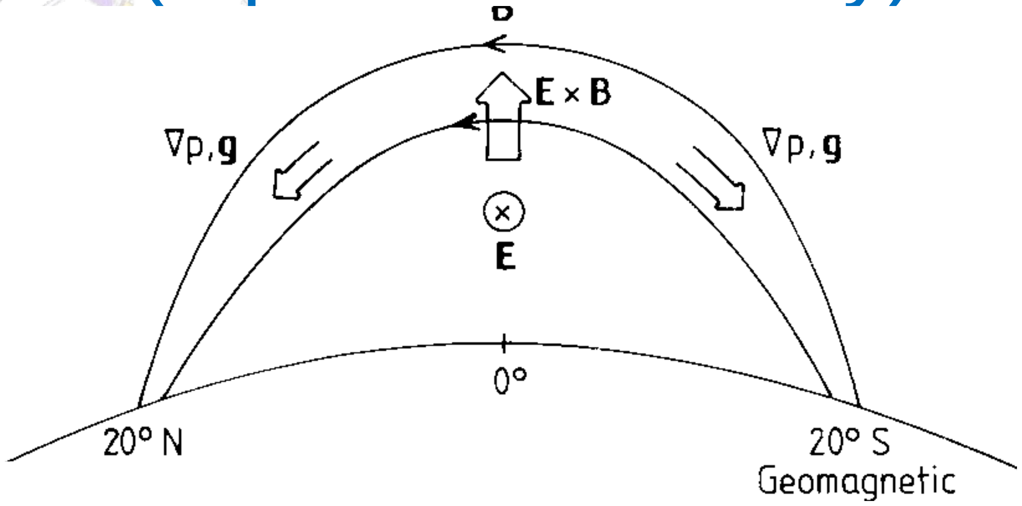


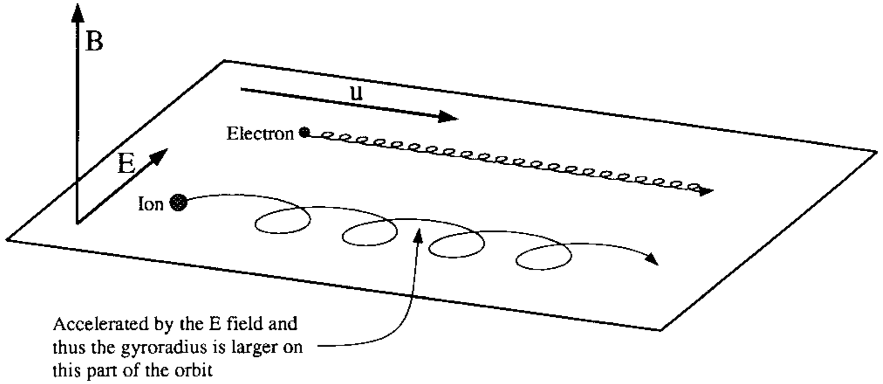


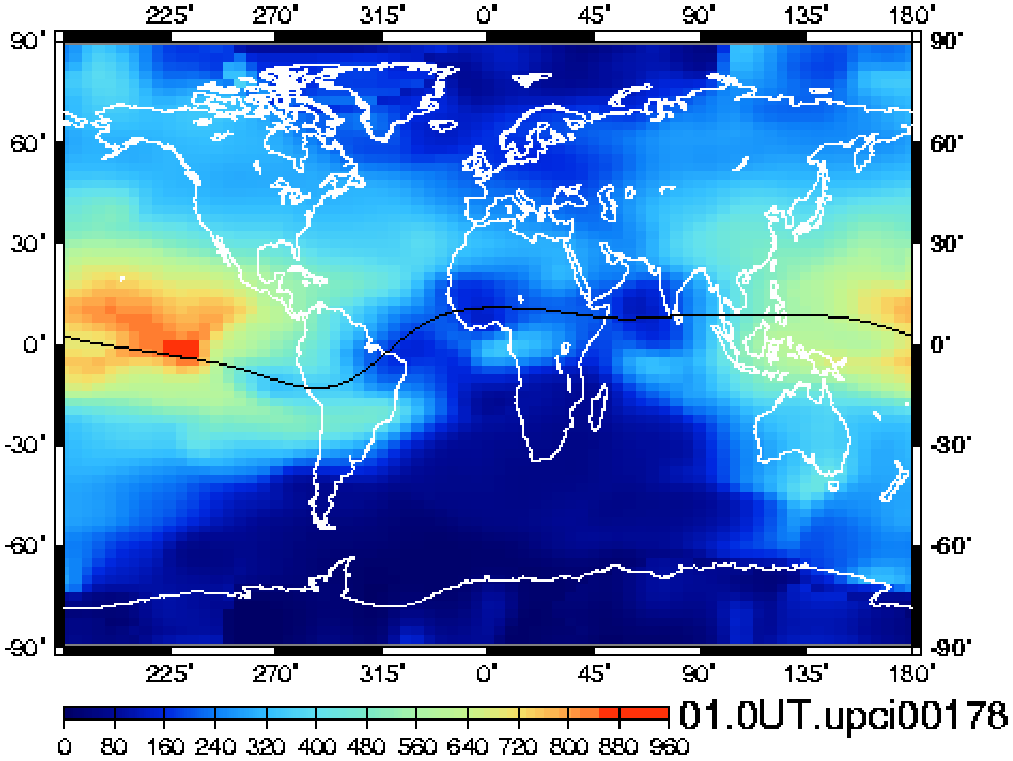


ExB drift, generates the fountain effect, and then, the equatorial anomaly and double peak, with a central role of the magnetic field, the magnetic equator in particular, in the distribution of the free electrons of the Earth ionosphere.

UNIVERSITAT POLITÈCNICA DE CATALUNYA BARCELONATECH

# And this? How can it be explained?

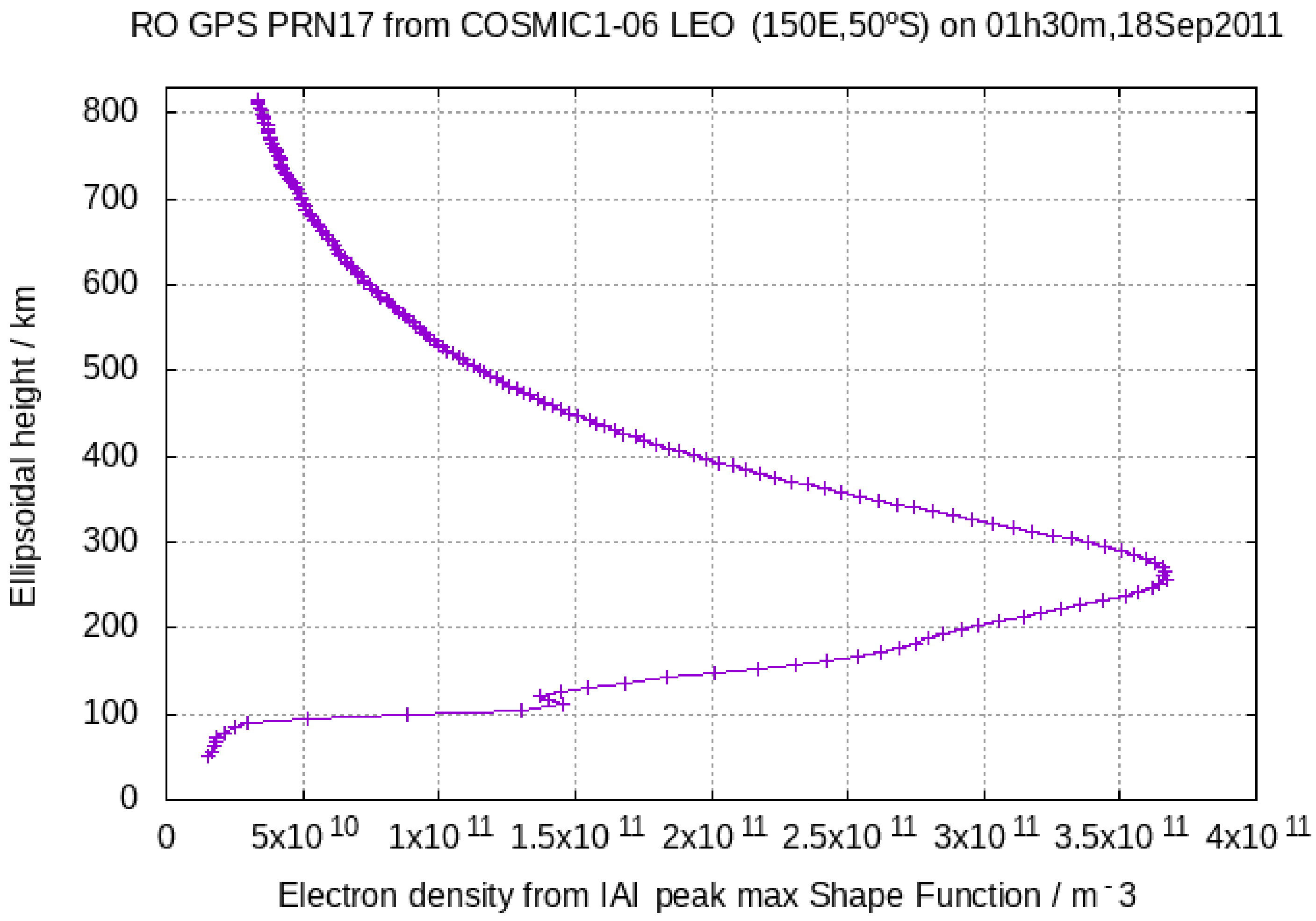

# And this? How can it be explained?

- The electron number density (hereinafter electron density) vs height(*).

- The intermediate electron density peak height can be understood as the optimal height of production of free electrons, a compromise between enough number of target molecules and enough ionizing solar radiation, specially in EUV.

(*) Estimated thanks to GNSS receivers flying on a Low Earth Orbiting satellite -in this case FORMOSAT-3/COSMIC- measuring multifrequency GNSS signals from transmitters below the LEO local horizon (radio-occultation scenario).

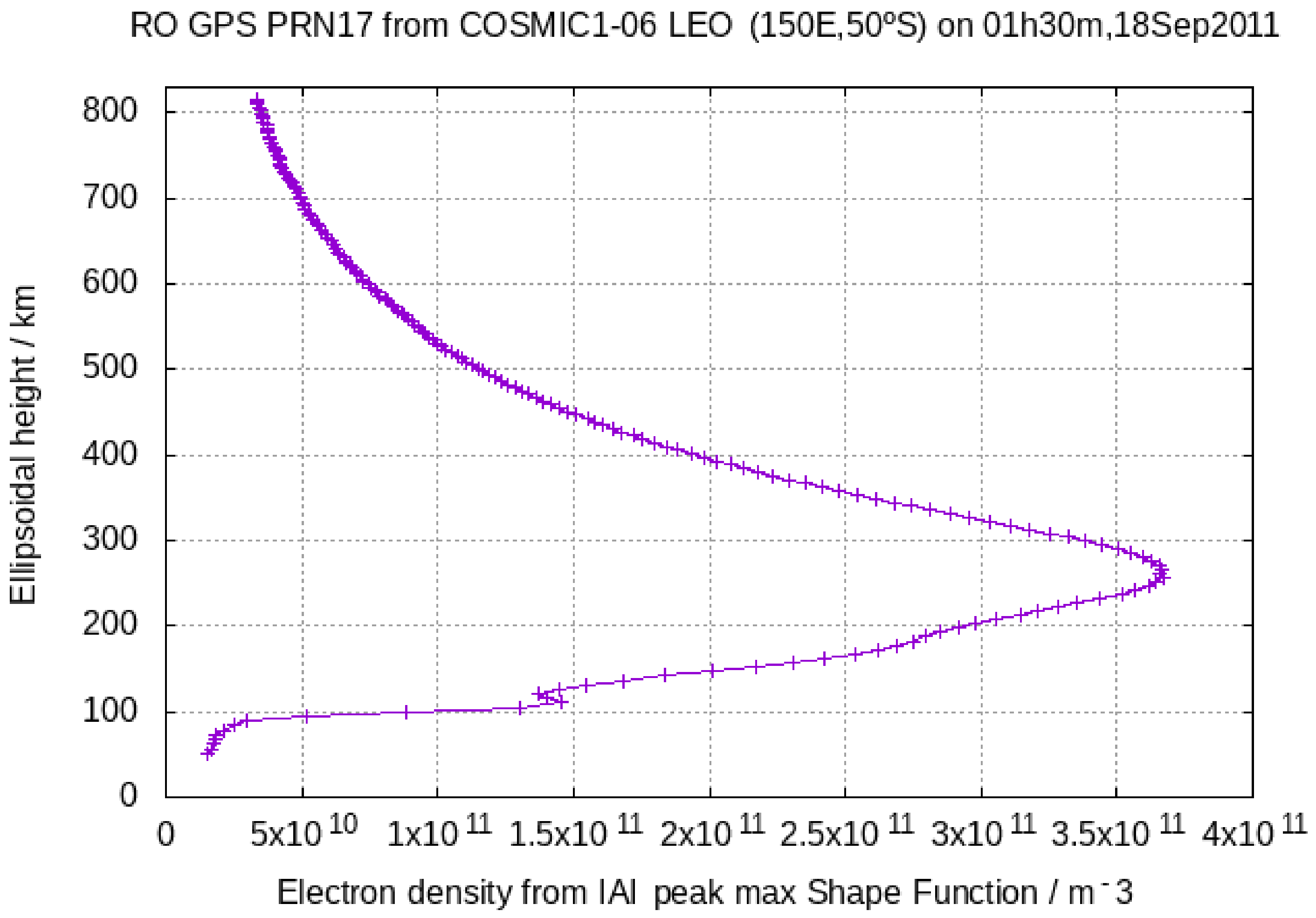

# And what about this? Any guess?

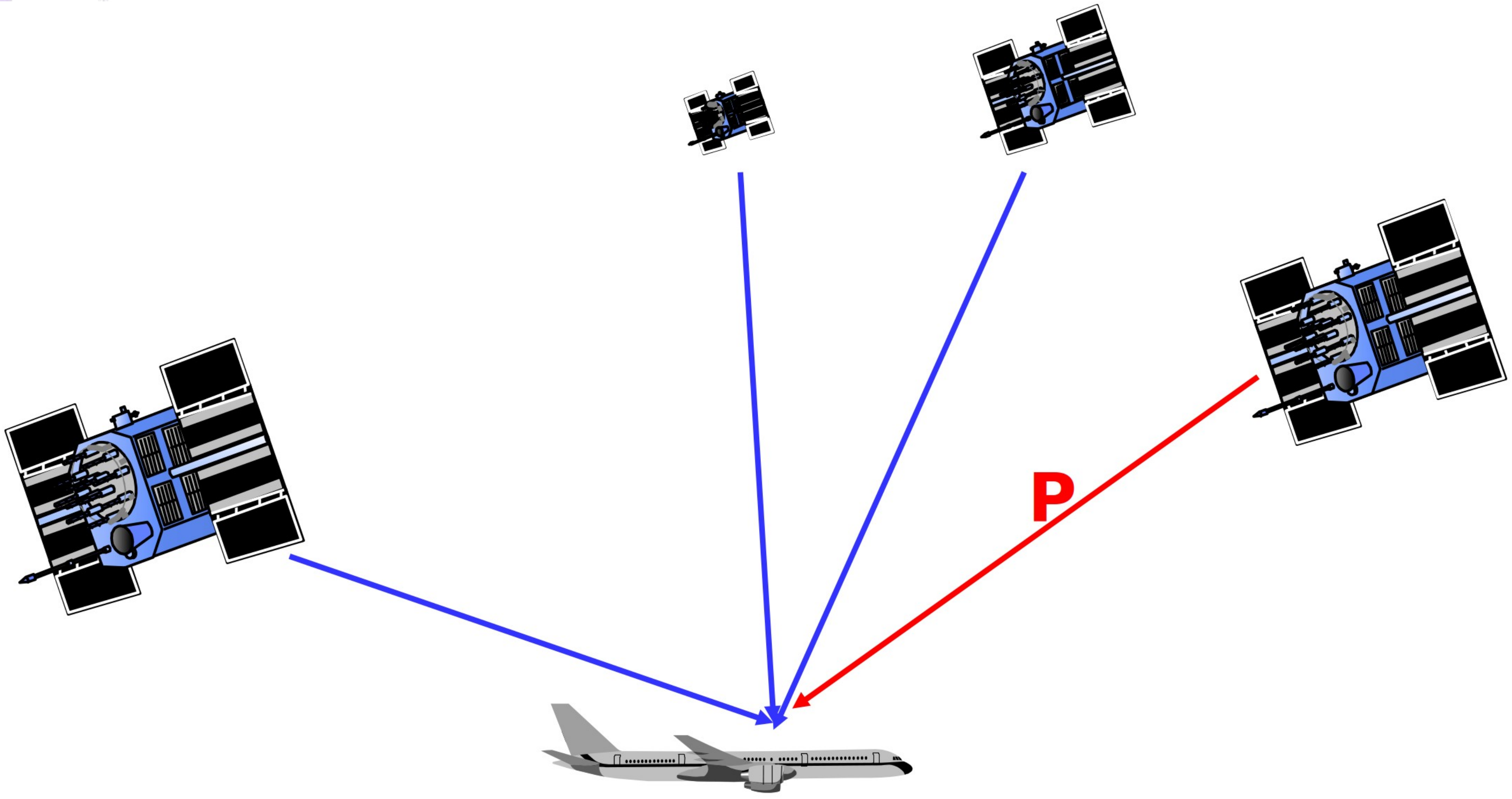

# And what about this? Any guess?

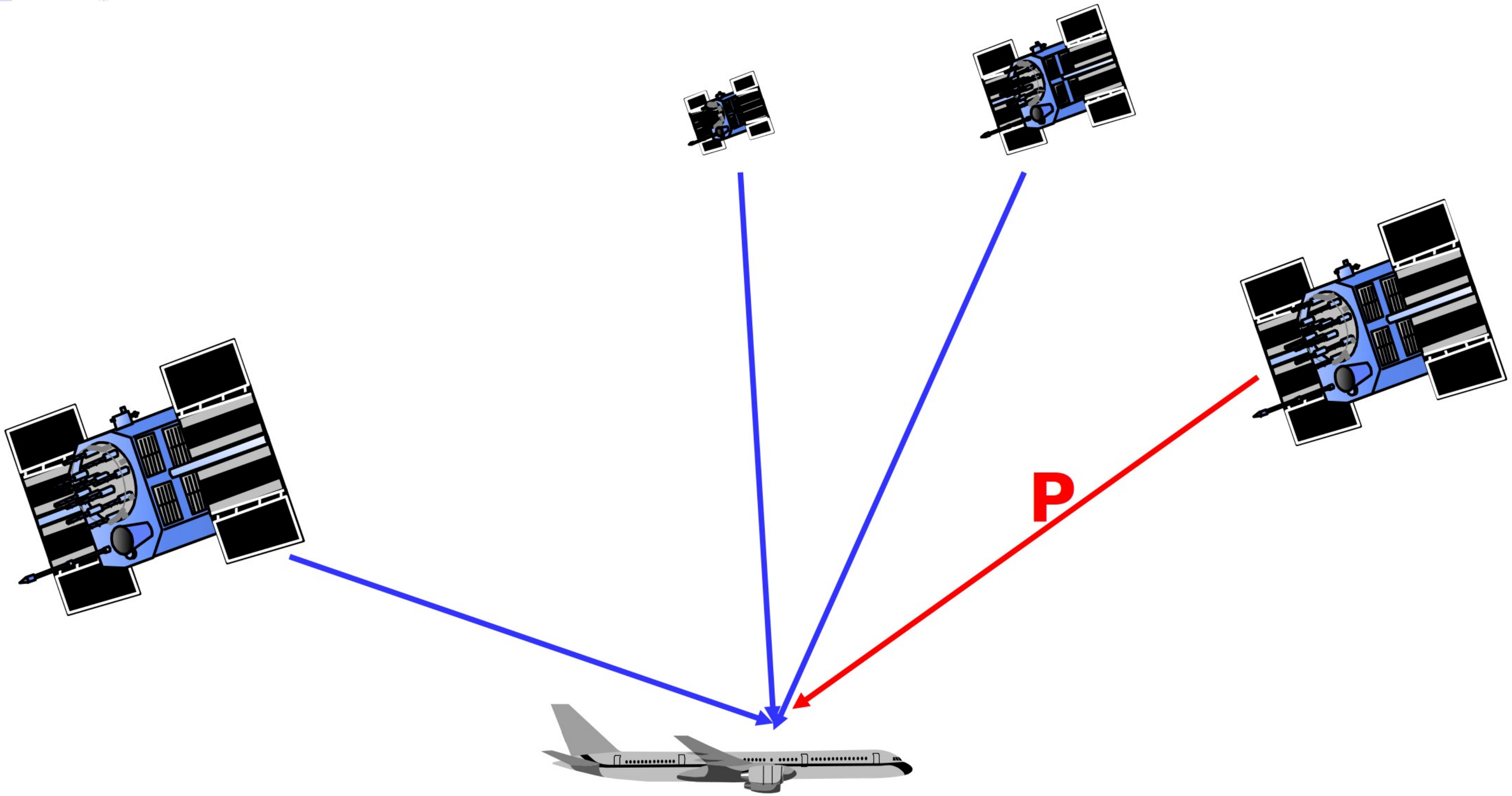


Yes, these are four Global Positioning System (GPS) transmitter providing pseudodistance signals to a receiver on board an airplane (this an “artistic” composition NOT following the real distance scale).

# And now, who can explain these layouts?

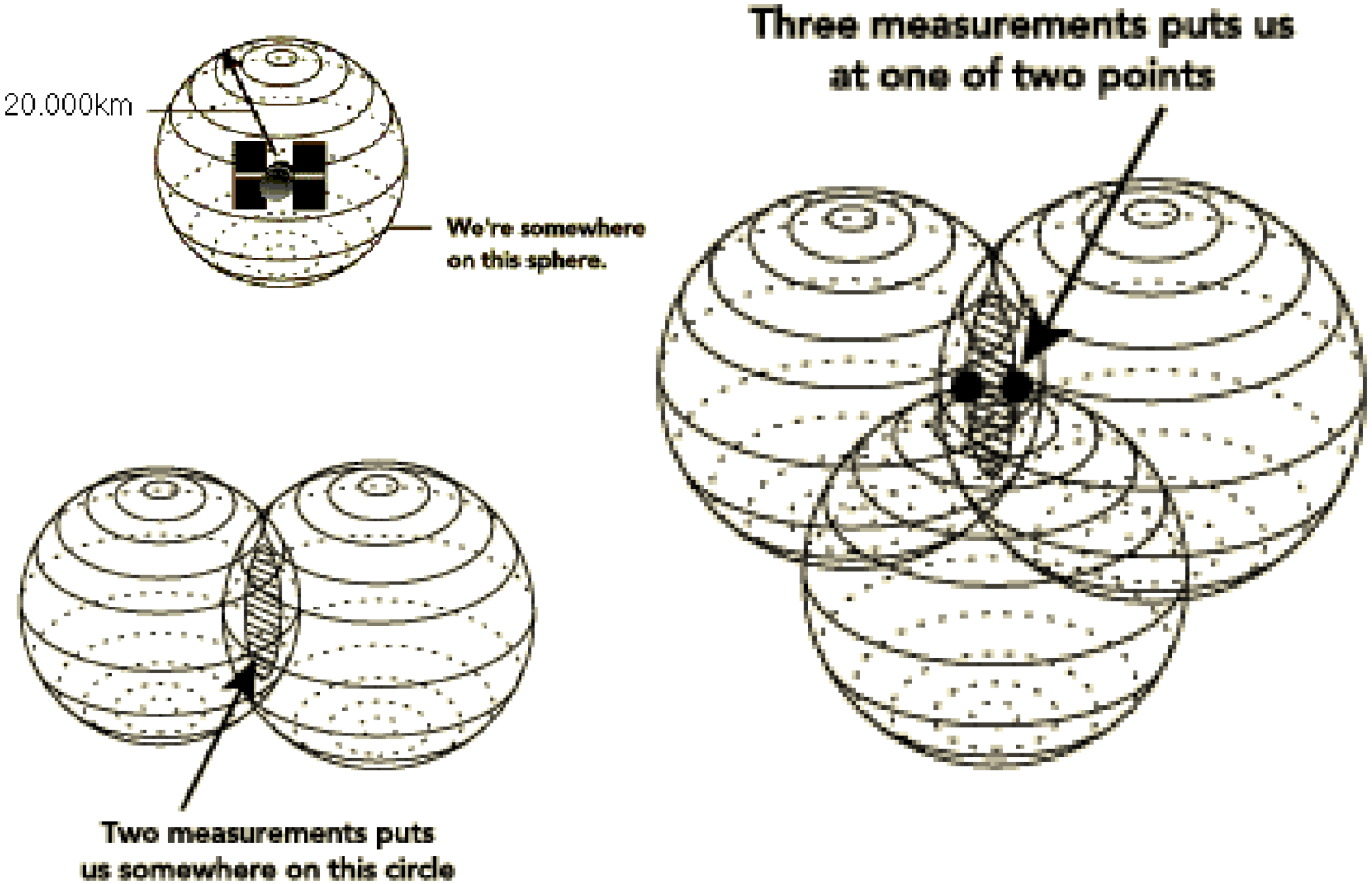

# And now, who can explain these layouts?

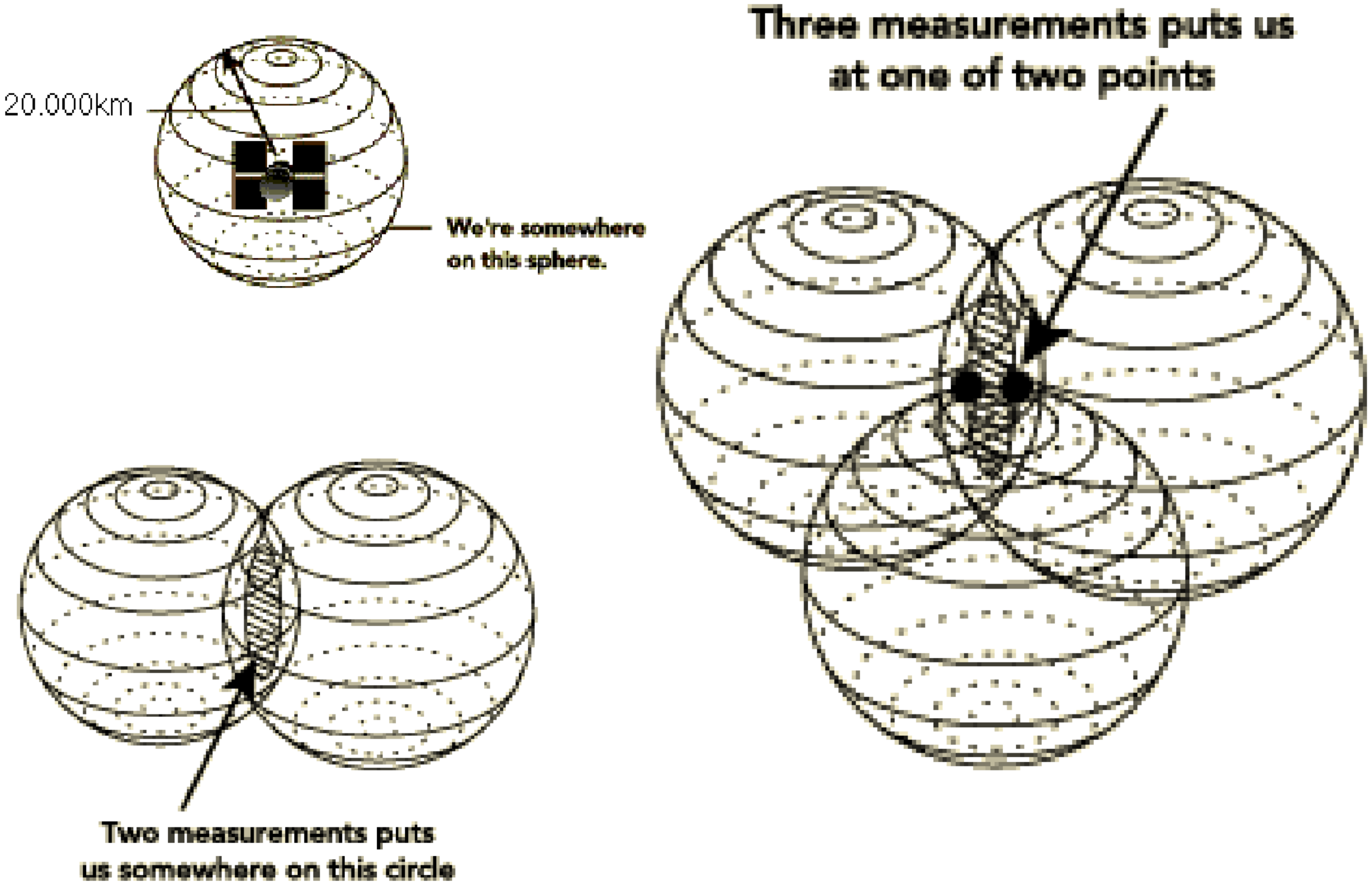


Yes, it illustrates the trilateration concept, foundation of GNSS for positioning: knowing the position of the center of at least three(*) spheres in different directions -GNSS transmitters on MEOs- and the radius of such spheres -from the pseudorange measurements-, we get the receiver position X,Y,Z -intersection-).



(*) at least four satellites are needed taking into account the receiver clock error

# But we need to get pseudoranges, right?

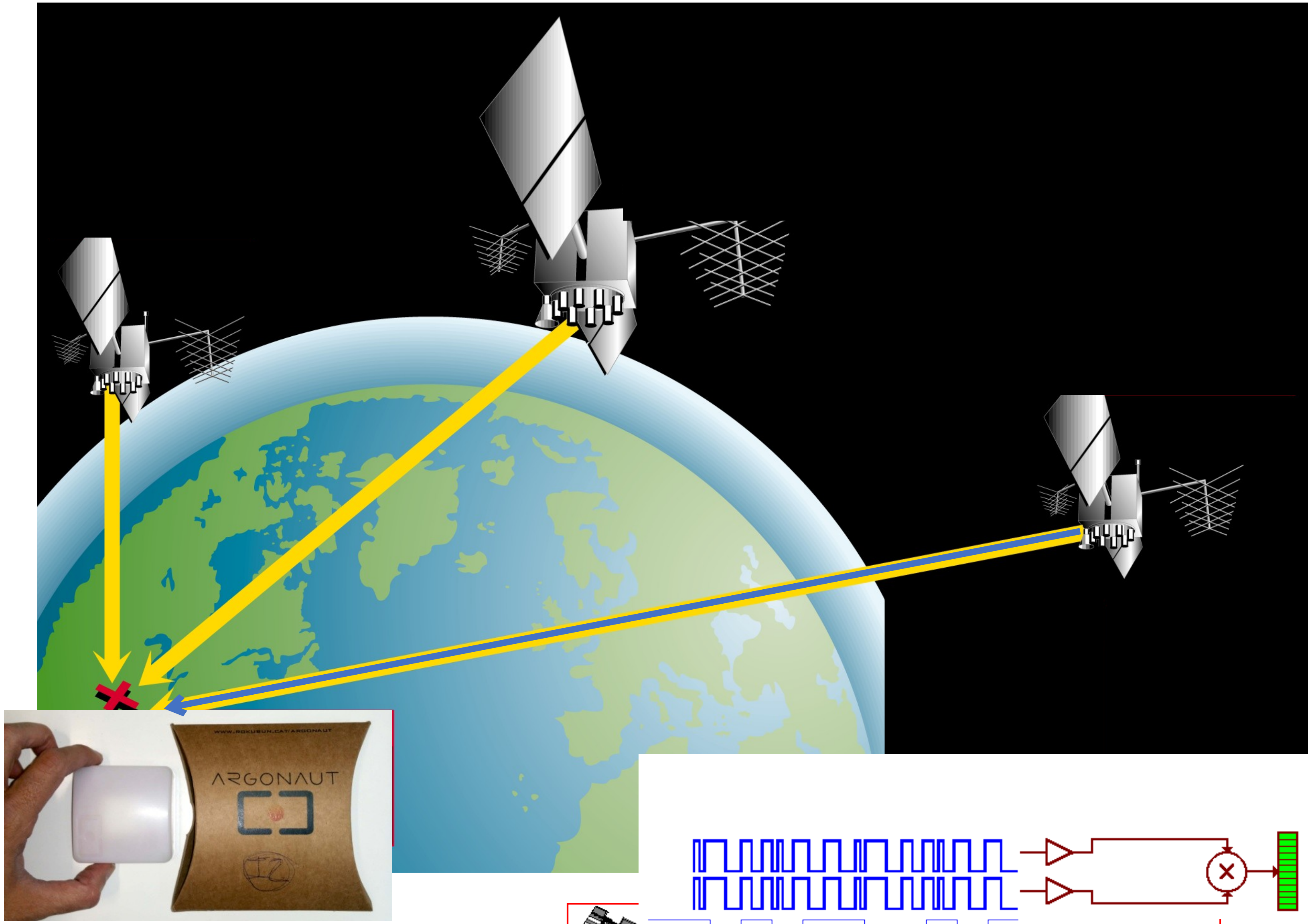


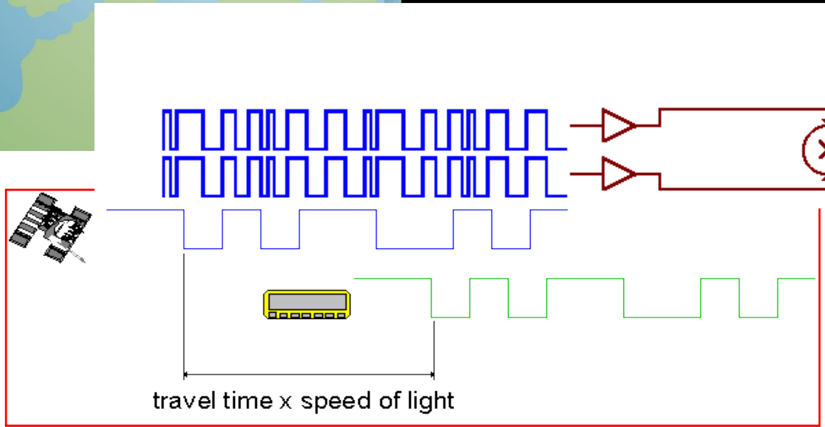

# But we need to get pseudoranges, right?

- “Pseudoranges” are computed from the apparent traveling time from GNSS transmitter to GNSS receiver.

- The pseudo-random noise transmitted signal, function of the atomic transmitter clock, is correlated at the receiver with its replica, generated from its typically quartz clock.

- Several “error” sources quickly arises, not only the transmitter and receiver clock errors, but also the atmospheric ones, including the ionospheric delay, all under the “pseudo” part of the observable pseudorange name.

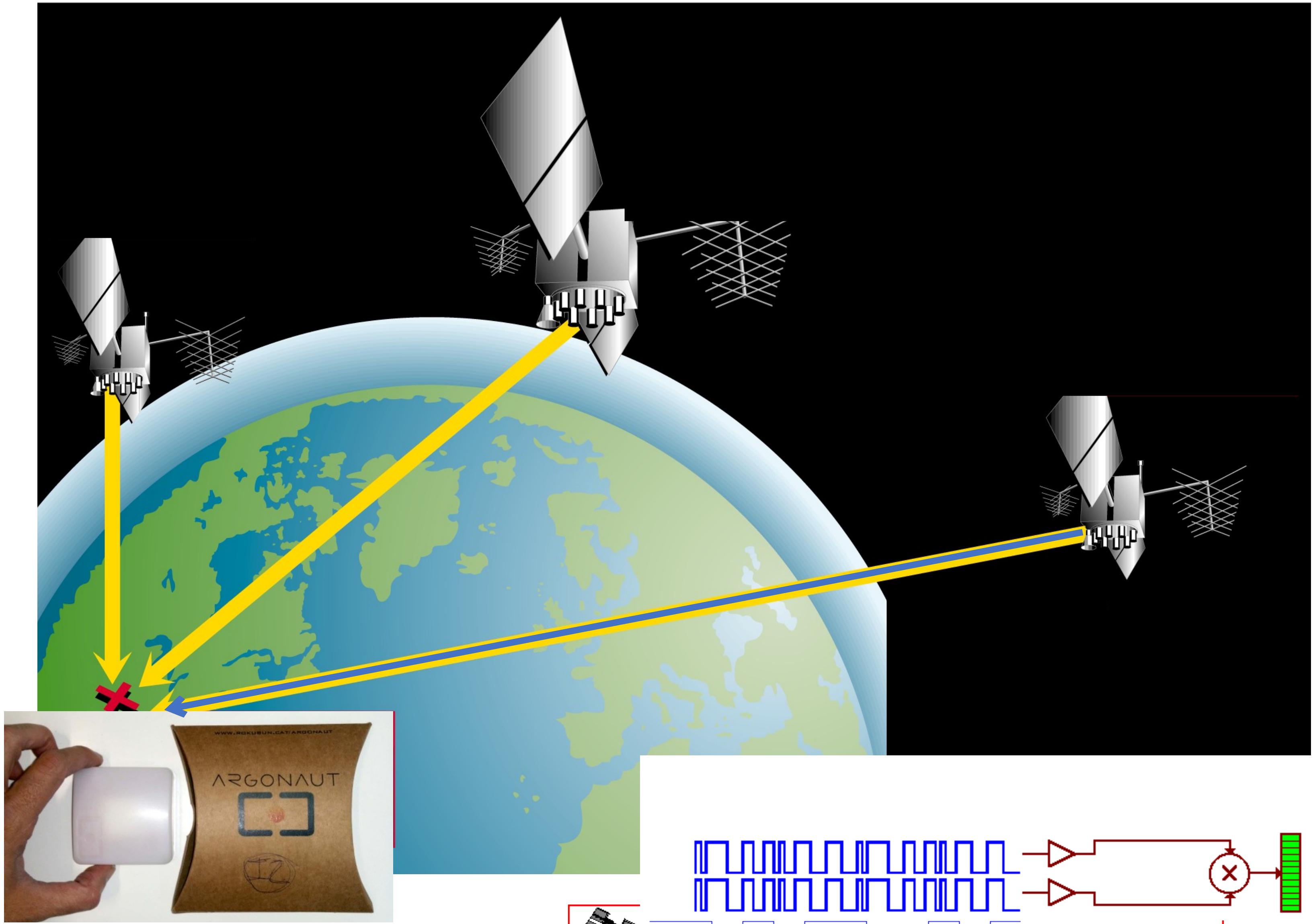


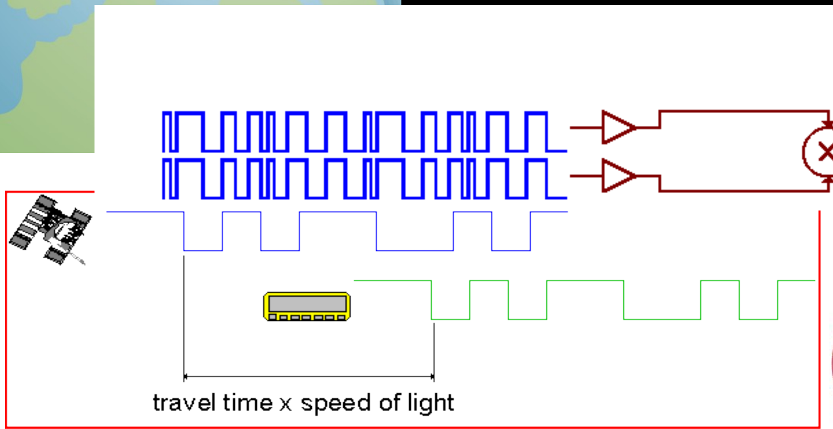

# But we need to get pseudorange measuremens, right?

# But we need to get pseudorange measuremens, right?



1. Code or pseudorange: This measurement is given by the apparent travel time $\tau$ of the EM signal propagated from GPS transmitter to receiver, scaled by the speed of light in the vacuum, $c$. This value can be partially considered as a range, i.e., a pseudorange $\tilde{\rho}$:

$$P \equiv c\tau = \tilde{\rho} \tag{3}$$

# And we have a second “invited” type of measurement to the “GNSS party”, very interesting, very precise: the carrier phase

# And we have a second "invited" type of measurement to the "GNSS party", very interesting, very precise: the carrier phase

2. Carrier phase: This measurement is computed in the receiver by continuously integrating the frequency Doppler shift, primarily due to the relative velocity, clocks, and tropospheric and ionospheric drifts. This value is scaled in unit lengths in such a way that it represents the pseudorange $\tilde{\rho}$ and basically refers to the last time the carrier phase was locked by the receiver $t_L$ (i.e., the pseudorange change since the last "cycle-slip" or the first acquisition epoch).

# And we have a second "invited" type of measurement to the "GNSS party", very interesting, very precise: the carrier phase

$$\int_{t_L}^{t} \dot{\tilde{\rho}}\, \mathrm{d}t = -\frac{c}{f} \int_{t_L}^{t} \delta f \cdot \mathrm{d}t. \qquad (5)$$

Thus, the carrier phase is finally defined as:

$$L \equiv -\lambda \int_{t_L}^{t} \delta f \cdot \mathrm{d}t = \tilde{\rho}(t) - \tilde{\rho}(t_L) = \tilde{\rho} + B_f, \qquad (6)$$

where $B_f$ is the carrier phase ambiguity for frequency $f$ and $\lambda = c/f$ is the corresponding carrier wavelength.

# Now, any guess or comment about this plot?



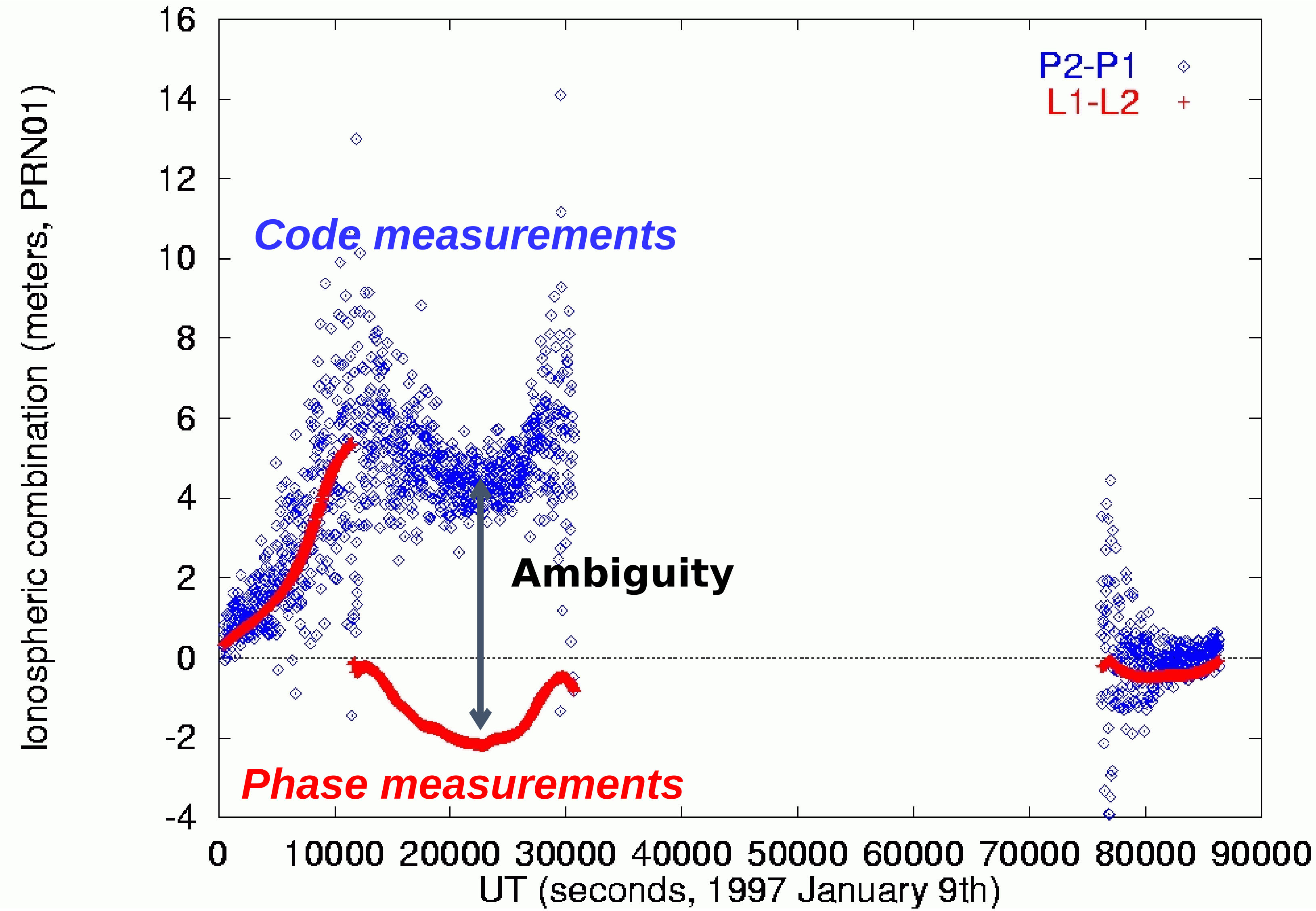

# Now, any guess or comment about this plot?



-We can see how the code (i.e. pseudorange) and phase measurements ("ionospheric combination") of a given GPS transmitter ("PRN01") from a given receiver, complement each other very well:

-The code measurements are accurate (pseudorange) but not precise (measurement noise and multipath >~1 m).

-The carrier phase measurements are not accurate (unknown ambiguity = pseudorange at phase lock) but very precise (measurement noise and multipath < 1cm).

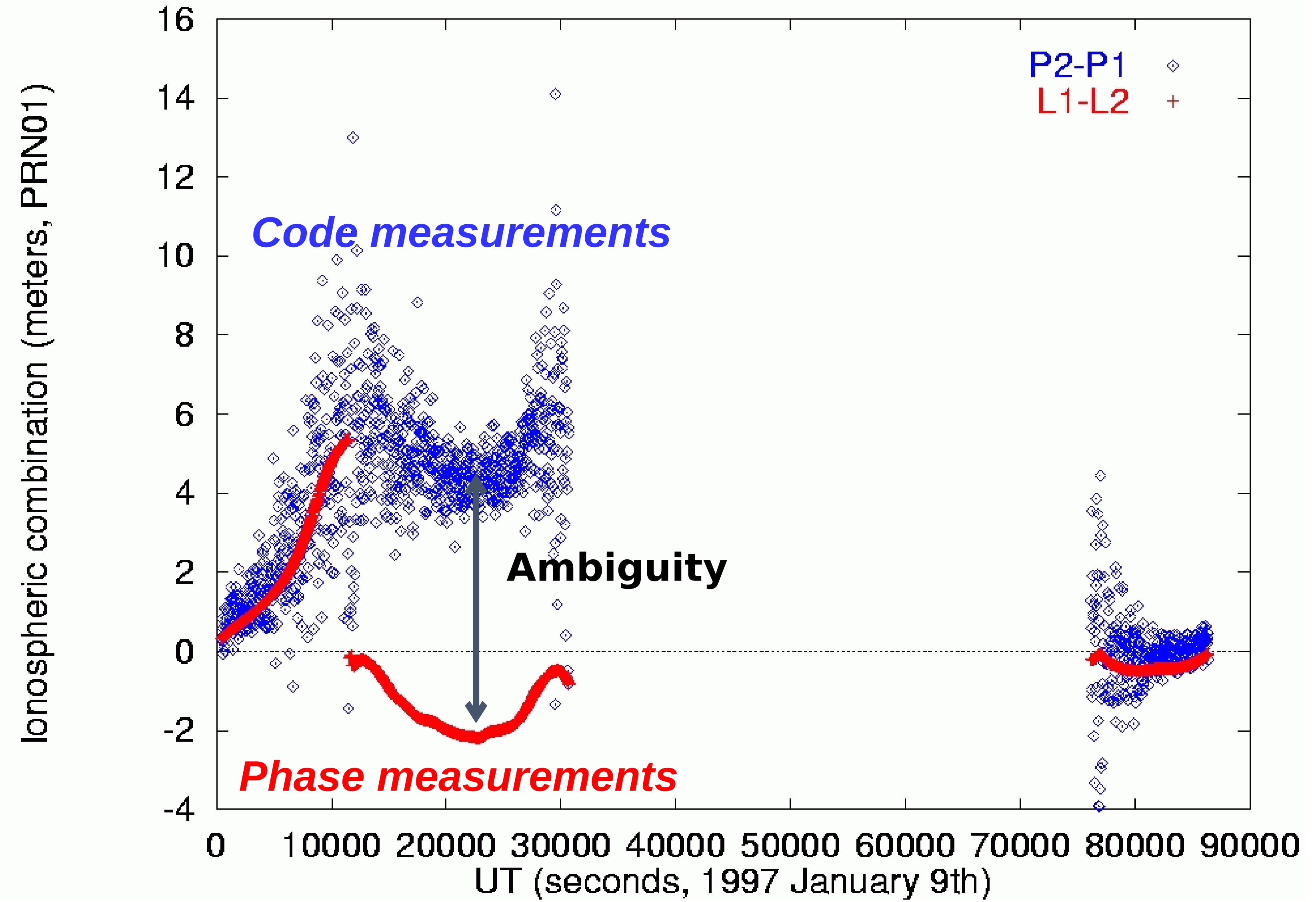

# Finally, the electron content is inside GNSS measurements!



$$P_m = \rho + c(\mathrm{d}t - \mathrm{d}t') + \boxed{\frac{40.309}{{f_m}^2} S} + T + D_m + D'_m \quad (15)$$

and

$$L_m = \rho + c(\mathrm{d}t - \mathrm{d}t') - \boxed{\frac{40.309}{{f_m}^2} S} + T + B_m + \frac{c}{f_m}\phi \quad (16)$$

$$S = \int_{r_\mathrm{T}}^{r_\mathrm{R}} N_\mathrm{e} \mathrm{d}l \quad (14)$$

# Finally, the electron content is inside GNSS measurements!



-The first-order approximation of the ionospheric delay term, deduced from the Appleton-Hartree equations of EM propogation, accounts for 99.9% of the the ionospheric delay of GNSS signals (L-band).

- It is positive (delay) for the pseudorange and negative (advance) for the carrier phase. BTW: Is this an issue vs the relativity principle of “maximum velocity” the light speed in the vaccum?.

- The ionospheric delay term is proportional to the Slant Total Electron Content (Slant TEC, STEC) and inversely proportional to the signal frequency.

$$P_m = \rho + c(\mathrm{d}t - \mathrm{d}t') + \boxed{\frac{40.309}{{f_m}^2} S} + T + D_m + D'_m \qquad (15)$$

and

$$L_m = \rho + c(\mathrm{d}t - \mathrm{d}t') - \boxed{\frac{40.309}{{f_m}^2} S} + T + B_m + \frac{c}{f_m}\phi \qquad (16)$$

$$S = \int_{r_\mathrm{T}}^{r_\mathrm{R}} N_\mathrm{e} \mathrm{d}l \qquad (14)$$

UNIVERSITAT POLITÈCNICA DE CATALUNYA BARCELONATECH

IonSAT

# Finally, the electron content is inside GNSS measurements!



$$L_I \equiv L_1 - L_2 = \alpha \cdot S - \beta \cdot \phi + B_I, \tag{17}$$

$$P_I \equiv P_2 - P_1 = \alpha \cdot S + D_I + D'_I + \epsilon_M + \epsilon_\mathrm{T}, \tag{18}$$

where $\alpha = 40.309\left(\frac{1}{f_2^2} - \frac{1}{f_1^2}\right) = 1.05 \cdot 10^{-17}\, m^3$, $\beta = c\left(\frac{1}{f_2} - \frac{1}{f_1}\right) = 0.054\,\mathrm{m}$, $B_I = B_1 - B_2$, $D_I = D_2 - D_1$ and $D'_I = D'_2 - D'_1$.[2] In this case, we also made explicit the two main components of the measurement error, both corresponding to the code: the multipath code error $\epsilon_\mathrm{M}$ and the thermal noise measurement error $\epsilon_\mathrm{T}$. Typically, the wind-up term $\beta \cdot \phi$ is a centimeter-level term. For the permanent receivers, this term can be corrected very accurately from their coordinates and orbital information, and it is not discussed explicitly herein.

# Finally, the electron content is inside GNSS measurements!



-Then the highly variable ionospheric magnitude, STEC, is directly given by the ionospheric combination of dual-frequency carrier phases and pseudoranges ($L_I$ & $P_I$): This is the main input data source for GNSS Ionosphere! (among the good performance of single-frequency measurements recently shown for certain ionospheric viewing problems such as plasma bubble detection).

-Other additional terms, are either constant at scales of hours (ambiguity BI, Differential Code Biases, DI, DI') or are small and can be very well modelled (wind-up term $\beta * \phi$).

$$L_I \equiv L_1 - L_2 = \alpha \cdot S - \beta \cdot \phi + B_I, \tag{17}$$

$$P_I \equiv P_2 - P_1 = \alpha \cdot S + D_I + D'_I + \epsilon_M + \epsilon_{\mathrm{T}}, \tag{18}$$

where $\alpha = 40.309\left(\frac{1}{f_2^2} - \frac{1}{f_1^2}\right) = 1.05 \cdot 10^{-17} m^3$, $\beta = c\left(\frac{1}{f_2} - \frac{1}{f_1}\right) = 0.054\,\mathrm{m}$, $B_I = B_1 - B_2$, $D_I = D_2 - D_1$ and $D'_I = D'_2 - D'_1$.[2] In this case, we also made explicit the two main components of the measurement error, both corresponding to the code: the multipath code error $\epsilon_{\mathrm{M}}$ and the thermal noise measurement error $\epsilon_{\mathrm{T}}$. Typically, the wind-up term $\beta \cdot \phi$ is a centimeter-level term. For the permanent receivers, this term can be corrected very accurately from their coordinates and orbital information, and it is not discussed explicitly herein.

# **Conclusion**: GNSS Ionosphere is well data-supported


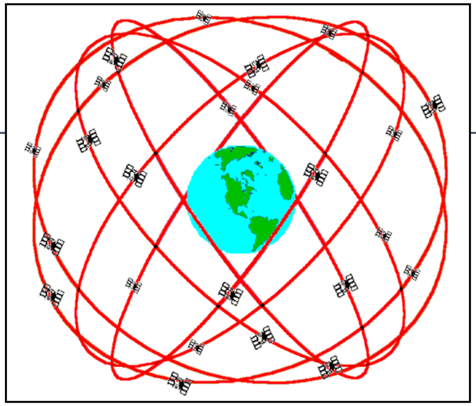

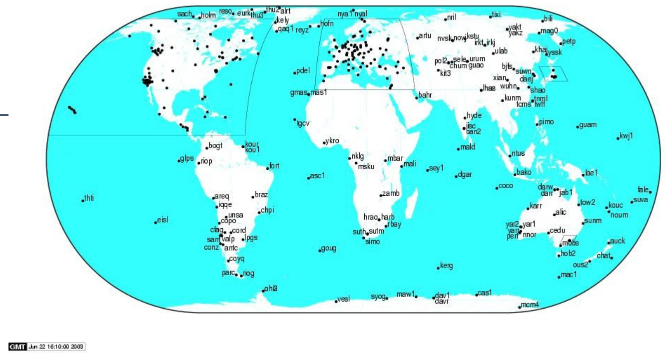

**~ 100 GNSS trans. & +1000 24/7 static GNSS rec. (+100 in RT)**

**Worldwide *scanner* of the Ionosphere, an excellent input to** generate ***Global Ionospheric Maps (GIMs) of VTEC maps*** (summarizing Big GNSS data), among **many other ways of modelling / studying the ionosphere**

UNIVERSITAT POLITÈCNICA DE CATALUNYA BARCELONATECH

IonSAT

# **Conclusion**: GNSS Ionosphere is well data-supported

**GNSS Ionosphere:**

***“Effects and computation of the distribution of free electrons, located at the partially ionized part of the atmosphere above 50 km height, from the Global Navigation Satellite Systems (GNSS) measurements, usually multi-frequency, crossing it; and its applications, such as Space Weather monitoring, precise real-time positioning and, in general, precise geodetic modelling among others”***


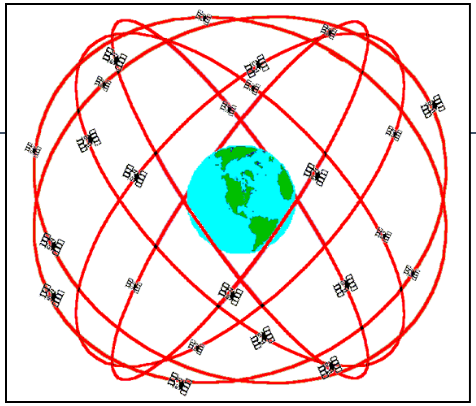

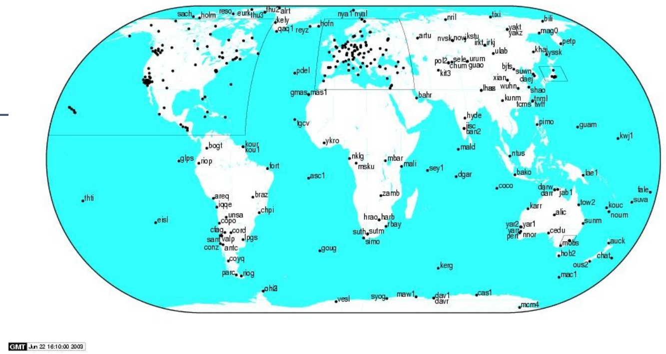

**~ 100 GNSS trans. & +1000 24/7 static GNSS rec. (+100 in RT)**

**Worldwide *scanner* of the Ionosphere, an excellent input to** generate ***Global Ionospheric Maps (GIMs) of VTEC maps*** (summarizing Big GNSS data), among **many other ways of modelling / studying the ionosphere**

UNIVERSITAT POLITÈCNICA DE CATALUNYA
BARCELONATECH

# **Conclusion**: GNSS Ionosphere is well data-supported

**GNSS Ionosphere:**

***"Effects and computation of the distribution of free electrons, located at the partially ionized part of the atmosphere above 50 km height, from the Global Navigation Satellite Systems (GNSS) measurements, usually multi-frequency, crossing it; and its applications, such as Space Weather monitoring, precise real-time positioning and, in general, precise geodetic modelling among others"***

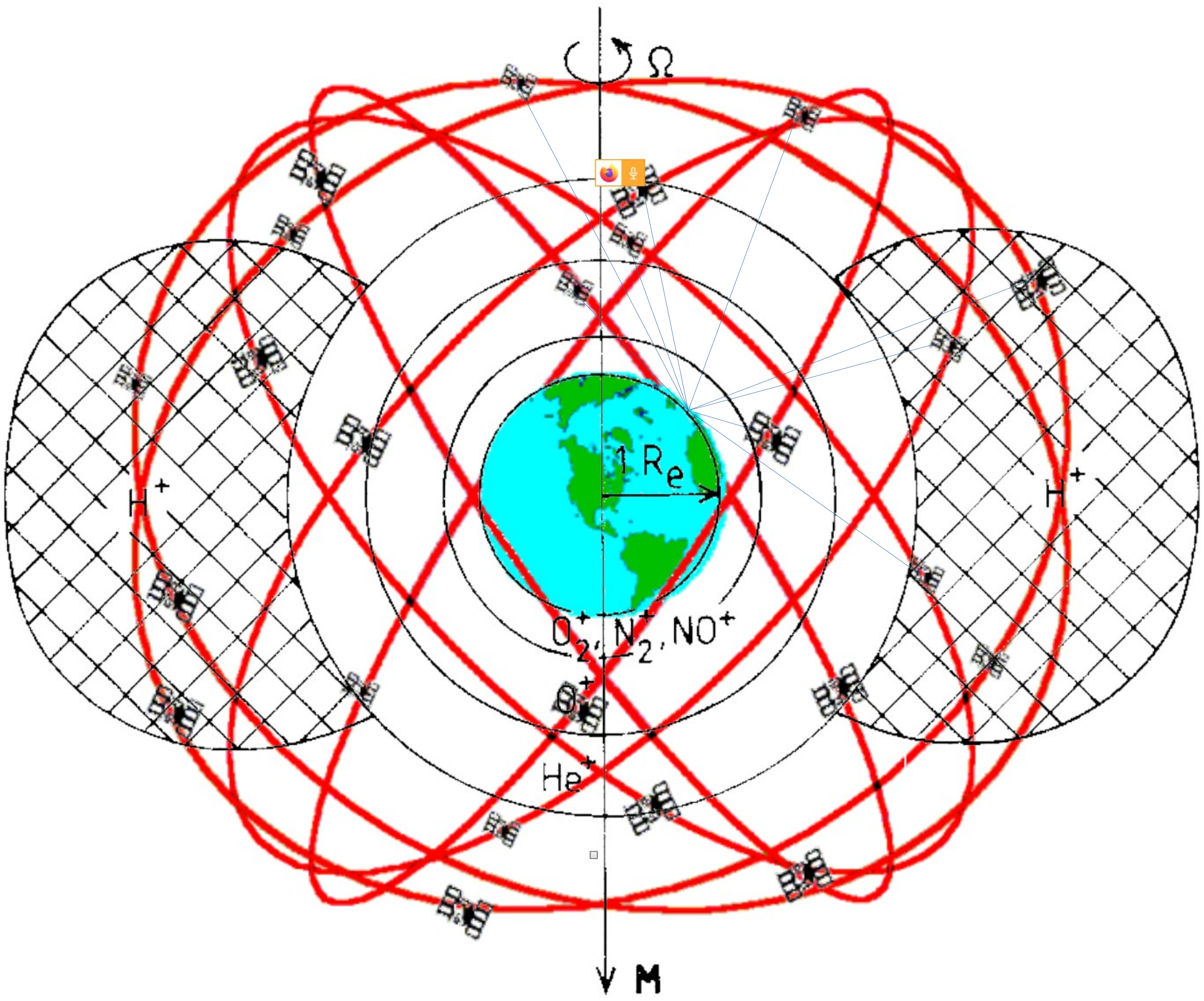


**Thank you!**

UNIVERSITAT POLITÈCNICA DE CATALUNYA
BARCELONATECH

IonSAT

# Set of backup slides #1

# Use Case 10: Access to UPC-IonSAT Global Ionospheric Maps registrations

***(AKA global VTEC maps every 15 minutes since end of 1996, i.e. ~1 million global VTEC maps & 5x10^9 VTECs computed so far)***

Manuel Hernández-Pajares, Victoria Graffigna, Alberto García-Rigo & Germán Olivares-Pulido on behalf of the UPC-IonSAT team

PITHIA-NRF TPW#5, Univ. Westminster, 12-13 September 2023

# GNSS Ionosphere

GNSS Ionosphere[1]: *Effects and computation of the distribution of free electrons, located at the partially ionized part of the atmosphere above 50 km height, from the Global Navigation Satellite Systems (GNSS) multi-frequency measurements crossing it; and its applications, such as Space Weather monitoring, precise real-time positioning and, among others.*

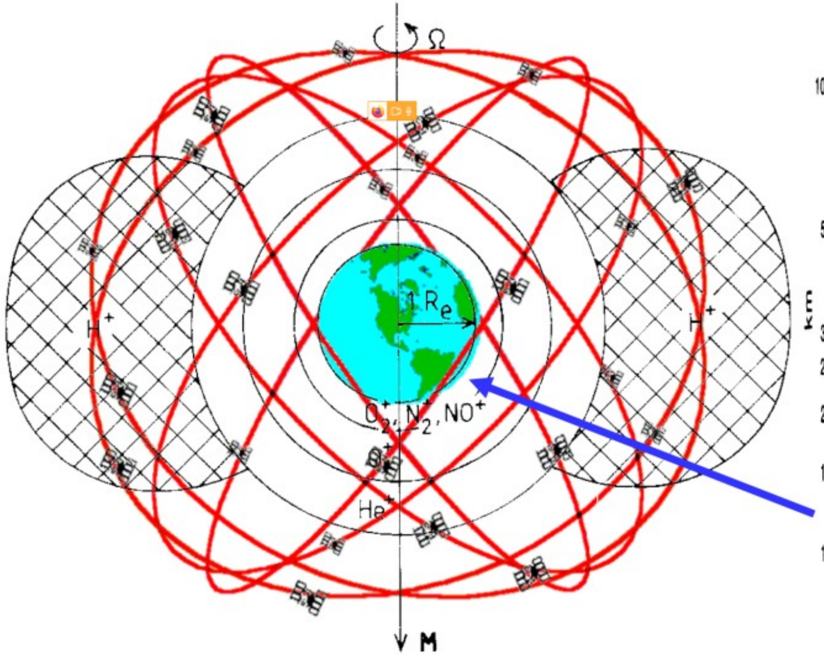


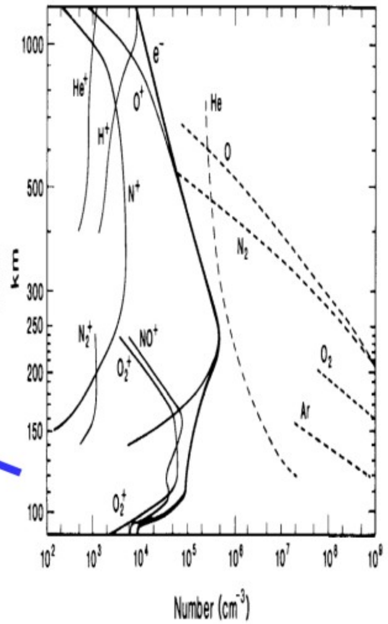


[1] Manuel Hernández-Pajares. "GNSS Ionosphere". In: *Encyclopedia of Geodesy* (2022). Ed. by Michael G. Sideris, pp. 1–7.

# The ionosphere in brief seen by GNSS

- The ionosphere is typically distributed from around 50 km to 1000 km height, where some predominant air molecules, such as $O_2$ and NO at the very bottom and mostly O above, are partially ionized respectively by the x-ray and specially Extreme Ultraviolet (EUV) solar flux (see for instance[2]).

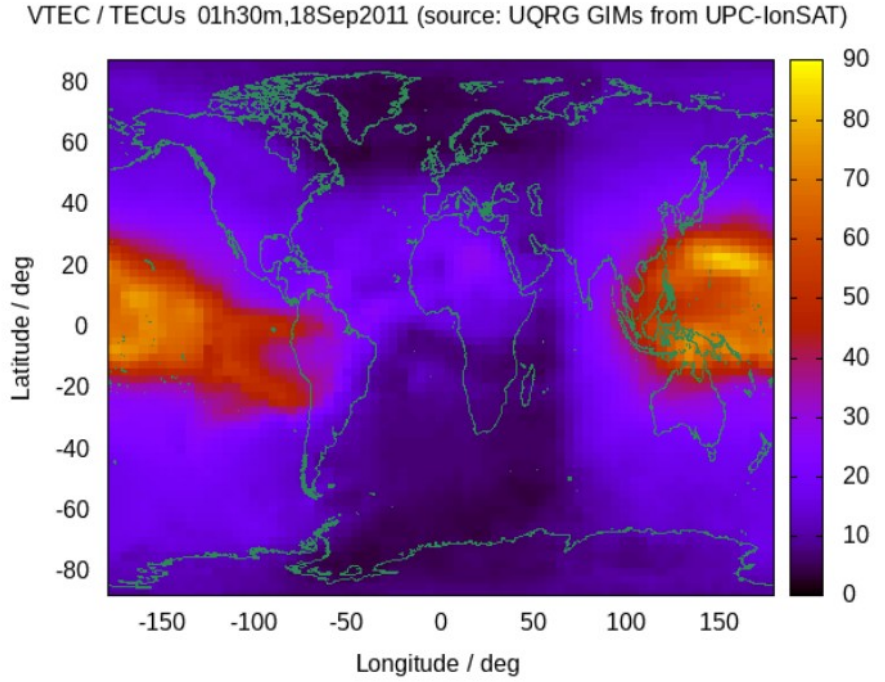


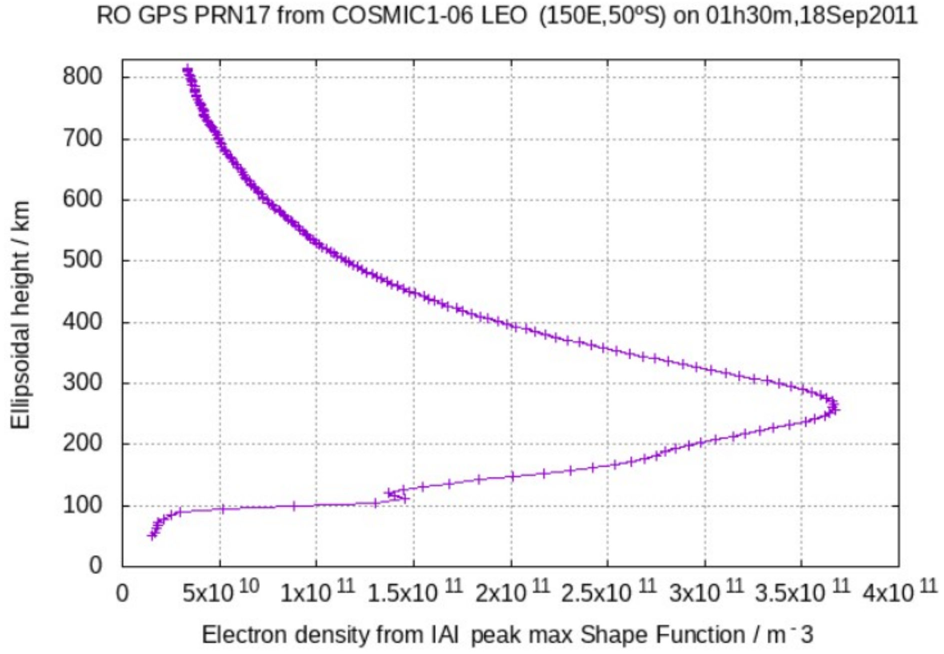


[2] Peter Teunissen and Oliver Montenbruck. *Springer handbook of global navigation satellite systems*. Springer, 2017, 1327, DOI: 10.1007/978–3–319–42928–1.

# Global Electron Content (GEC)

As consequence of its main origin, the total number of ionosphere free electrons (GEC) follows closely the solar activity, specially in normal (undisturbed) conditions: see the GEC time series obtained from the UQRG GIMs, computed every 15 minutes since end of 1996. The origin of features, like the semiannual and annual anomalies, are still under discussion ([3]).

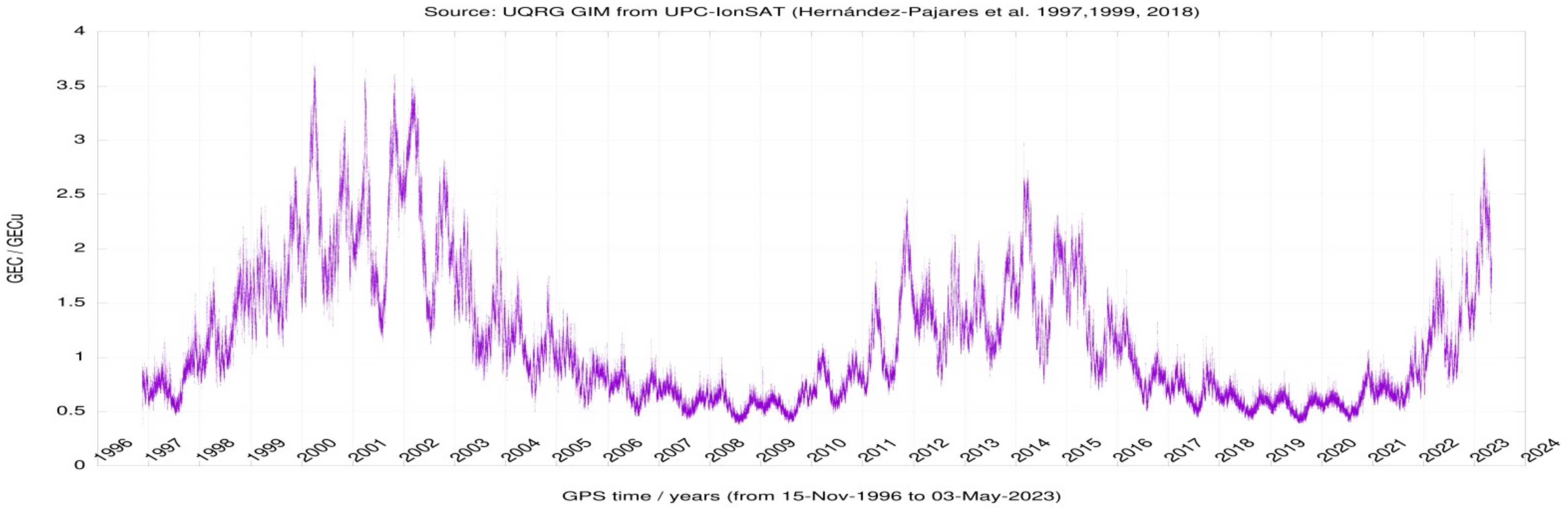


[3] Francisco Azpilicueta and Claudio Brunini. “A new concept regarding the cause of ionosphere semiannual and annual anomalies”. In: *Journal of Geophysical Research: Space Physics* 116.A1 (2011).

# GIMs with TOMION

multi-frequency carrier phases

positions of GNSS Receivers

positions of GNSS Transmitters

TOMION preprocessing (Cycle-slips, Line-Of-Sight), voxel-based Jacobian (for each given transmitter-receiver):

$$L_j - L_k = \alpha \sum_{m=1}^{n} (\mathbf{N_e})_\mathbf{m} \Delta s_m + \mathbf{B_{j,k}}$$

Solving $\{(\mathbf{N_e})_\mathbf{m}\}$ and $\{\mathbf{B_{j,k}}\}$ with Kalman filter in local time x latitude ref. frame

Slant & Vertical Total Electron Content values ($S$, $V$): $S = (L_j - L_k - \mathbf{B_{j,k}})/\alpha \Rightarrow V = S/M$

VTEC interpolation (Kriging / Atomic Decomposition in rapid / RT latencies)

Global Ionospheric Maps $\{\mathbf{V_m}, \sigma_\mathbf{m}\}$

Applications (ionospheric storm state, gradients, precise navigation,...)

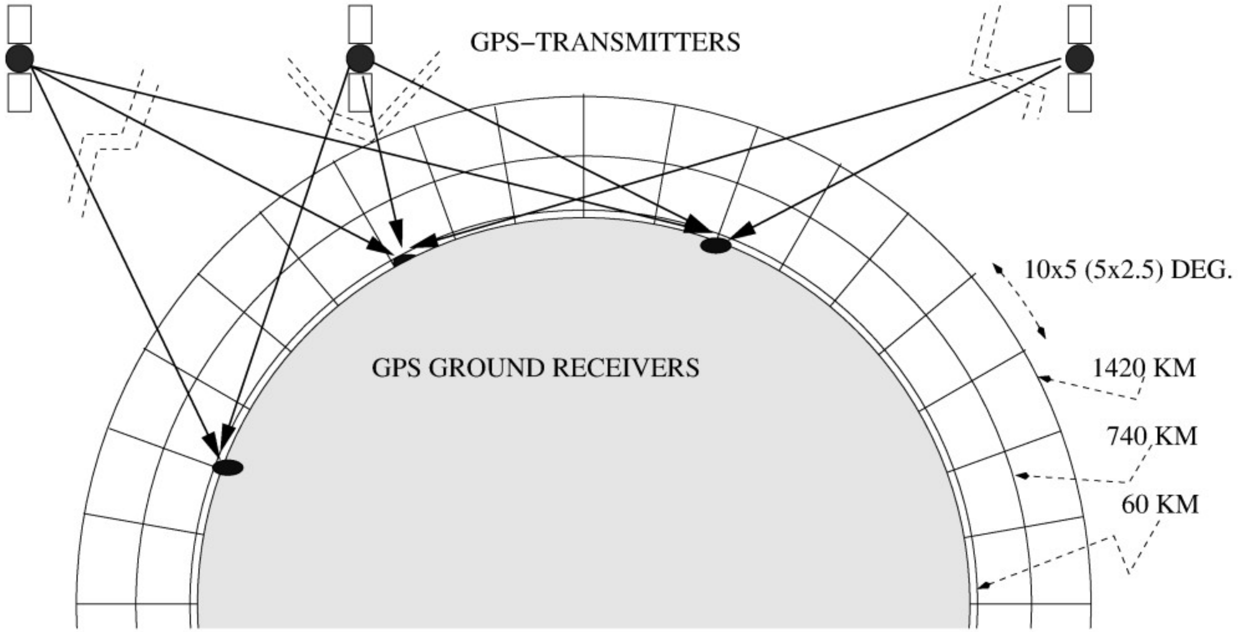

# Introduction to TOMION model (2 of 3)

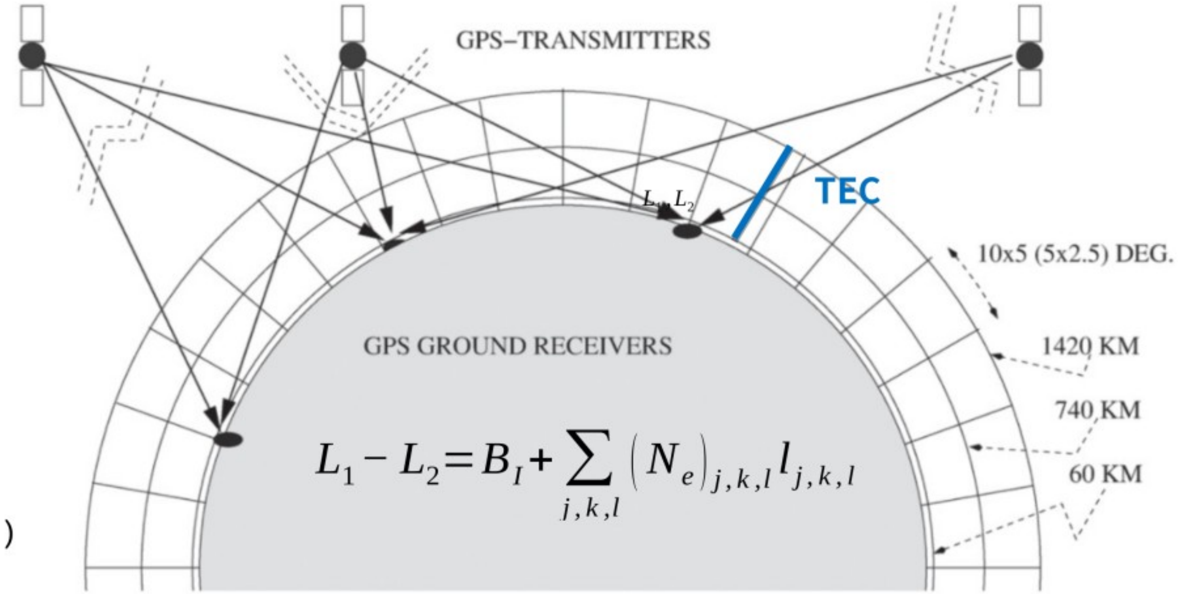


**UPC Quarter-of-an-hour time resolution Rapid GIM (UQRG)**

- It incorporates a Kalman filter and a kriging-based interpolation for the vertically integrated electron density (the vertical total electron content, VTEC, see[6],[7],[8]).

---

[6] M Hernandez-Pajares, JM Juan, and J Sanz. "Neural network modeling of the ionospheric electron content at global scale using GPS data". In: *Radio Science* 32.3 (1997), pp. 1081–1089.

[7] M Hernández-Pajares, JM Juan, and J Sanz. "New approaches in global ionospheric determination using ground GPS data". In: *Journal of Atmospheric and Solar-Terrestrial Physics* 61.16 (1999), pp. 1237–1247.

[8] R Orús et al. "Improvement of global ionospheric VTEC maps by using kriging interpolation technique". In: *Journal of Atmospheric and Solar-Terrestrial Physics* 67.16 (2005), pp. 1598–1609.

# Introduction to TOMION model (3 of 3)

- TOMION is the software used in the generation of UPC-IonSAT GIMs of VTEC for the International GNSS Service (IGS), such as the UQRG one, one of the best behaving GIMs in IGS ([9],[10],[11]).
- The tomography performed by TOMION is able to combine different data and geometries ([12]), in agreement with independent measurements and models ([13],[14]), also in the polar regions ([15]).

[9] M Hernández-Pajares et al. "The IGS VTEC maps: a reliable source of ionospheric information since 1998". In: *Journal of Geodesy* 83.3-4 (2009), pp. 263–275.

[10] Manuel Hernández-Pajares et al. "Methodology and consistency of slant and vertical assessments for ionospheric electron content models". In: *Journal of Geodesy* 91.doi:10.1007/s00190-017-1032-z (2017), pp. 1405–1414.

[11] David Roma-Dollase et al. "Consistency of seven different GNSS global ionospheric mapping techniques during one solar cycle". In: *Journal of Geodesy* 92.6 (2018), pp. 691–706.

[12] Manuel Hernández-Pajares et al. "A new way of improving global ionospheric maps by ionospheric tomography: consistent combination of multi-GNSS and multi-space geodetic dual-frequency measurements gathered from vessel-, LEO-and ground-based receivers". In: *Journal of Geodesy* 94.8 (2020), pp. 1–16.

[13] DV Kotov et al. "Coincident observations by the Kharkiv IS radar and ionosonde, DMSP and Arase (ERG) satellites, and FLIP model simulations: Implications for the NRLMSISE-00 hydrogen density, plasmasphere, and ionosphere". In: *Geophysical Research Letters* 45.16 (2018), pp. 8062–8071.

[14] DV Kotov et al. "Weak magnetic storms can modulate ionosphere-plasmasphere interaction significantly: Mechanisms and manifestations at mid-latitudes". In: *Journal of Geophysical Research: Space Physics* 124.11 (2019), pp. 9665–9675.

[15] Manuel Hernández-Pajares et al. "Polar Electron Content From GPS Data-Based Global Ionospheric Maps: Assessment, Case Studies, and Climatology". In: *Journal of Geophysical Research: Space Physics* 125.6 (2020), e2019JA027677.

https://esc.pithia.eu

PITHIA-NRF
e-Science Centre

HOME SEARCH & BROWSE

Home

# PITHIA-NRF e-Science Centre

## Search & Browse Metadata

Search Data Collections

Browse Data Collections

Browse Catalogues

Browse Metadata

## Space Physics Ontology

Space Physics Ontology

## Data Registration

UNIVERSITAT POLITÈCNI
DE CATALUNYA
BARCELONATECH

UPC

IonSAT

- EIS foF2 Forecasts Over Digisonde Stations
- EIS foF2 Long Term Prediction Maps
- EIS foF2 Nowcast Maps
- EIS hmF2 Nowcast Maps
- EIS Ionospheric Alerts
- EIS Near Real-Time TEC Maps
- EPB_detectionTool
- eSWua: Ionograms database, autoscaled records
- eSWua: Ionograms database, manually scaled records
- eSWua: Scintillation Indices and Total Electron Content (TEC) database
- EUHFORIA: EUropean Heliospheric FORecasting Information Asset
- GIM: Global Ionosphere Maps
- hmF2_qModel
- IAP-P Doppler sounder spectrograms
- IPIM : Ionosphere-Plasmasphere IRAP Model
- IRI: International Reference Ionosphere version 2001
- IRTAM 3D global real-time assimilative model of ionospheric electron density
- NOA Athens Digisonde (AT138) Data
- RayTRIX-CQP: Oblique ionogram synthesizer with E, F1, F2 layer echo traces and MUFs, driven by IRTAM ionospheric nowcast
- ROB-IONO Near-Real Time European Ionospheric Maps
- SWIF Model
- TechTIDE LSTID activity index

# GIM: Global Ionosphere Maps

Global Vertical Total Electron Content 2D map computed using UPC Rapid Network of GPS receivers

## Interact

| Interaction Method | Description | Data Format | Link |
|---|---|---|---|
| Direct Link to Data Collection | The GIM landing page has the list of data the 15-minutes maps. | text/html (click the link to show information on this ontology term) | Open GIM Landing Page in new tab |

## Properties

| Property | Value |
|---|---|
| Type (1/2) | Receiver of GNSS signals (click the link to show information on this ontology term) |
| Type (2/2) | Assimilative Model (click the link to show information on this ontology term) |
| Project | GIM: Global Ionospheric Maps (click the link to show information on this metadata registration) |
| Data Level | Level 3 (click the link to show information on this ontology term) |
| Result | *Not used* |
| Permission | Creative Commons Attribution-NonCommercial-ShareAlike (click the link to show information on this ontology term) |

### Identifier Properties

| | |
|---|---|
| **Local ID** | DataCollection_UPC-RapidNetwork_GIM |
| **Namespace** | pithia |
| **Version** | 1 |
| **Created** | Tuesday 20th Dec. 2022, 09:30:00 |
| **Last Modified** | Tuesday 20th Dec. 2022, 09:30:00 |

| | |
|---|---|
| **Role** *(from Related Party* ***(1/2)*** *> Responsible Party Info)* | Point of contact (click the link to show information on this ontology term) |
| **Party** *(from Related Party* ***(1/2)*** *> Responsible Party Info)* | Manuel Hernandez-Pajares (click the link to show information on this metadata registration) |
| **Role** *(from Related Party* ***(2/2)*** *> Responsible Party Info)* | Data Provider (click the link to show information on this ontology term) |
| **Party** *(from Related Party* ***(2/2)*** *> Responsible Party Info)* | UPC-IonSAT (click the link to show information on this metadata registration) |
| **Result Time** | *Not used* |
| **Name** *(from Collection Results > Source > Online Resource)* | GIM Landing Page |
| **URL** *(from Collection Results > Source > Online Resource > Linkage)* | http://cabrera.upc.es/upc_ionex_GPSonly-RINEXv3 |
| **Protocol** *(from Collection Results > Source > Online Resource)* | HTTP |
| **Data Format** *(from Collection Results > Source > Online Resource)* | text/html (click the link to show information on this ontology term) |
| **Description** *(from Collection Results > Source > Online Resource)* | The GIM landing page has the list of the 15-minutes ionex files. |

HORIZON 2020
The EU Framework Programme for Research and Innovation

UNIVERSITAT POLITÈCNIC DE CATALUNYA
BARCELONATECH

# Index of /upc_ionex_GPSonly-RINEXv3

| Name | Last modified | Size | Description |
|---|---|---|---|
| Parent Directory | | - | |
| 1996/ | 2022-10-09 15:56 | - | |
| 1997/ | 2020-04-08 10:56 | - | |
| 1998/ | 2020-04-08 10:56 | - | |
| 1999/ | 2020-04-08 10:56 | - | |
| 2000/ | 2020-04-08 10:56 | - | |
| 2001/ | 2020-04-08 10:56 | - | |
| 2002/ | 2022-10-09 16:23 | - | |
| 2003/ | 2020-04-08 10:56 | - | |
| 2004/ | 2020-04-08 10:56 | - | |
| 2005/ | 2020-04-08 10:56 | - | |
| 2006/ | 2022-10-09 16:22 | - | |
| 2007/ | 2020-04-08 10:56 | - | |
| 2008/ | 2020-04-08 10:56 | - | |
| 2009/ | 2020-04-08 10:56 | - | |
| 2010/ | 2020-04-08 10:56 | - | |
| 201 | 2020-04-08 10:56 | - | |
| 2012/ | 2020-04-08 10:56 | - | |
| 2013/ | 2020-04-08 10:56 | - | |
| 2014/ | 2020-04-08 10:56 | - | |
| 2015/ | 2020-04-08 10:56 | - | |
| 2016/ | 2020-04-08 10:56 | - | |

UNIVERSITAT POLITÈCNICA DE CATALUNYA
BARCELONATECH

HORIZON 2020
The EU Framework Programme for Research and Innovation

PITHIA-NRF Research Infrastructure

IonSAT

# Index of /upc_ionex_GPSonly-RINEXv3/2010

| Name | Last modified | Size | Description |
|---|---|---|---|
| Parent Directory | | - | |
| 001_100101.15min/ | 2020-04-08 10:56 | - | |
| 002_100102.15min/ | 2020-04-08 10:56 | - | |
| 003_100103.15min/ | 2020-04-08 10:56 | - | |
| 004_100104.15min/ | 2020-04-08 10:56 | - | |
| 005_100105.15min/ | 2020-04-08 10:56 | - | |
| 006_100106.15min/ | 2020-04-08 10:56 | - | |
| 007_100107.15min/ | 2020-04-08 10:56 | - | |
| 008_100108.15min/ | 2020-04-08 10:56 | - | |
| 009_100109.15min/ | 2020-04-08 10:56 | - | |
| 010_100110.15min/ | 2020-04-08 10:56 | - | |
| 011_100111.15min/ | 2020-04-08 10:56 | - | |
| 012_100112.15min/ | 2020-04-08 10:56 | - | |
| 013_100113.15min/ | 2020-04-08 10:56 | - | |
| 014_100114.15min/ | 2020-04-08 10:56 | - | |
| 015_100115.15min/ | 2020-04-08 10:56 | - | |
| 016_100116.15min/ | 2020-04-08 10:56 | - | |
| 017_100117.15min/ | 2020-04-08 10:56 | - | |
| 018_100118.15min/ | 2020-04-08 10:56 | - | |
| 019_100119.15min/ | 2020-04-08 10:56 | - | |
| 020_100120.15min/ | 2020-04-08 10:56 | - | |
| 021_100121.15min/ | 2020-04-08 10:56 | - | |

Format: $DOY_$YY$MM$DD.15min

Day of Year · Year · Month · Day · Resolution

# Index of /upc_ionex_GPSonly-RINEXv3/2010/015_100115.15min

| Name | Last modified | Size | Description |
|---|---|---|---|
| Parent Directory | | - | |
| uqrg0150.10i.Z | 2018-11-09 19:12 | 919K | |

$$\text{Format (IGS): } \underbrace{\text{uqrg}}_{\text{Center}}\underbrace{\text{\$DOY}}_{\text{Day of Year}}\text{0.}\underbrace{\text{\$YY}}_{\text{Year}}\overset{\text{IONEX}}{\text{i}}\text{.}\underset{\text{Compressed}}{\text{Z}}$$

# Index of /upc_ionex_GPSonly-RINEXv3/2010/015_100115.15min

| Name | Last modified | Size | Description |
|---|---|---|---|
| Parent Directory | | - | |
| uqrg0150.10i.Z | 2018-11-09 19:12 | 919K | |

*Apache/2.4.29 (Ubuntu) Server at cabrera.upc.es Port 80*

Do you want to allow downloads on "cabrera.upc.es"?

You can change which websites can download files in Websites Preferences.

Cancel Al

UNIVERSITAT
DE CATALUNYA
BARCELONATECH

Terminal — more ◂ sh - /usr/bin/zmore

```
     1.0           IONOSPHERE MAPS     GPS                 IONEX VERSION / TYPE
tecrms2ionex_4.awk UPC-IonSAT          11/09/18 1711UT     PGM / RUN BY / DATE
Global ionosphere maps for day  15, 2010 (15- 1-2010)      DESCRIPTION
Contact address: Manuel Hernandez-Pajares                  DESCRIPTION
                 IonSAT research group                     DESCRIPTION
                 Technical Univ. of Catalonia (UPC-IonSAT) DESCRIPTION
                 Mod. C3 Campus Nord UPC                   DESCRIPTION
                 E08034-Barcelona, SPAIN                   DESCRIPTION
                 e-mail:  manuel@ma4.upc.edu               DESCRIPTION
                                                           DESCRIPTION
                                                           DESCRIPTION
P1-P2 DCBs(UPC3-BRDC)  15 2010: Bias=  0.000 RMS= 0.855 [ns]DESCRIPTION
                                                           DESCRIPTION
  2010     1    15     0     0     0                       EPOCH OF FIRST MAP
  2010     1    15    23    59    24                       EPOCH OF LAST MAP
   900                                                     INTERVAL
    97                                                     # OF MAPS IN FILE
  COSZ                                                     MAPPING FUNCTION
     0.0                                                   ELEVATION CUTOFF
   300                                                     # OF STATIONS
    32                                                     # OF SATELLITES
  6371.0                                                   BASE RADIUS
     2                                                     MAP DIMENSION
   450.0 450.0   0.0                                       HGT1 / HGT2 / DHGT
    87.5 -87.5  -2.5                                       LAT1 / LAT2 / DLAT
  -180.0 180.0   5.0                                       LON1 / LON2 / DLON
    -1                                                     EXPONENT
TEC values in  0.1 TECUs; 9999 if no value available       COMMENT
IGS GPS stations used in the computations:                 COMMENT
019b ab02 ab07 ab08 ab11 ab14 ab25 ab27 ab37 ab39 ab41 ab43 COMMENT
ab44 abmf abpo ac03 ac12 ac60 ac61 acor acso acu5 ade1 adks COMMENT
agmt ahid aira ajac alac alam albh algo alic allg alon alrt COMMENT
amc2 ankr antc areq arli artu asky aspa auck autf baie bake COMMENT
bako bamo ban2 barh bcyi bdos bell bjfs bla1 blmm bluf boav COMMENT
bogt bomj brft brib brip brmu brst brus bshm bsmk bucu bue1 COMMENT
buri bysp cabl cagl call cand cant cas1 casc ccj2 cedu cefe COMMENT
cfag chan chat chiz chme chum chur cjtr ckis clrk cmbl cnmr COMMENT
coco cont copo cosa coyq crao crar cuib cusv daej dane darw COMMENT
dav1 devi dgar dgjg dksg drao dres dum1 dupt ecsd edoc eur2 COMMENT
faa1 falk fall flin flrs func g101 g107 g117 g124 g201 g202 COMMENT
ganp gisb glps glsv gmas gmma guat harb hdil helg her2 hil1 COMMENT
hilb hlfx hmbg hnlc hob2 hobu hofn holm howe hrst hueg hugo COMMENT
hvlk hvwy hyde ifr1 impz ineg invk iqal iqqe irkj isba ispa COMMENT
ista jct1 joen karr kerg khaj khar kir0 kiri kit3 kouc kour COMMENT
ksnb kuaq kunm kuuj kvtx lafe lamt laut lhaz lpal lthw mac1 COMMENT
```

PITHIA-NRF Research Infrastructure

The EU Framework Programme for Research and Innovation
HORIZON 2020

UNIVERSITAT POLITÈCNICA DE CATALUNYA
BARCELONATECH

IonSAT

| | | |
|---|---|---|
| 2014/ | 2020-04-08 10:56 | - |
| 2015/ | 2020-04-08 10:56 | - |
| 2016/ | 2020-04-08 10:56 | - |
| 2017/ | 2020-04-08 10:56 | - |
| 2018/ | 2023-09-04 16:57 | - |
| 2019/ | 2023-09-04 16:59 | - |
| 2020/ | 2023-09-04 17:05 | - |
| 2021/ | 2023-09-04 17:08 | - |
| 2022/ | 2023-01-01 20:40 | - |
| 2023/ | 2023-09-05 06:14 | - |
| tmp/ | 2023-03-05 21:19 | - |
| uqrg.latest.Z | 2023-09-05 05:00 | 1.1M |
| uqrg.latest.rms.gif | 2023-09-05 07:45 | 4.5M |
| uqrg.latest.tec.gif | 2023-09-05 07:45 | 4.8M |

# THANK YOU!

# Set of backup slides #2

# Ionospheric scales derived from UPC-IonSAT Global Ionospheric Maps

## 3rd URSI Atlantic / Asia-Pacific Radio Science Meeting
## 29 May - 3 June 2022

by

**Qi Liu(1), Manuel Hernandez Pajares(1,2), Haixia Lyu(3,1) , Heng Yang(4,1), Enric Monte-Moreno(5), Alberto García-Rigo(2,1), Germán Olivares-Pulido(1) , Raül Orús-Pérez(6)**

(1) UPC-IonSAT, Barcelona, Spain; (2) IEEC, Barcelona, Spain; (3) GNSS Research Center, Wuhan University, China; (4) Yangtze Normal University, Chongqing, China; (5) UPC-TALP, Barcelona, Spain; (6) ESA ESTEC, Noordwijk, the Netherlands.

contact e-mails: manuel.hernandez@upc.edu, q.liu@upc.edu

UNIVERSITAT POLITÈCNICA DE CATALUNYA BARCELONATECH

IonSAT

# 0. Motivation

In this work we summarize the approach, results and answer to the question that we did ourselves almost two years ago:

**Can the high temporal resolution VTEC Global Ionospheric Maps** (GIM, such as UQRG generated by UPC-IonSAT since end 1996) directly provide **reliable estimation** of the spatial and temporal components of the **VTEC gradients**, and of a sensitive **Ionospheric storm scale index**, with **comparable results** to the corresponding indices proposed and generated by other colleagues from **raw GNSS data** (respectively Jakowski & Hoque 2019, and Nishioka et al. 2017)?

*Jakowski, N., & Hoque, M. M. (2019). Estimation of spatial gradients and temporal variations of the total electron content using ground-based GNSS measurements. Space Weather, 17, 339–356. https://doi.org/10.1029/2018SW002119.*

*Nishioka, M., T. Tsugawa, H. Jin, and M. Ishii (2017), A new ionospheric storm scale based on TEC and f o F 2 statistics, Space Weather, 15, 228–239, doi:10.1002/2016SW001536.*

# 1. Context: GNSS-based UQRG Global Ionospheric Map (GIM)

LOS Carrier phases in length units: **L1-L2** (measurement, corrected from wind-up)

Associated L1-L2 ambiguity, **BI** (unknown)

Electron density of LOS illuminated voxels: **Ne** (unknowns)

Straight line LOS length within given voxel: **l_{j,k,l}**

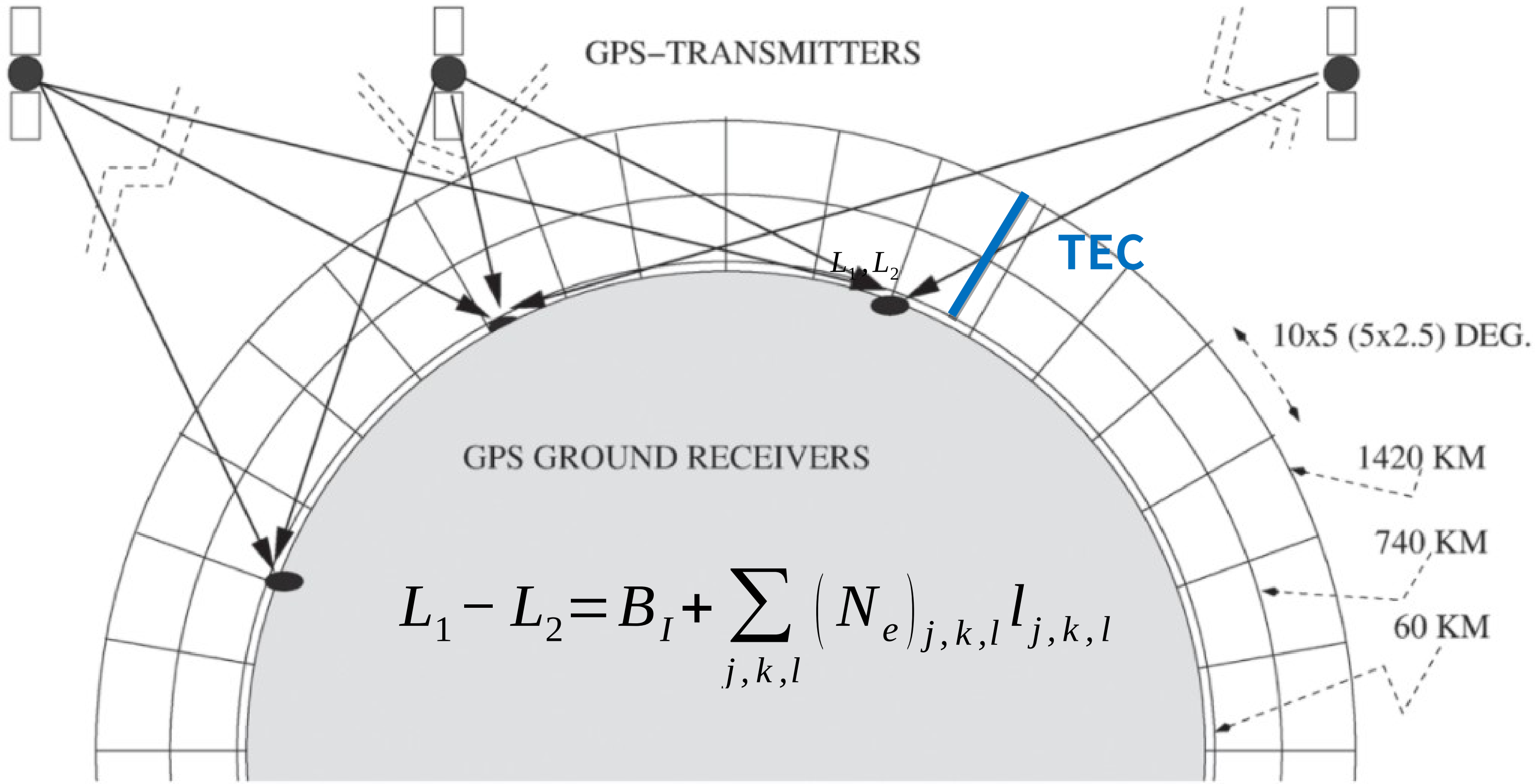


$$L_1 - L_2 = B_I + \sum_{j,k,l} \left(N_e\right)_{j,k,l} l_{j,k,l}$$

**UPC Quarter-of-an-hour time resolution Rapid GIM (UQRG)**

**Two-Layer voxel tomographic** estimation **without ionospheric background model** and with **dual-frequency carrier phase input data only**. with in-house TOMION software.

Kriging **interpolation** which **preserves the details**

**Resolution: 15min x 5º x 2.5º in time x lon.xlat**

UNIVERSITAT POLITÈCNICA DE CATALUNYA BARCELONATECH

# 1. Context: TOMION software

- TOMION is a data driven ionospheric model originally developed by the second authors of this presentation during the latest 25 years
- It allows a tomographic estimation of the density of free ionospheric electrons from GNSS carrier phase dual-frequency data only, without any background model.
- It incorporates a Kalman filter and a kriging-based interpolation for the vertically integrated electron density (the vertical total electron content, VTEC, see Hernández-Pajares et al. 1997, 1999, Orús et al. 2005).
- TOMION is the software used in the generation of UPC-IonSAT global ionospheric maps (GIMs) of VTEC for the International GNSS Service (IGS), such as the UQRG one, one of the outperforming GIMs, or even the best behaving GIM in IGS (Hernández-Pajares et al. 2009,2017, Roma-Dollase et al. 2018).
- UQRG GIM produced by TOMION is, for instance, able to detect realistic features of the polar ionosphere as well (Hernández-Pajares et al. 2020a) and to provide a realistic and sensitive storm index (Qi et al. 2021).
- The tomography performed by TOMION is able to ingest different geometries and types of input measurements (Hernández-Pajares et al. 2020b), in agreement with independent measurements and models (Kotov et al. 2018, 2019).

# 2. Defining the components of VTEC gradient from the GIM

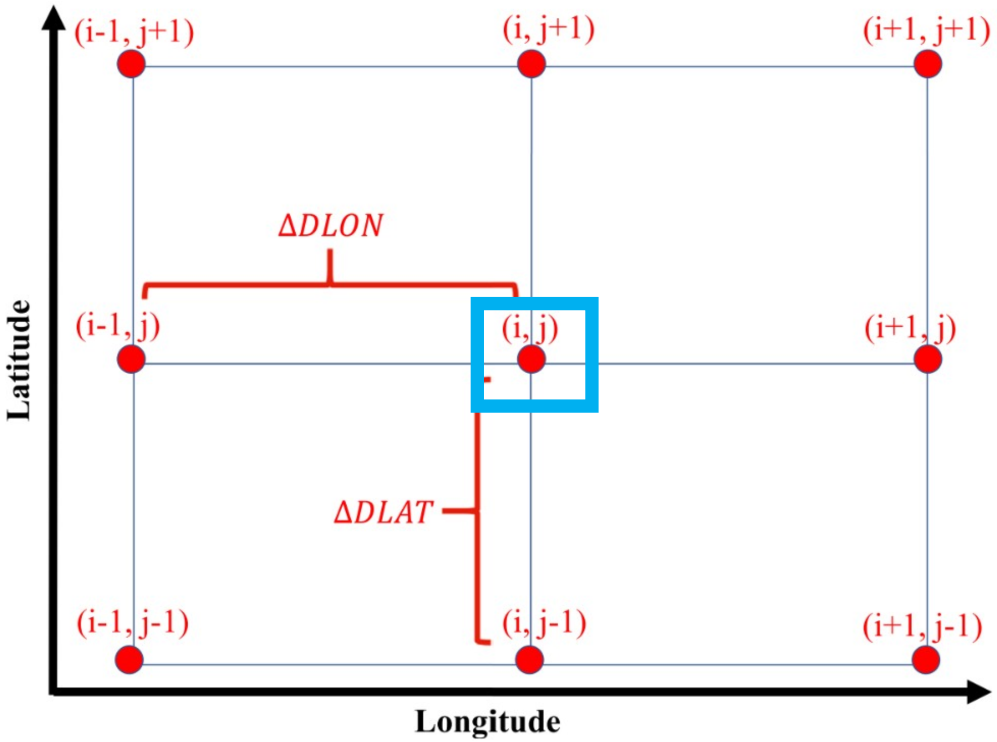


The **spatial and temporal components of VTEC gradient at grid points of** UQRG **GIM** on a global scale are introduced.

The VTEC gradient derived from UQRG GIMs (VgUG, Liu et al. 2022), **allows** to obtain full (non-relative) values of TEC spatial gradients and temporal variations **separately at any worldwide grid point**, considering the distances on the corresponding parallels and meridians at the ionospheric efective height, ΔDLON & ΔDLAT, separated 5º & 2.5º respectively, and the time difference between GIMs Δt (30 minutes, centered, 15 minutes, uncentered).

$$\begin{cases} \nabla V_{x,i,j} = (VTEC_{i,j} - VTEC_{i-1,j})/\Delta DLON \\ \nabla V_{y,i,j} = (VTEC_{i,j} - VTEC_{i,j-1})/\Delta DLAT \\ \nabla V_{i,j} = \sqrt{\nabla V^2_{x,i,j} + \nabla V^2_{y,i,j}} \\ \nabla\vec{V} = (\nabla V_{x,i,j}, \nabla V_{y,i,j}) \end{cases}$$

$$\dot{V}_{i,j} = \Delta VTEC_{i,j}/\Delta t = (VTEC_{i,j,t} - VTEC_{i,j,t-1})/\Delta t$$

# 2.1 Example of global distribution of VTEC spatial gradient

Compared with the quiet ionospheric state, the VTEC spatial and temporal gradient directly derived from the GIM are able to capture the extraordinary VTEC variations during the disturbed ionospheric state, splitted in north, east and time components.

St. Patrick's Day 2015 Geomagnetic Storm

Quiet

St. Patrick's day storm

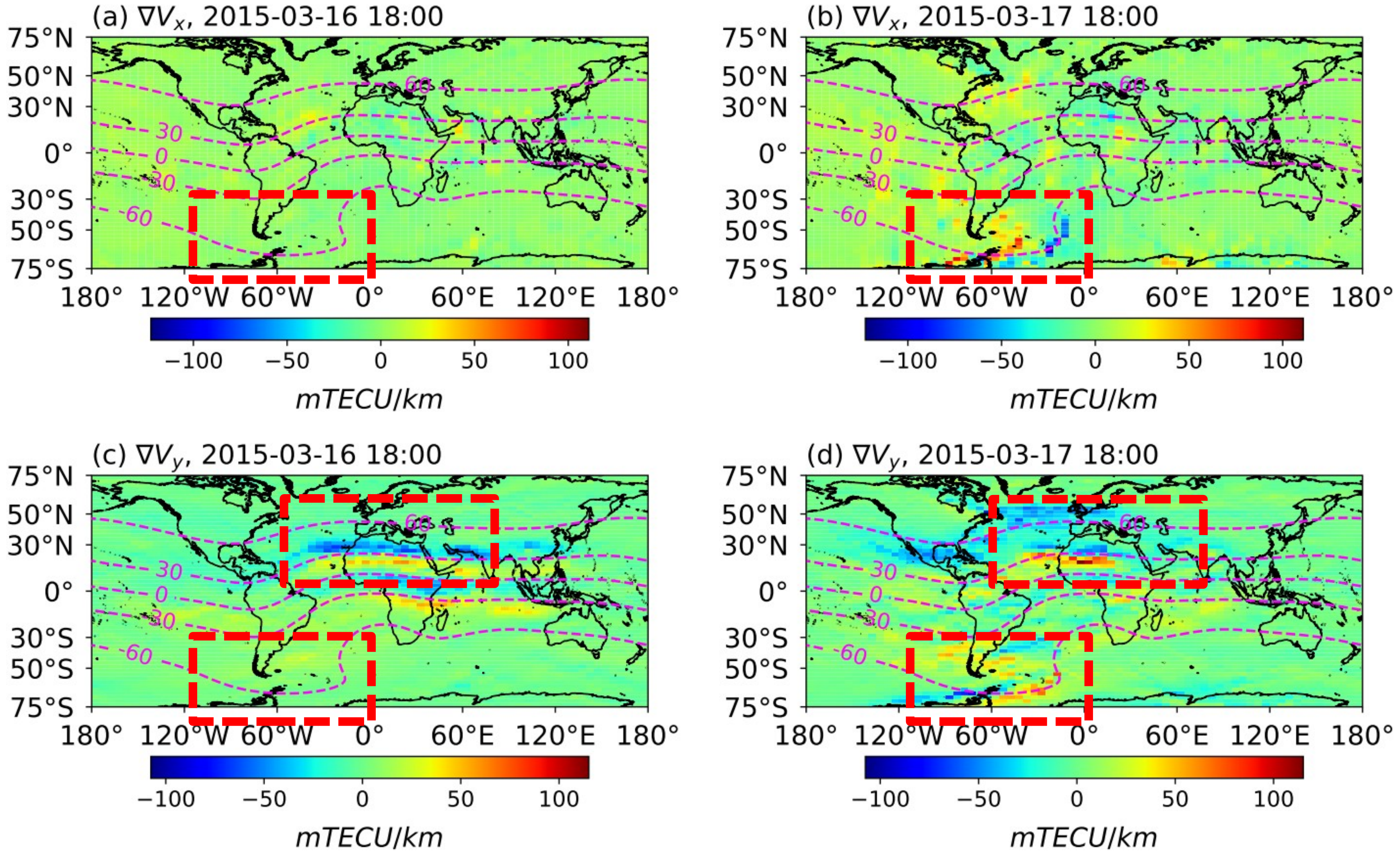


UNIVERSITAT POLITÈCNICA DE CATALUNYA
BARCELONATECH

# 3. Definition of regional indices from the VTEC gradient

Indeed the **Regional VTEC spatial Gradient indices**, based on UQRG (***RVGU***) and the temporal one, the **Regional Ionospheric Disturbance index** based on UQRG (***RIDU***), are proposed to estimate the regional ionospheric perturbation degree over selected regions. And they allow us **to compare them with similar indices computed previously and independently with different approaches** by other research groups.

$$\begin{cases} \overline{\nabla V_x} = \sum_{i=1}^{N} \sum_{j=1}^{M} \nabla V_{x,i,j} / N_S \\ \nabla V_{x,P_{95+}} = P_{95}(\nabla V_{x,i,j,p}) \\ \nabla V_{x,P_{95-}} = -P_{95}(|\nabla V_{x,i,j,n}|) \\ \overline{\nabla V_y} = \sum_{i=1}^{N} \sum_{j=1}^{M} \nabla V_{y,i,j} / N_S \\ \nabla V_{y,P_{95+}} = P_{95}(\nabla V_{y,i,j,p}) \\ \nabla V_{y,P_{95-}} = -P_{95}(|\nabla V_{y,i,j,n}|) \end{cases}$$

$$\begin{cases} \overline{\nabla V} = \sum_{i=1}^{N} \sum_{j=1}^{M} \nabla V_{i,j} / N_S \\ \sigma_{\nabla V} = \sqrt{\left( \sum_{i=1}^{N} \sum_{j=1}^{M} \nabla {V_{i,j}}^2 \right) / N_S - \overline{\nabla V}^2} \\ \nabla V_{P_{95}} = P_{95}(\nabla V_{i,j}) \end{cases}$$

$$RIDU = \sum_{i=1}^{n} \sum_{j=1}^{m} \dot{V}_{i,j} / N_S$$

# 3.1 Example of comparison of GIM- vs raw-GNSS data- based regional **spatial** indices over Europe: **Quiet conditions** (20-25 May 2015)

From **UQRG GIM (VgUG)**
(Liu et al. 2022)

From **raw GNSS data**
**(**Jakowski & Hoque (2017)

**Spatial gradient norm**

**Latitudinal gradient component**

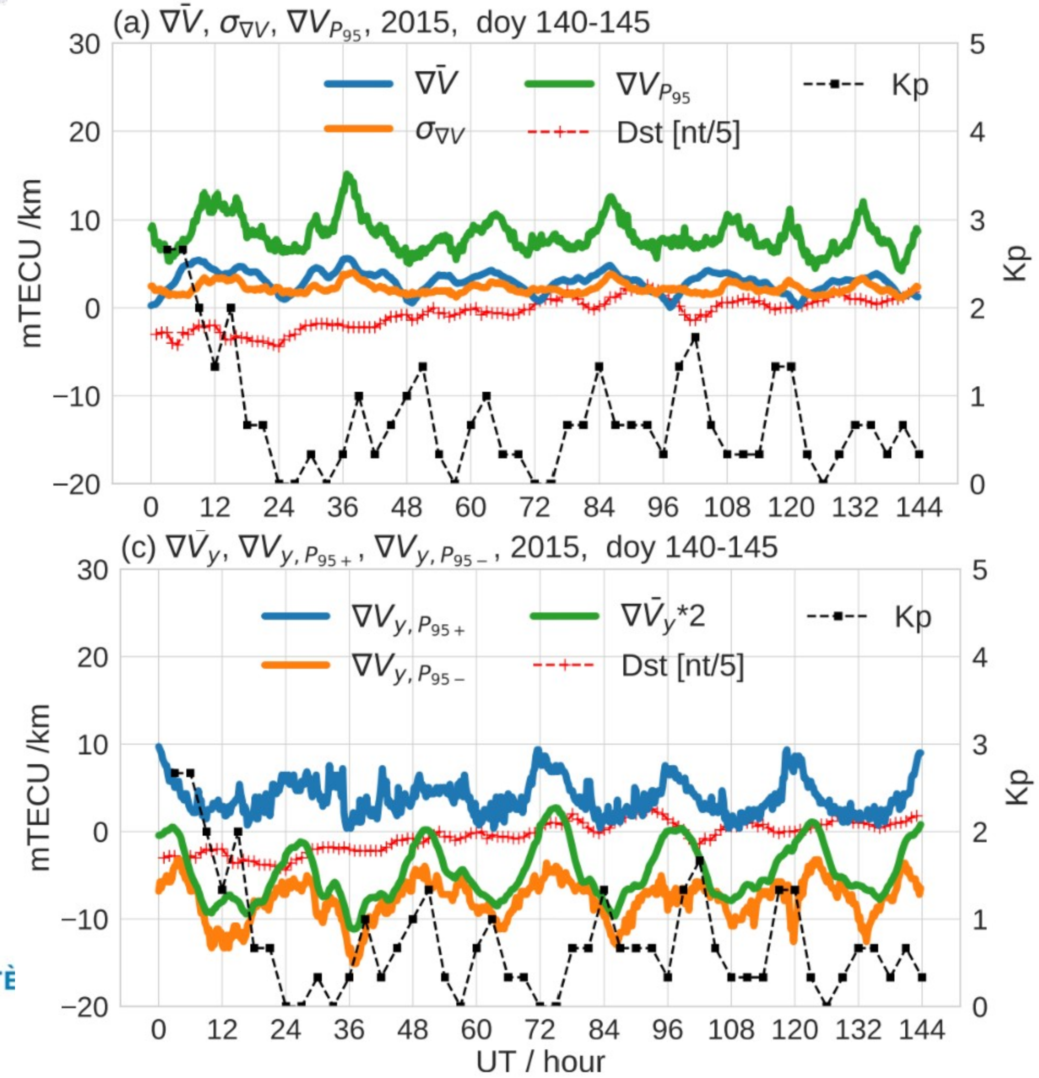


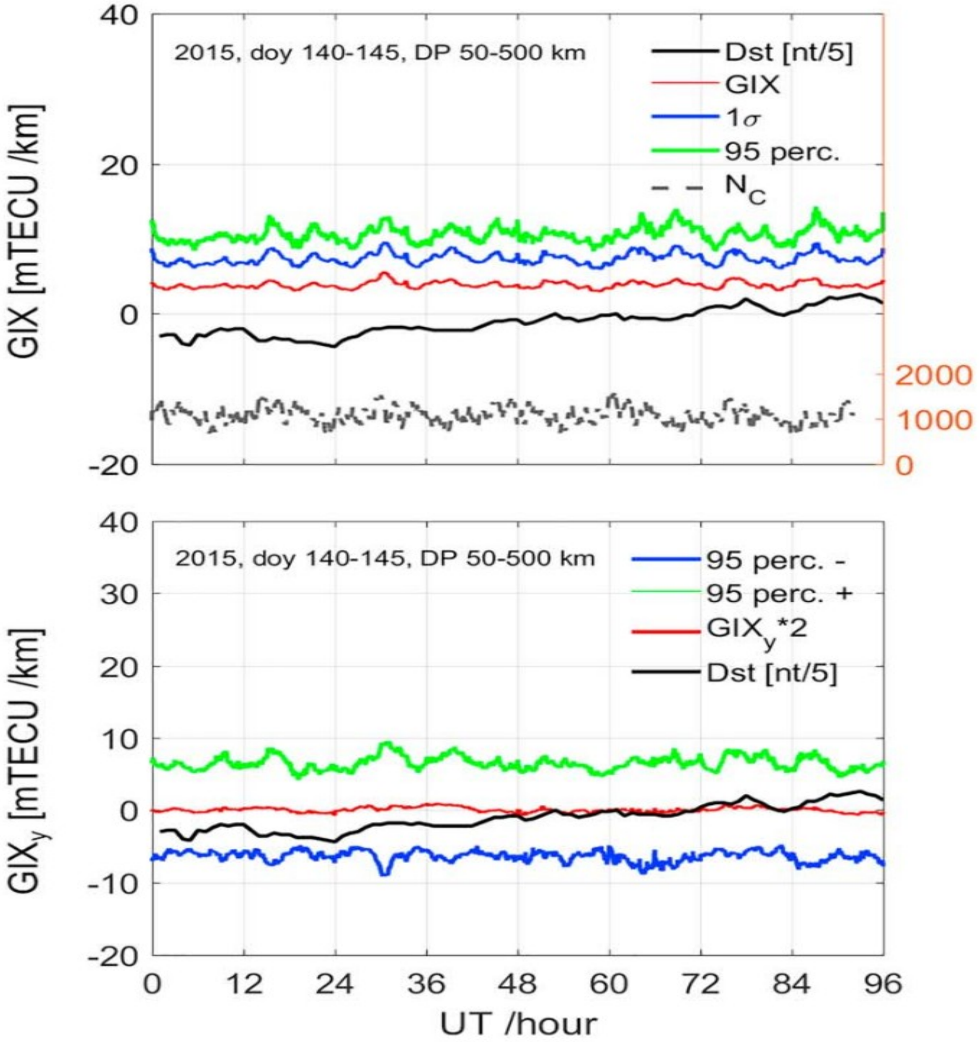


UNIVERSITAT POLITÈCNICA DE CATALUNYA
BARCELONATECH

# 3.1 Example of comparison of GIM- vs raw-GNSS data- based regional **spatial** indices over Europe: **Quiet conditions** (20-25 May 2015) -Continued-

From **UQRG GIM (VgUG)** (Liu et al. 2022)

From **raw GNSS data** (Jakowski & Hoque (2017)

**Longitudinal gradient component**

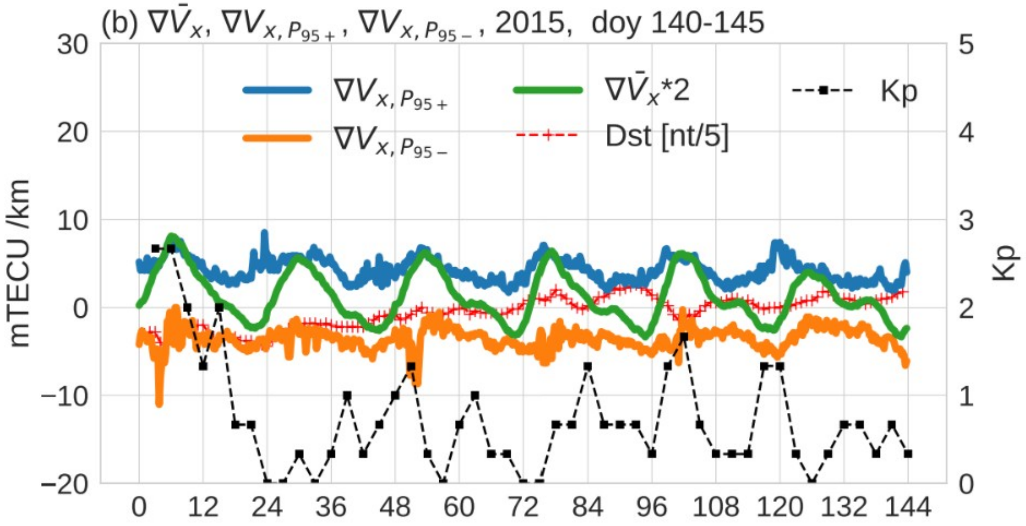


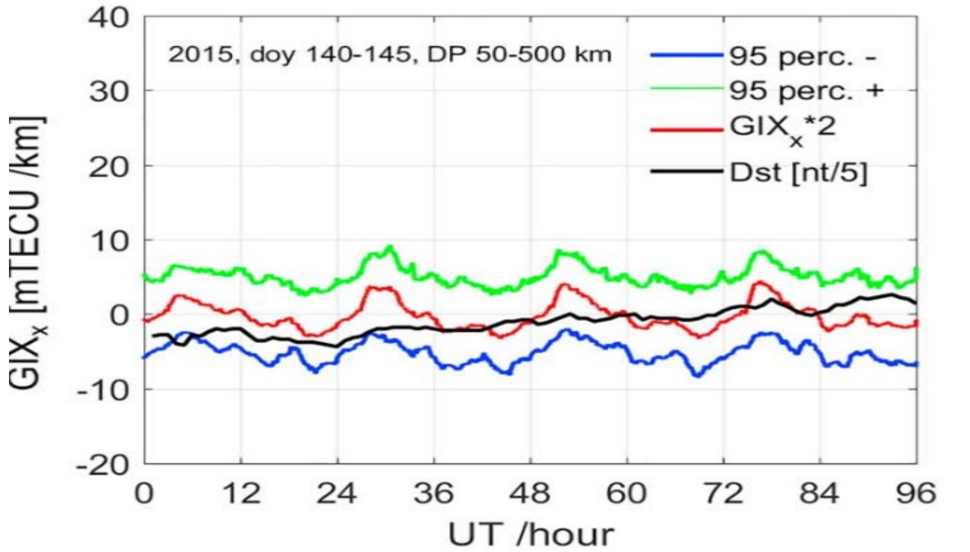


**Input receivers / IPPs used in the region**

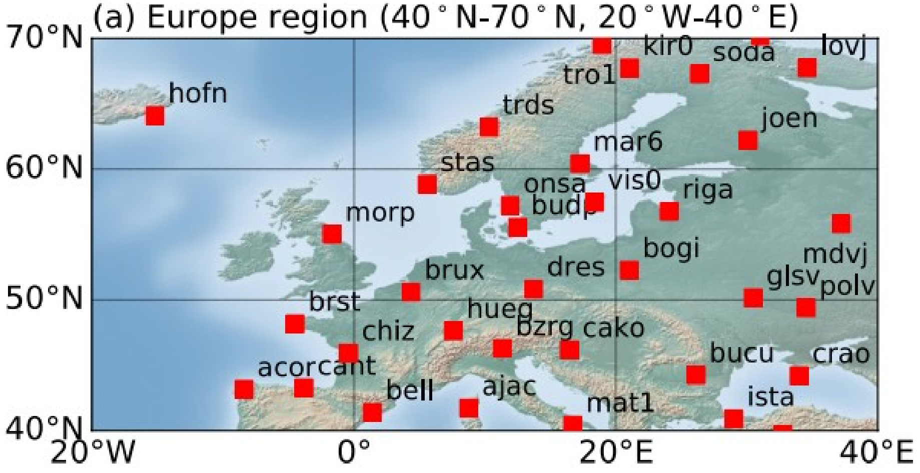


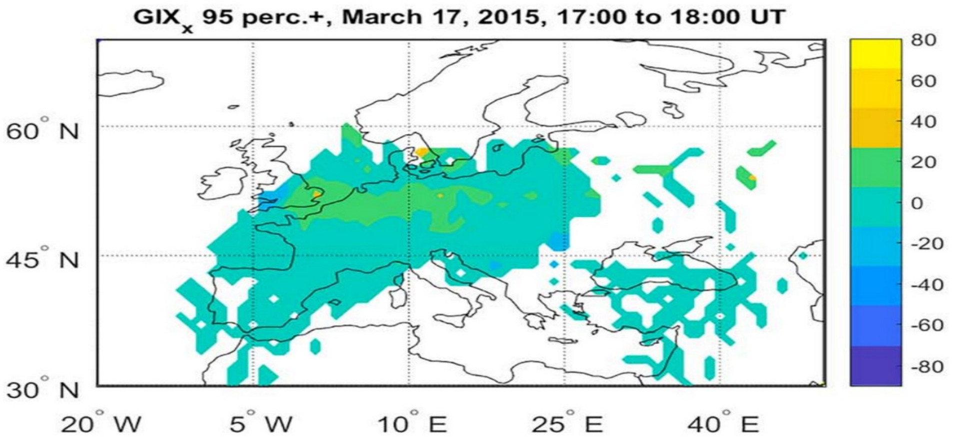


UNIVERSITAT POLITÈCNICA DE CATALUNYA
BARCELONATECH

# 3.2 Example of comparison of GIM- vs raw-GNSS data- based regional **spatial** indices over Europe: **St. Patrick**s Day iono. **storm** (16-20 March 2015)

From **UQRG GIM (VgUG)**
(Liu et al. 2022)

From **raw GNSS data**
**(**Jakowski & Hoque (2017)

**Spatial gradient norm**

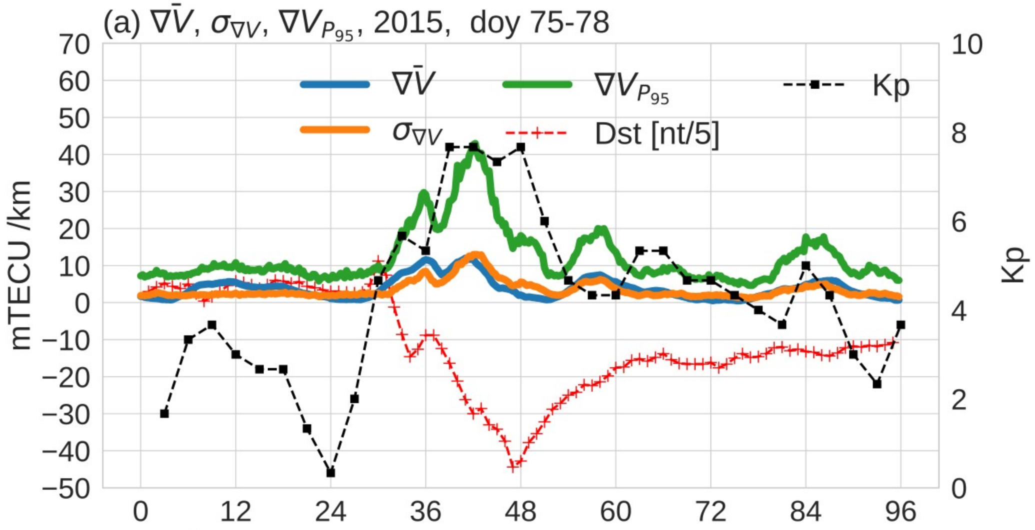


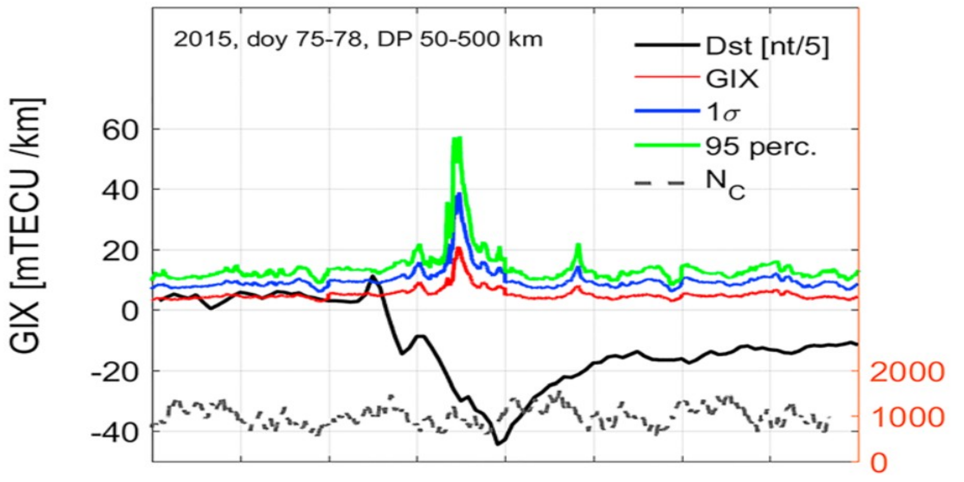


**Latitudinal gradient component**

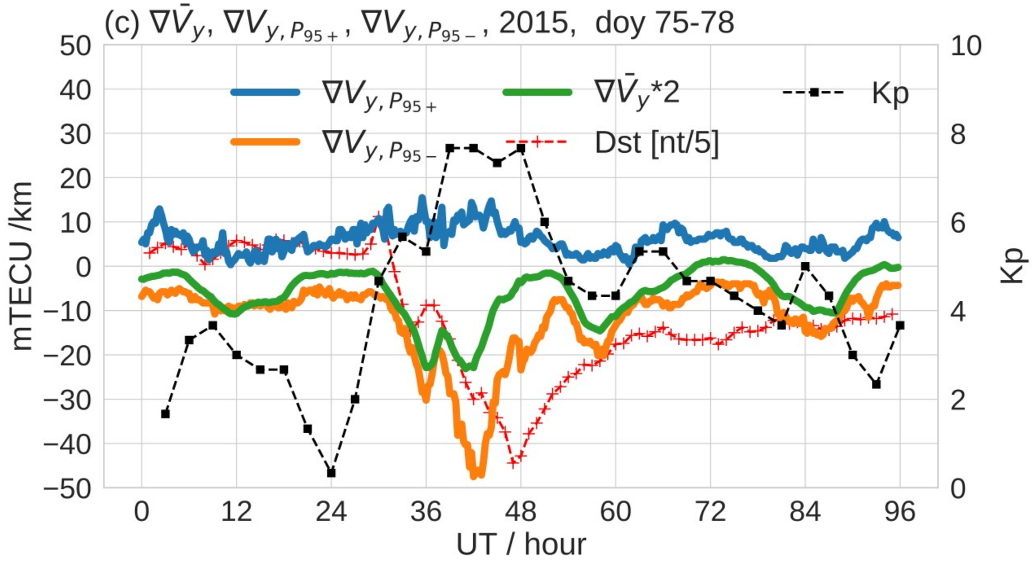


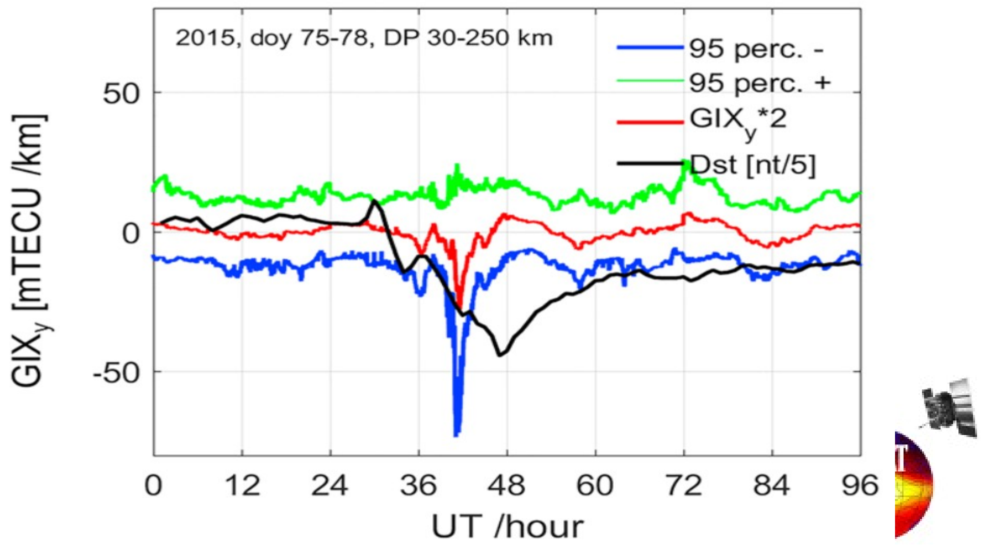


UNIVERSITAT POLITÈCNICA DE CATALUNYA
BARCELONATECH

# 3.2 Example of comparison of GIM- vs raw-GNSS data- based regional **spatial** indices over Europe: **St. Patrick**s Day ionospheric **storm** (16-20 March 2015) -Continued-

From **UQRG GIM (VgUG)**
(Liu et al. 2022)

From **raw GNSS data**
**(**Jakowski & Hoque (2017)

**Longitudinal gradient component**

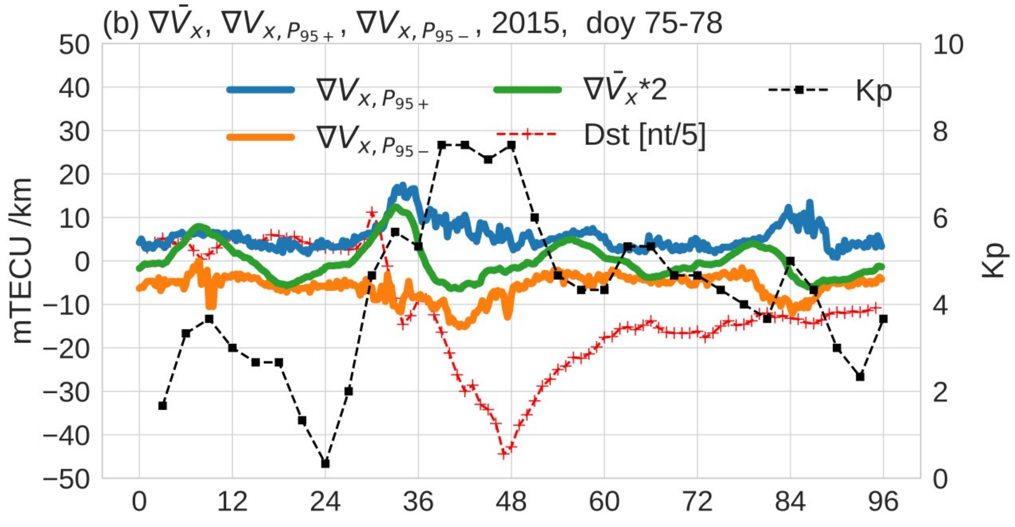


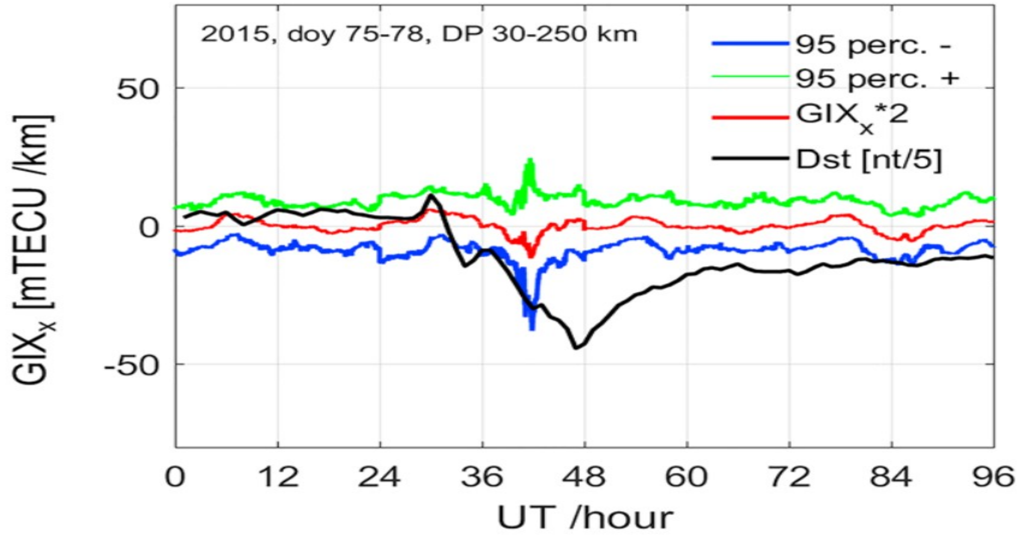

# 3.3 Example of comparison of GIM- vs raw-GNSS data- based regional **spatial** indices over Europe: **Halloween storm** (28 Oct -1 Nov 2003)

From **UQRG GIM (VgUG)**
(Liu et al. 2022)

From **raw GNSS data**
**(**Jakowski & Hoque (2017)

**Spatial gradient norm**

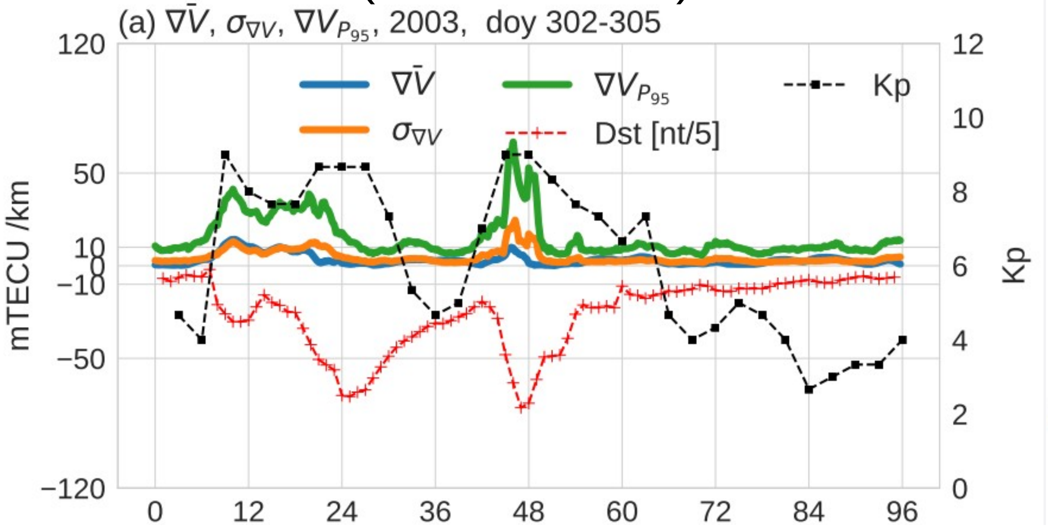


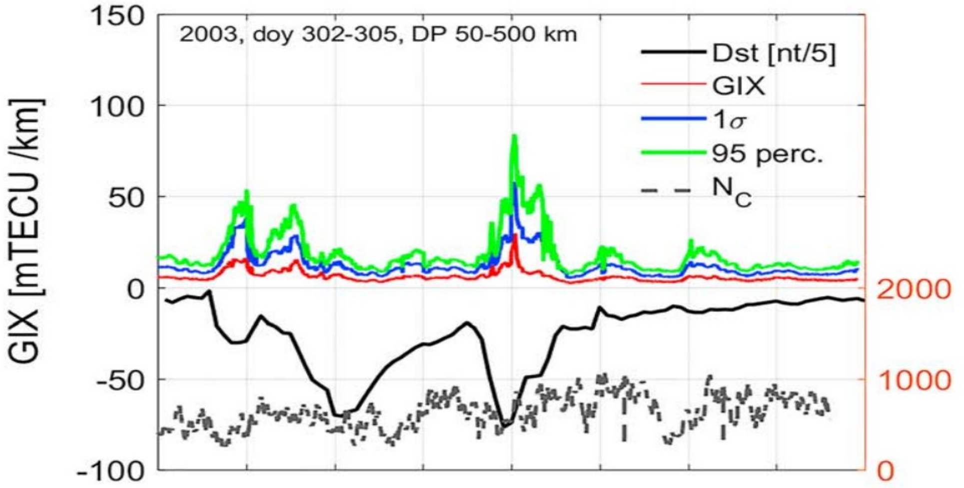


**Latitudinal gradient component**

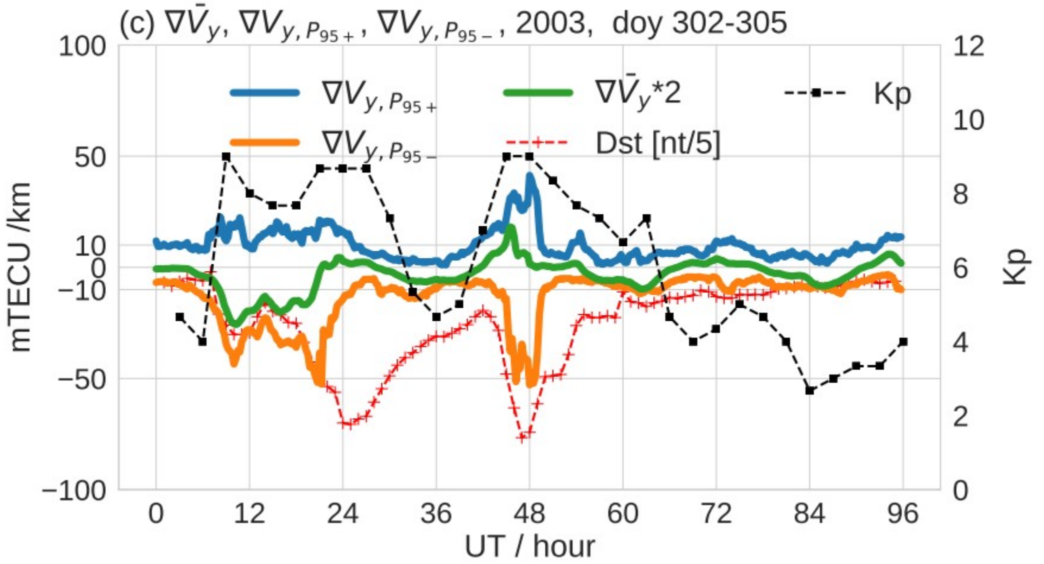


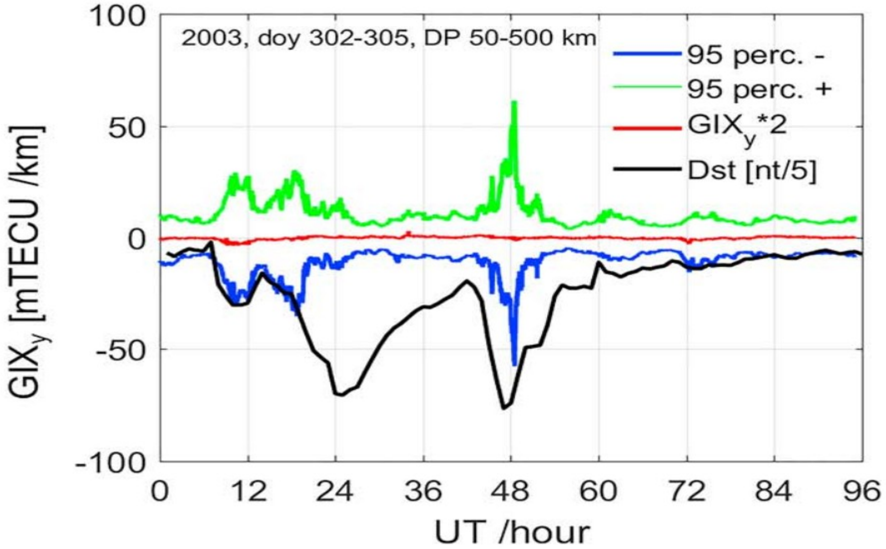


UNIVERSITAT POLITÈCNICA DE CATALUNYA
BARCELONATECH

# 3.3 Example of comparison of GIM- vs raw-GNSS data- based regional **spatial** indices over Europe: **Halloween storm** (28 Oct -1 Nov 2003) -Continued-

**Longitudinal gradient component**

From **UQRG GIM (VgUG)**
(Liu et al. 2022)

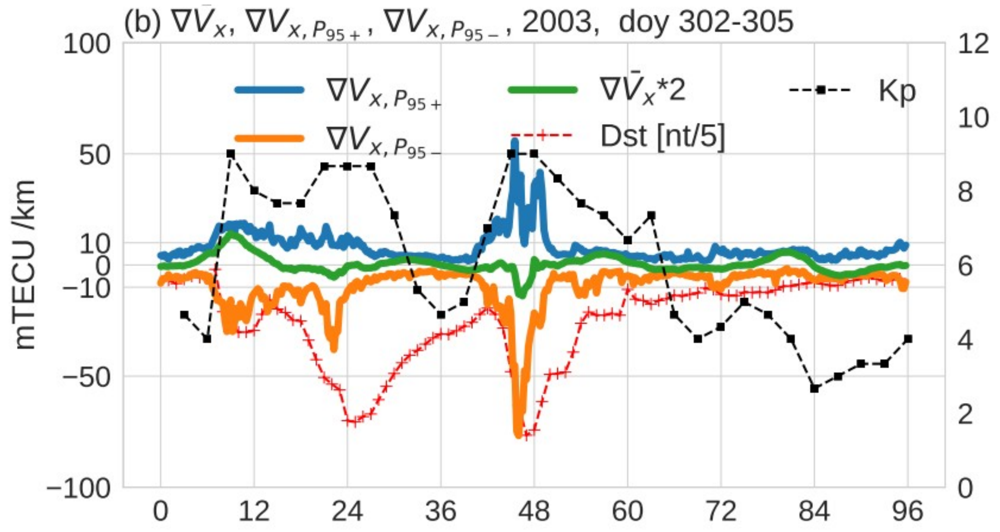


From **raw GNSS data**
**(**Jakowski & Hoque (2017)

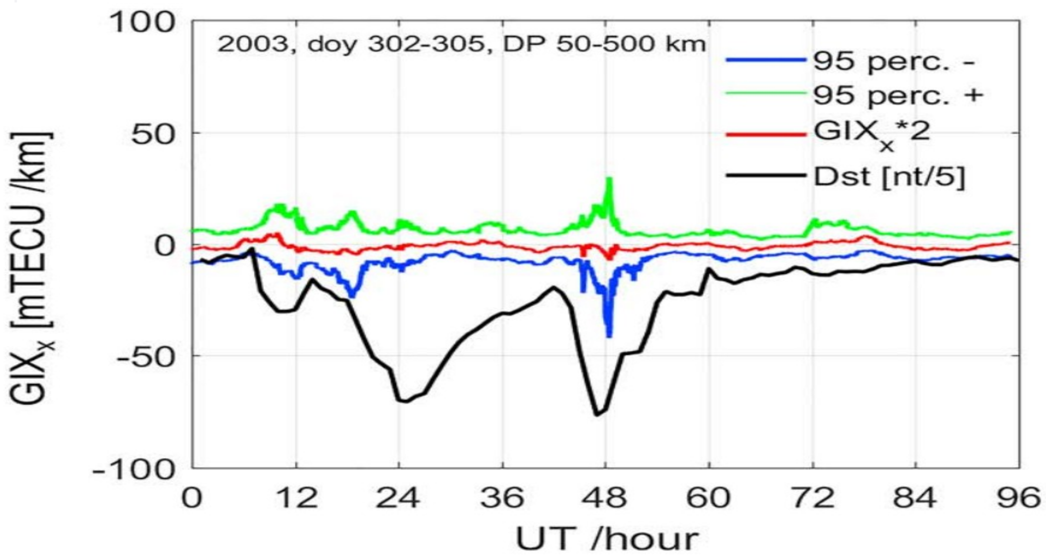


**Both regional indices based on the VTEC gradient norm and on the VTEC gradient latitudinal components provide results very comparable when GIM-based and raw-GNSS-based results are considered**. The longitudinal component of the VTEC gradient appear correlated but smaller when they are computed from GIMs.

UNIVERSITAT POLITÈCNICA DE CATALUNYA
BARCELONATECH

# 3.3 Example of comparison of GIM- vs raw-GNSS data- based regional **temporal** indices over Europe: Solar flare X17.0 class preceding **Halloween storm** (28 Oct 2003)

From **UQRG GIM (VgUG),**
Regional Ionospheric Disturbance index
(Liu et al. 2022)

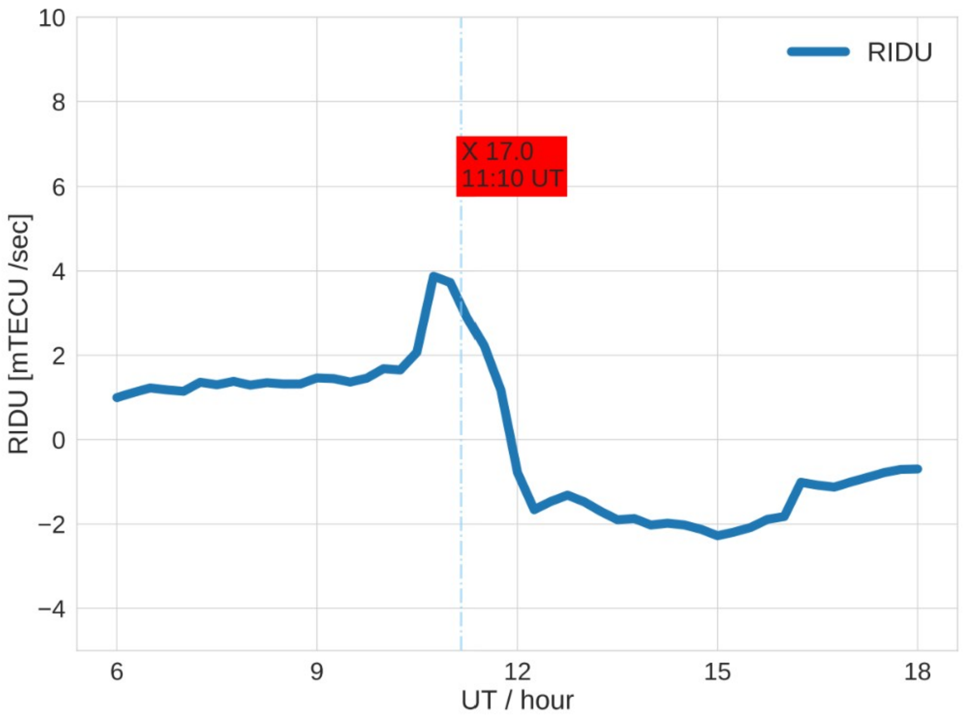


$$\begin{cases} \dot{V}_{i,j} = \Delta VTEC_{i,j}/\Delta t = (VTEC_{i,j,t} - VTEC_{i,j,t-1})/\Delta t \\ RIDU = \sum_{i=1}^{n} \sum_{j=1}^{m} \dot{V}_{i,j} / N_S \end{cases}$$

From **raw GNSS data,**
Sudden Ionospheric Disturbance indeX (**SIDX**)
**(**Jakowski & Hoque (2017)

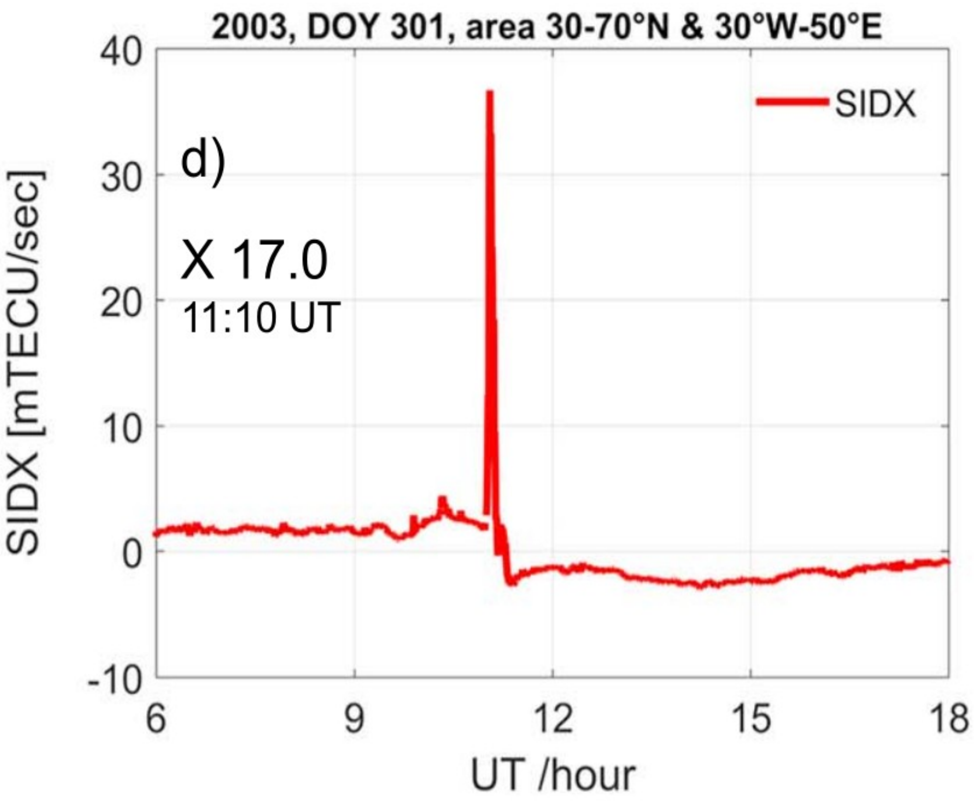


The **GIM-based** temporal component of the VTEC gradient is **only sensitive to very strong flares**, and it appears smoothed, as it might be expected from the GIM interpolation procedure in space and time.
For detecting and measuring the solar EUV flux rate during flares (two products provided by UPC-IonSAT to the Space Weather community in RT), the global raw GNSS measurements in the day-light hemisphere, perform in an excellent way (Hernández-Pajares et al. 2012).

IonSAT

# 4. Extending the definition of the Ionospheric storm scale index to GIMs (IsUG)

We propose the Ionospheric Storm Scale Index Based on UQRG (IsUG) as a direct extension of the I-scale index proposed at regional level (Japan) and from raw GNSS data by Nishioka et al. (2017):

$$P_{TEC} = \frac{100 \times (O_{TEC} - R_{TEC})}{R_{TEC}} \qquad \hat{P}_{TEC} = \frac{P_{TEC} - \mu}{\sigma}$$

It is defined as the standardized Ptec, $\hat{P}_{TEC}$, where Ptec is the percentage deviation of VTEC, Otec is the hourly median VTEC derived at grid points of GIM. The hourly median VTEC is the median of the five VTEC values during 1-h interval, under the GIM VTEC temporal resolution of 15 min. The hourly median VTEC is calculated every hour (for example, 0, 1, 2 UT). Rtec is the reference median value at the same local time and geographic location in the past 27 days.

| IsUG | Description | Definition | Probability on a global scale (%) |
|---|---|---|---|
| IP3 | Severe positive storm | $5 < \hat{P}$ | 0.17 |
| IP2 | Strong positive storm | $3 < \hat{P} \leq 5$ | 0.72 |
| IP1 | Moderate positive storm | $1 < \hat{P} \leq 3$ | 12.43 |
| I0 | Quiet | $-1 < \hat{P} \leq 1$ | 73.96 |
| IN1 | Moderate negative storm | $-2 < \hat{P} \leq -1$ | 11.72 |
| IN2 | Strong negative storm | $-3 < \hat{P} \leq -2$ | 0.95 |
| IN3 | Severe negative storm | $\hat{P} < -3$ | 0.06 |

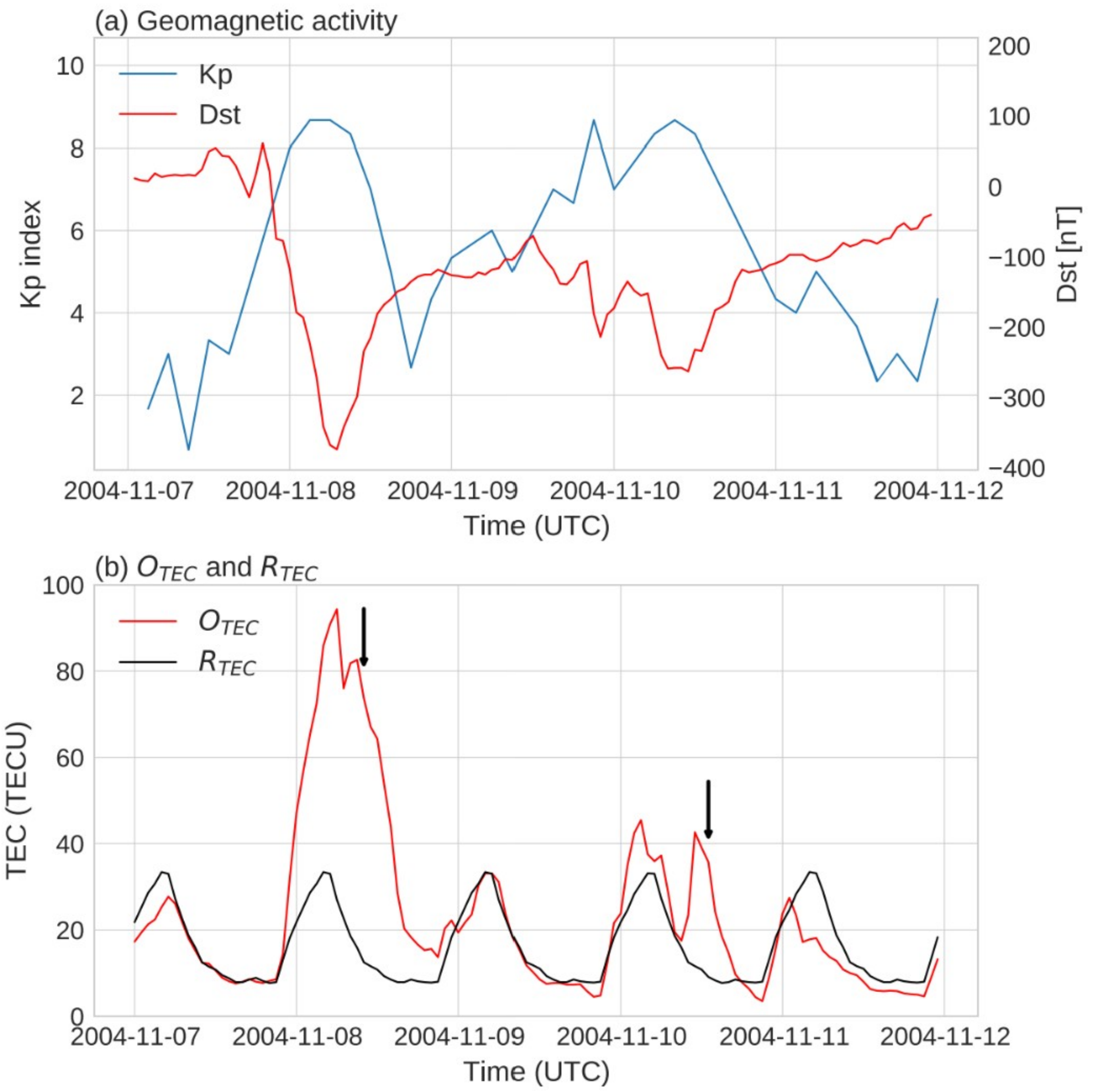


(130°E, 30°N)

# 4.1 Comparing Ptec from GIM with Ptec from raw GNSS data over Japan since 1997 to 2014 (3 months of seasonal data per year)

From **UQRG GIM (VgUG)**
(Liu et al. 2021)

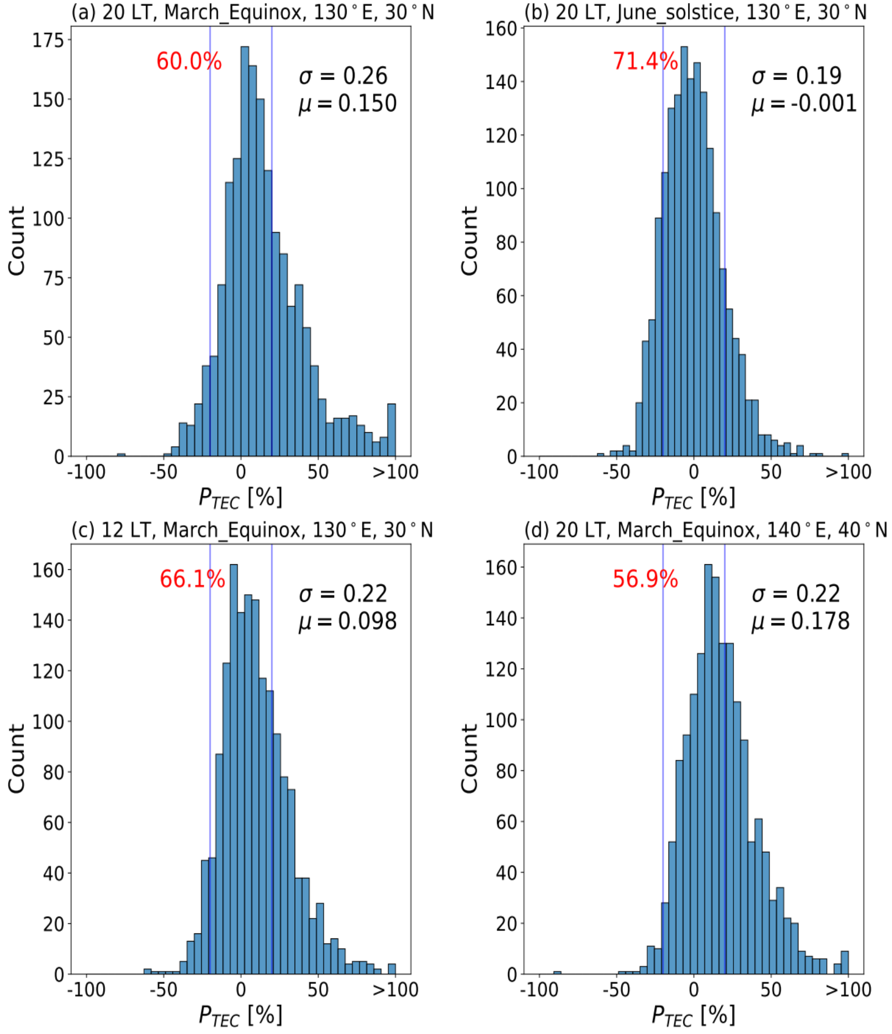


From **raw GNSS data**
**(**Nishioka et al., 2017))

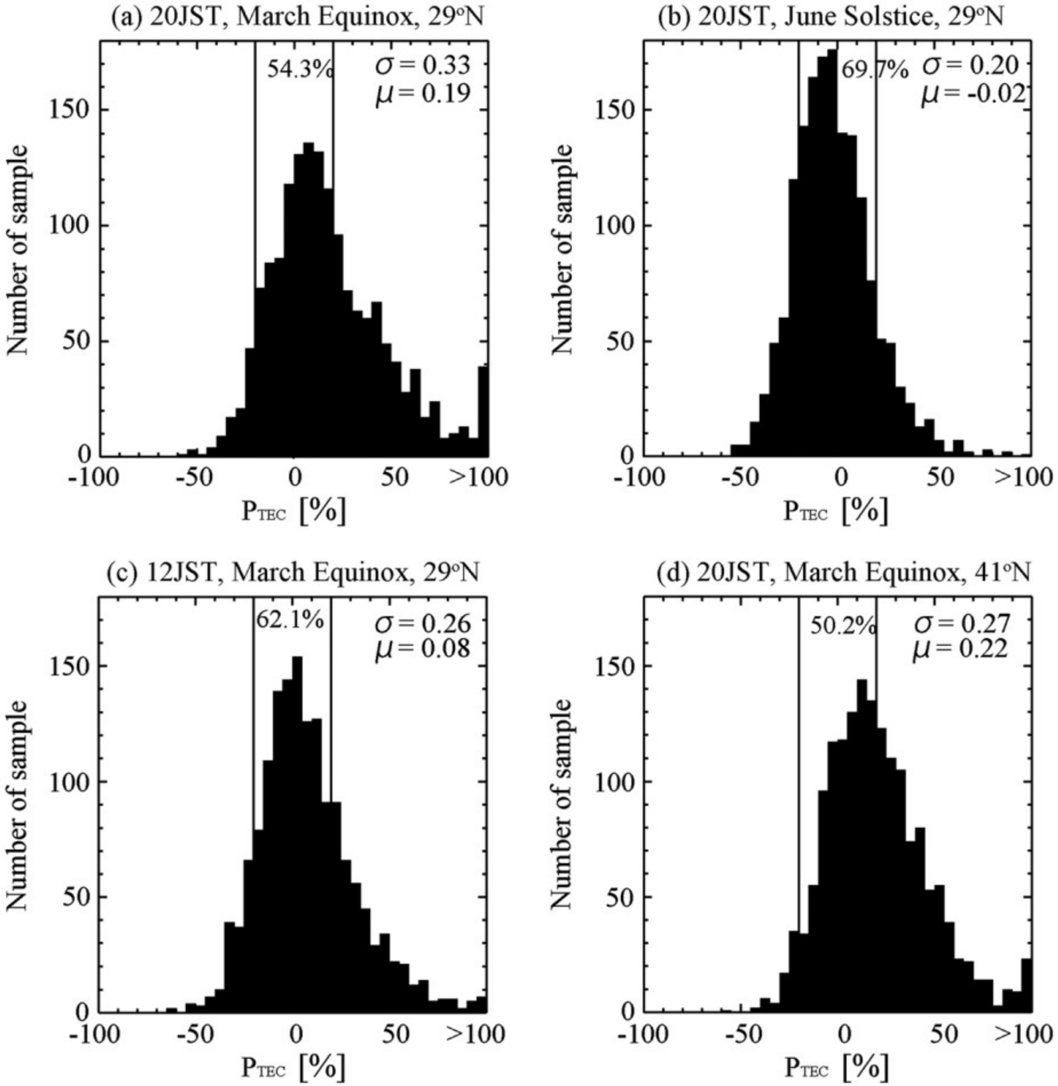


UNIVERSITAT POLITÈCNICA DE CATALUNYA BARCELONATECH UPC

# 4.2 Comparing $\hat{P}_{TEC}$ from GIM $\hat{P}_{TEC}$ from raw GNSS data over Japan since 1997 to 2014 (3 months of seasonal data per year)

From **UQRG GIM (VgUG)**
(Liu et al. 2021)

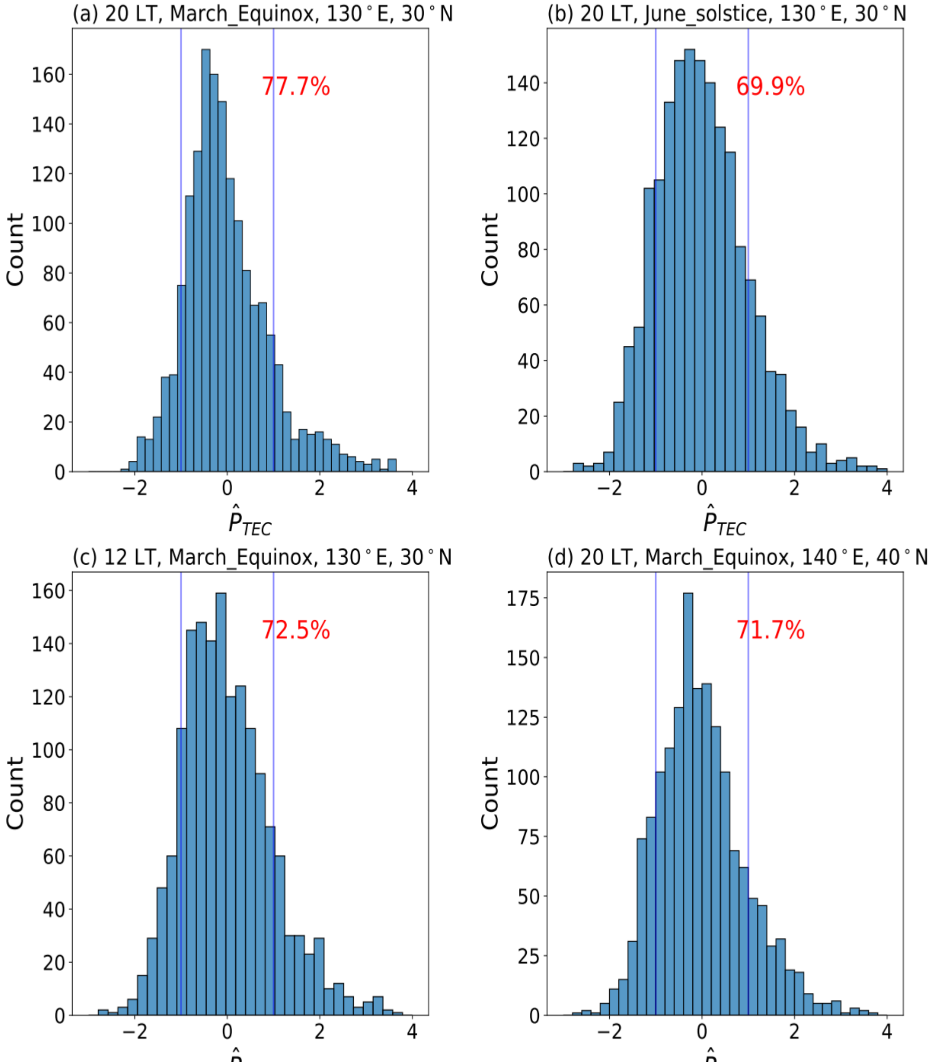


From **raw GNSS data**
**(**Nishioka et al., 2017))

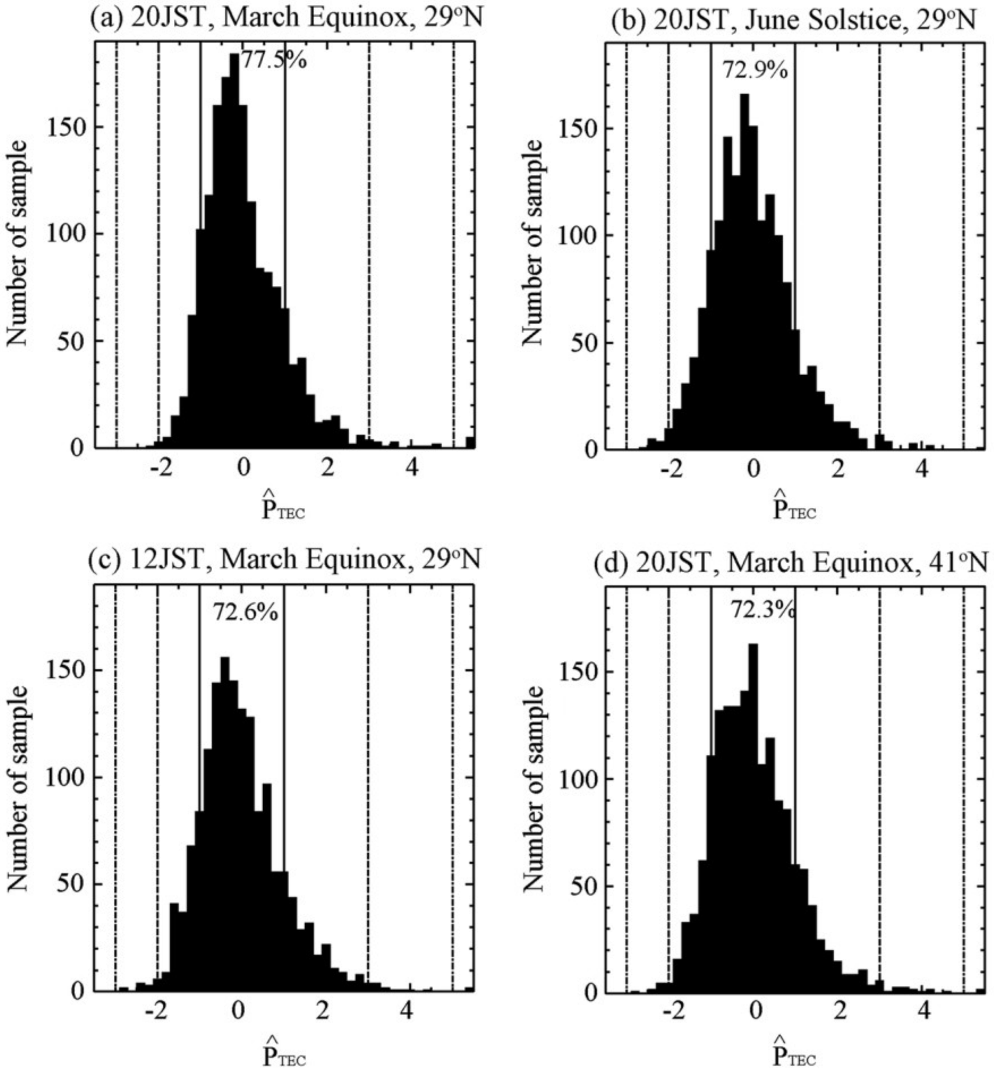


UNIVERSITAT
DE CATALUN
BARCELONAT
UPC

# 4.3 Summary of Ptec and $\hat{P}_{TEC}$ comparison from GIM vs. from raw GNSS data over Japan since 1997 to 2014 (3 months of seasonal data per year)

**Ptec**

**Table 1**
*Comparison of $P_{TEC}$ Distribution Parameters During 1997–2014 Between the Values Derived From UQRG (Input for IsUG Index) and the Values Derived in Nishioka et al. (2017) as Input to I-Scale*

| | | | | $P_{TEC}$(UQRQ-GIM) (this work) | | | $P_{TEC}$(raw-GNSS-data) (Nishioka et al., 2017) | | |
|---|---|---|---|---|---|---|---|---|---|
| Season | LT | Long. | Lat. | $\sigma$ | $\mu$ | per. 20% | $\sigma$ | $\mu$ | per. 20% |
| March Equi. | 20 h | 130°E | 30°N | 0.28 | 0.150 | 60.0 | 0.33 | 0.19 | 54.3 |
| June Equi. | 20 h | 130°E | 30°N | 0.19 | −0.001 | 71.4 | 0.20 | −0.02 | 69.7 |
| March Equi. | 12 h | 130°E | 30°N | 0.22 | 0.098 | 66.1 | 0.26 | 0.08 | 62.1 |
| March Equi. | 20 h | 140°E | 40°N | 0.23 | 0.178 | 56.9 | 0.27 | 0.22 | 50.2 |

$\hat{P}_{TEC}$

**Table 2**
*Comparison of the Percentiles for $|\hat{P}_{TEC}| \leq 1$ During 1997–2014 Between the Values Derived From UQRG (Input for IsUG Index) and the Values Derived in Nishioka et al. (2017) as Input to I-Scale*

| | | | | $\hat{P}_{TEC}$(UQRQ-GIM) (this work) | $\hat{P}_{TEC}$(raw-GNSS-data) (Nishioka et al., 2017) |
|---|---|---|---|---|---|
| Season | LT | Long. | Lat. | perc. $|\hat{P}_{TEC}| \leq 1$ | perc. $|\hat{P}_{TEC}| \leq 1$ |
| March Equi. | 20 h | 130°E | 30°N | 77.7 | 77.5 |
| June Equi. | 20 h | 130°E | 30°N | 69.7 | 72.9 |
| March Equi. | 12 h | 130°E | 30°N | 72.5 | 72.6 |
| March Equi. | 20 h | 140°E | 40°N | 71.7 | 72.3 |

UNIVERSITAT POLITÈCNICA DE CATALUNYA
BARCELONATECH

# 4.5 Snapshots of IsUG maps of November 7 2004 (severe geomagnetic storm)

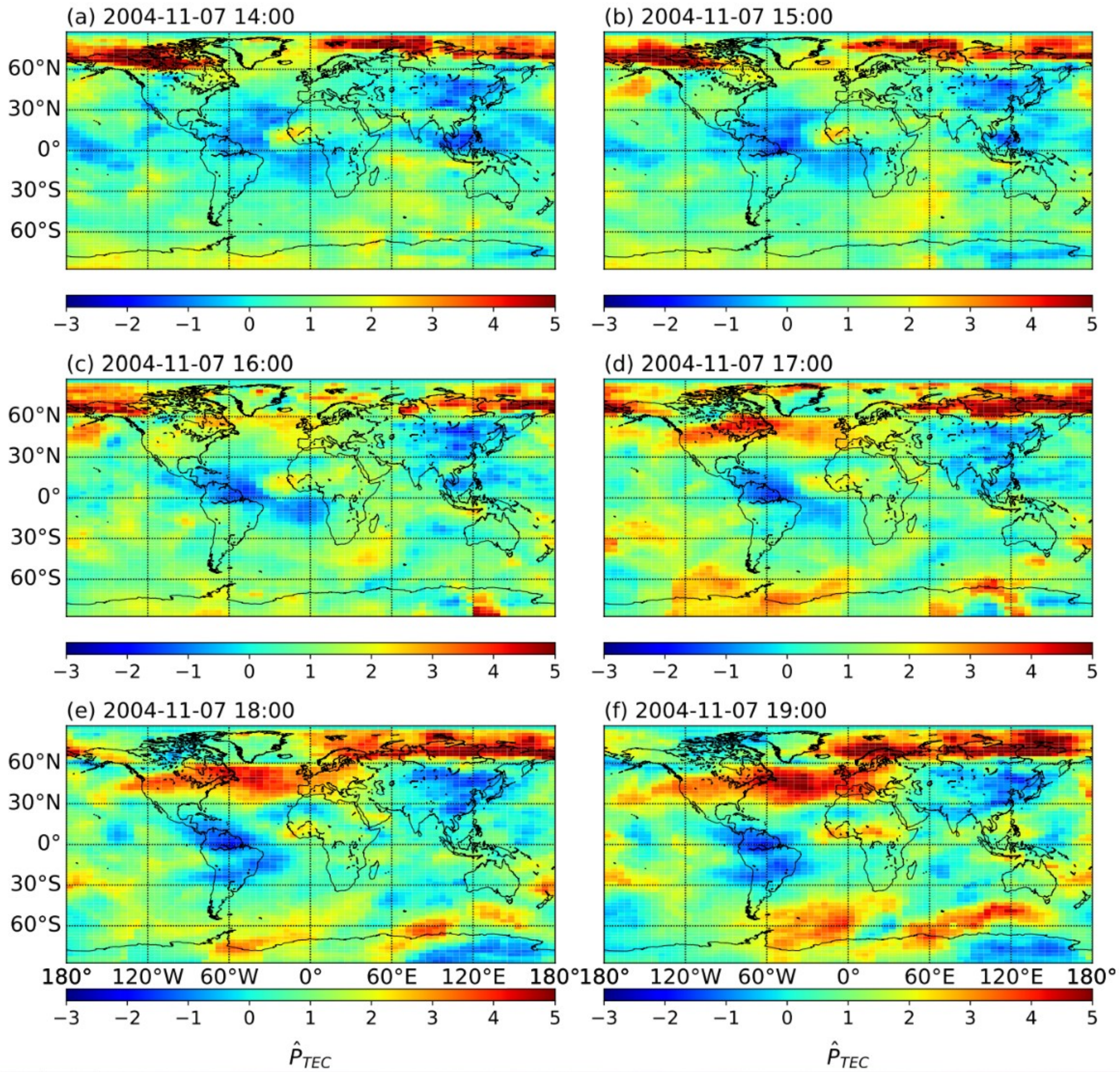

# 4.5 Snapshots of IsUG maps during November 7-November 8 2004 (severe geomagnetic storm) -Continued-

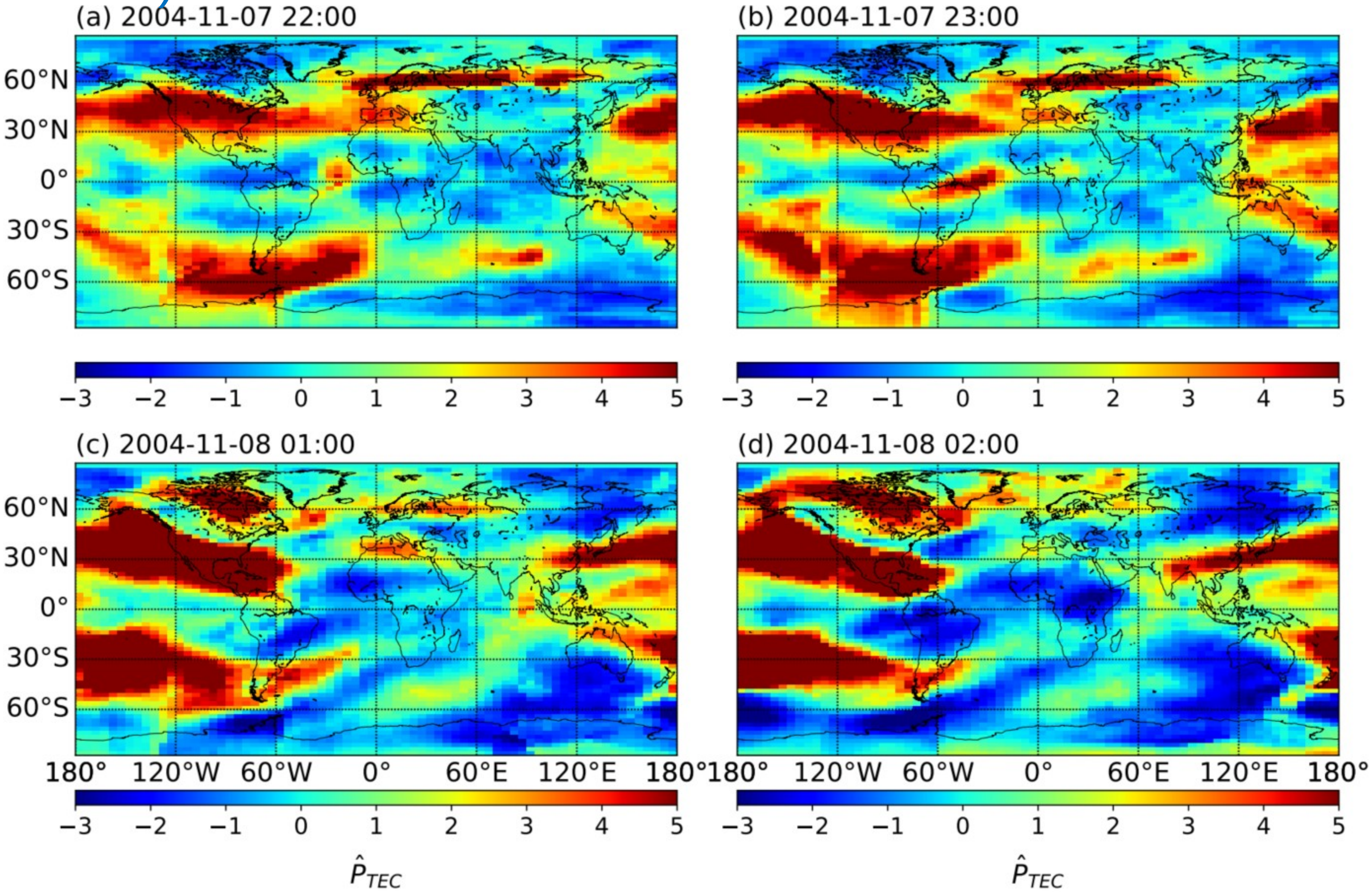

# 4.6 Animation of IsUG maps during a quiet period



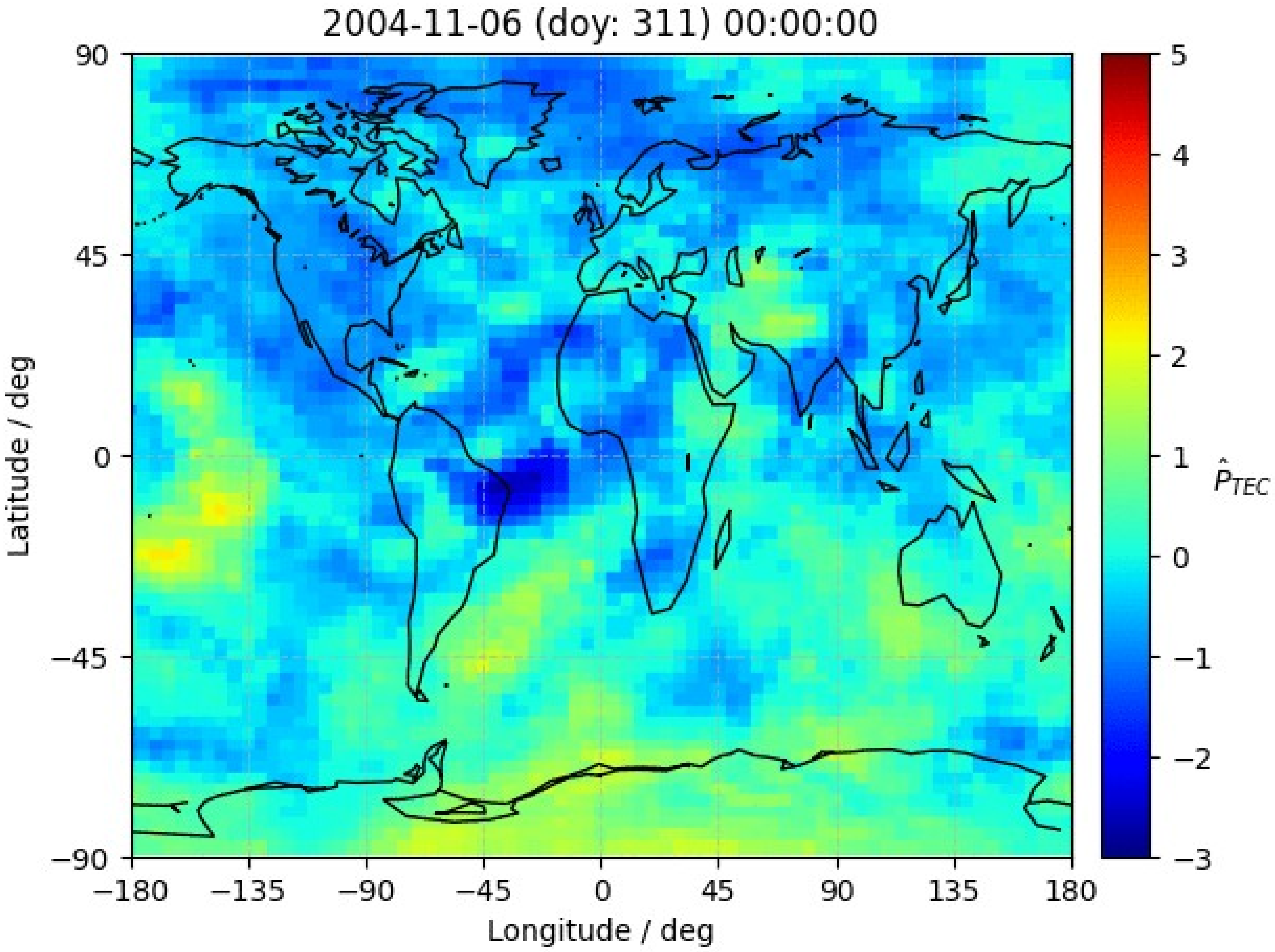

# 4.6 Animation of IsUG maps during a ionospheric storm period

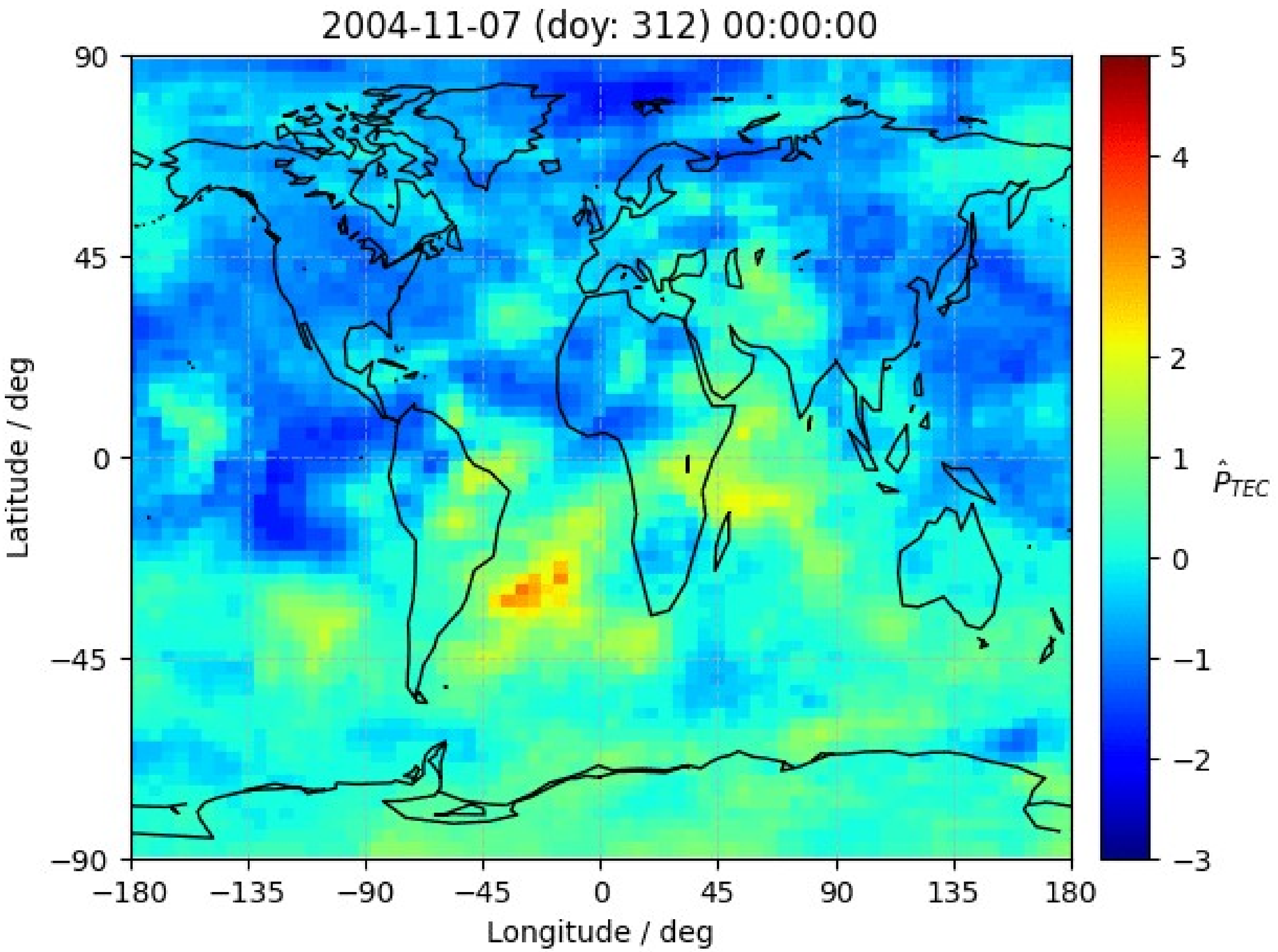

# 5. Conclusions

- ✓ The regional gradient indices based on UQRG open a new way to estimate the ionospheric perturbation degree at selected regions, consistent in a large extent with direct raw-GNSS based approaches. And the spatial and temporal VTEC gradient at each grid point of UQRG allow the representation of ionospheric perturbations on a global scale.
- ✓ The new ionospheric storm scale, IsUG, has a great potential for characterization of ionospheric state and the scientific study of ionospheric storms from a global perspective, being consistent with the raw-GNSS based original implementation in Japan during one and half solar cycles (1997-2014).
- ✓ More details can be found at:


Liu, Q., Hernández-Pajares, M., Lyu, H., Nishioka, M., Yang, H., Monte-Moreno, E., ... & Orús-Pérez, R. (2021). Ionospheric Storm Scale Index Based on High Time Resolution UPC-IonSAT Global Ionospheric Maps (IsUG). Space Weather, 19(11), e2021SW002853.

Liu, Q., Hernández-Pajares, M., Yang, H., Monte-Moreno, E., García-Rigo, A., Lyu, H., ... & Orús-Pérez, R. (2022). A New Way of Estimating the Spatial and Temporal Components of the Vertical Total Electron Content Gradient Based on UPC-IonSAT Global Ionosphere Maps. Space Weather, 20(2), e2021SW002926.

Space Weather

RESEARCH ARTICLE
10.1029/2021SW002853

## Ionospheric Storm Scale Index Based on High Time Resolution UPC-IonSAT Global Ionospheric Maps (IsUG)

Qi Liu[1], Manuel Hernández-Pajares[1,2], Haixia Lyu[3,1], Michi Nishioka[4], Heng Yang[5,1], Enric Monte-Moreno[6], Tamara Gulyaeva[7], Yannick Béniguel[8], Volker Wilken[9], Germán Olivares-Pulido[1], and Raül Orús-Pérez[10]

[1]Universitat Politècnica de Catalunya (UPC-IonSAT), Barcelona, Spain, [2]Institut d'Estudis Espacials de Catalunya (IEEC), Barcelona, Spain, [3]GNSS Research Center, Wuhan University, China, [4]National Institute of Information and Communications Technology (NICT), Tokyo, Japan, [5]School of Electronic Information and Engineering, Yangtze Normal University, Chongqing, China, [6]Department of TSC, TALP, Universitat Politècnica de Catalunya, Barcelona, Spain, [7]IZMIRAN, Moscow, Russia, [8]Informatique, Electromagnétisme, Electronique, Analyse numérique (IEEA), Courbevoie, France, [9]German Aerospace Center (DLR), Neustrelitz, Germany, [10]Wave Interaction and Propagation Section (TEC-EFW) ESA ESTEC, Noordwijk, The Netherlands

**Key Points:**

- The new ionospheric storm scale, IsUG, is presented
- The IsUG is based on the high resolution and rapid UPC-IonSAT Global Ionosphere Maps (UQRG)
- Statistical analysis is carried out on a global scale from 1997 to 2014 comparing well with the available raw GNSS data based I-scale index

**Supporting Information:**

Supporting Information may be found

Space Weather

RESEARCH ARTICLE
10.1029/2021SW002926

## A New Way of Estimating the Spatial and Temporal Components of the Vertical Total Electron Content Gradient Based on UPC-IonSAT Global Ionosphere Maps

Qi Liu[1], Manuel Hernández-Pajares[1,2], Heng Yang[1,3], Enric Monte-Moreno[4], Germán Olivares-Pulido[1], and Raül Orús-Pérez[6], Alberto García-Rigo[1,2], Haixia Lyu[1,5]

[1]Universitat Politècnica de Catalunya (UPC-IonSAT), Barcelona, Spain, [2]Institut d'Estudis Espacials de Catalunya (IEEC), Barcelona, Spain, [3]School of Electronic Information and Engineering, Yangtze Normal University, Chongqing, China, [4]Department of TSC, TALP, Universitat Politècnica de Catalunya, Barcelona, Spain, [5]GNSS Research Center, Wuhan University, Wuhan, China, [6]Wave Interaction and Propagation Section (TEC-EFW) ESA ESTEC, Noordwijk, The Netherlands

**Key Points:**

- A new ionospheric temporal and spatial gradient index based on UPC-IonSAT Global Ionosphere Maps (UQRG) are presented at the selected region
- The new ionospheric spatial gradients indices at grid points of UQRG are presented
- The derived ionospheric spatial gradients and temporal variations indices are analyzed during quiet and disturbed ionosphere states

# Thanks for your attention!

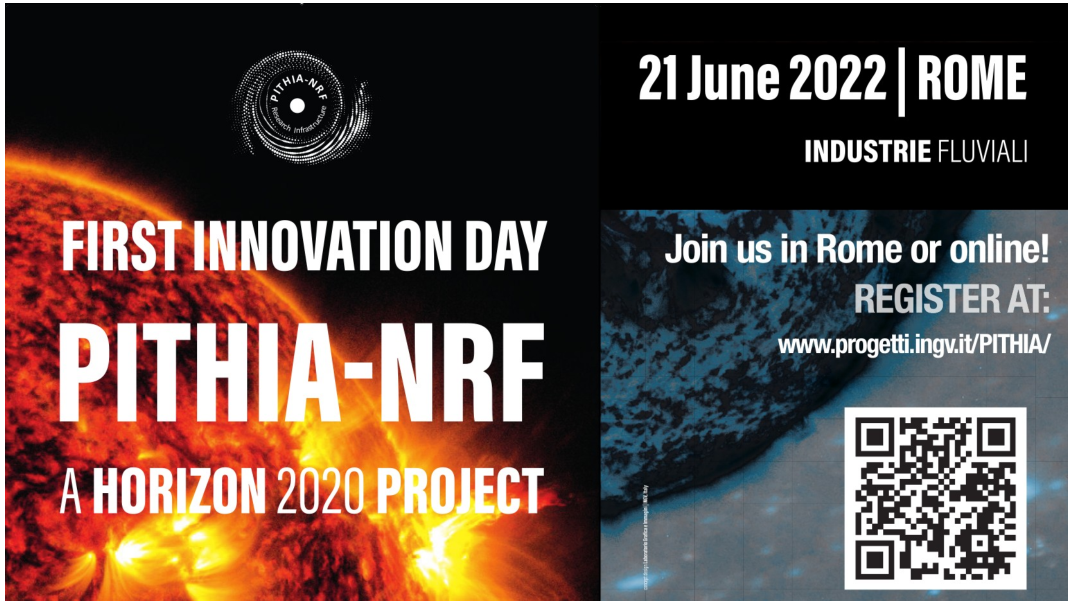


UNIVERSITAT POLITÈCNICA DE CATALUNYA
BARCELONATECH

IonSAT

# 4. References


- Hernandez-Pajares, M., Juan, J. M., & Sanz, J. (1997). Neural network modeling of the ionospheric electron content at global scale using GPS data. Radio Science, 32(3), 1081-1089.
- Hernández-Pajares, M., Juan, J. M., & Sanz, J. (1999). New approaches in global ionospheric determination using ground GPS data. Journal of Atmospheric and Solar-Terrestrial Physics, 61(16), 1237-1247.
- Hernández-Pajares, M., García-Rigo, A., Juan, J. M., Sanz, J., Monte, E., & Aragón-Àngel, A. (2012). GNSS measurement of EUV photons flux rate during strong and mid solar flares. Space Weather, 10(12).
- Hernández-Pajares, M., Juan, J. M., Sanz, J., Orus, R., Garcia-Rigo, A., Feltens, J., ... & Krankowski, A. (2009). The IGS VTEC maps: a reliable source of ionospheric information since 1998. Journal of Geodesy, 83(3), 263-275.
- Hernández-Pajares, M., Roma-Dollase, D., Krankowski, A., García-Rigo, A., & Orús-Pérez, R. (2017). Methodology and consistency of slant and vertical assessments for ionospheric electron content models. Journal of Geodesy, 91(12), 1405-1414.
- Hernández-Pajares, M., Lyu, H., Aragón-Àngel, À., Monte-Moreno, E., Liu, J., An, J., & Jiang, H. (2020). Polar Electron Content From GPS Data-Based Global Ionospheric Maps: Assessment, Case Studies, and Climatology. Journal of Geophysical Research: Space Physics, 125(6), e2019JA027677.
- Hernández-Pajares, M., Lyu, H., Garcia-Fernandez, M., & Orus-Perez, R. (2020). A new way of improving global ionospheric maps by ionospheric tomography: consistent combination of multi-GNSS and multi-space geodetic dual-frequency measurements gathered from vessel-, LEO-and ground-based receivers. Journal of Geodesy, 94(8), 1-16.
- Jakowski, N., & Hoque, M. M. (2019). Estimation of spatial gradients and temporal variations of the total electron content using ground-based GNSS measurements. Space Weather, 17, 339–356. https://doi.org/10.1029/2018SW002119.

# 4. References


- Kotov, D. V., Richards, P. G., Truhlík, V., Bogomaz, O. V., Shulha, M. O., Maruyama, N., ... & Chepurnyy, Y. M. (2018). Coincident observations by the Kharkiv IS radar and ionosonde, DMSP and Arase (ERG) satellites, and FLIP model simulations: Implications for the NRLMSISE-00 hydrogen density, plasmasphere, and ionosphere. Geophysical Research Letters, 45(16), 8062-8071.
- Kotov, D. V., Richards, P. G., Truhlík, V., Maruyama, N., Fedrizzi, M., Shulha, M. O., ... & Domnin, I. F. (2019). Weak magnetic storms can modulate ionosphere-plasmasphere interaction significantly: Mechanisms and manifestations at mid-latitudes. Journal of Geophysical Research: Space Physics, 124(11), 9665-9675.
- Liu, Q., Hernández-Pajares, M., Lyu, H., Nishioka, M., Yang, H., Monte-Moreno, E., ... & Orús-Pérez, R. (2021). Ionospheric Storm Scale Index Based on High Time Resolution UPC-IonSAT Global Ionospheric Maps (IsUG). Space Weather, 19(11), e2021SW002853.
- Liu, Q., Hernández-Pajares, M., Yang, H., Monte-Moreno, E., García-Rigo, A., Lyu, H., ... & Orús-Pérez, R. (2022). A New Way of Estimating the Spatial and Temporal Components of the Vertical Total Electron Content Gradient Based on UPC-IonSAT Global Ionosphere Maps. Space Weather, 20(2), e2021SW002926.
- Nishioka, M., T. Tsugawa, H. Jin, and M. Ishii (2017), A new ionospheric storm scale based on TEC and f o F 2 statistics, Space Weather, 15, 228–239, doi:10.1002/2016SW001536.
- Orús R., Hernández-Pajares, M., Juan, J. M., & Sanz, J. (2005). Improvement of global ionospheric VTEC maps by using kriging interpolation technique. Journal of atmospheric and solar-terrestrial physics, 67(16), 1598-1609.
- Roma-Dollase, D., Hernández-Pajares, M., Krankowski, A., Kotulak, K., Ghoddousi-Fard, R., Yuan, Y., ... & Gómez-Cama, J. M. (2018). Consistency of seven different GNSS global ionospheric mapping techniques during one solar cycle. Journal of Geodesy, 92(6), 691-706.

# Backup Slides

# Abstract


The ionospheric response to high geomagnetic activity, the ionospheric storm, can enlarge GNSS positioning errors by the increase of ionospheric electron density and disable high-frequency communications by the decrease of the ionospheric electron density. In addition, the ionospheric perturbations with high spatial and temporal components of VTEC gradient might also enlarge GNSS positioning errors and even incapacitate Satellite-Based Augmentation System (SBAS) and Ground-Based Augmentation System (GBAS) services[1][2]. UPC Quarter-of-an-hour time resolution Rapid GIM (UQRG) is derived from GNSS carrier phase measurements assuming a two-layer tomographic TEC model and interpolated by Kriging technique with a spatial resolution of 5° and 2.5° in longitude and latitude, respectively[3]. The characteristics and performance of UQRG GIMs[4][5] have allowed us to define two new GIM-derived ionospheric scales:

(1) The Ionospheric storm scale derived from UQRG GIMs (IsUG[6]) is defined as the percentage deviations of hourly median VTEC extracted at each grid point of historical UQRG (from 1997 to 2014), and it is normalized (subtract the mean and divide by the corresponding standard deviation) in order to remove the dependence of VTEC variations on season, local time and geographical location. The level of ionospheric storm from the proposed ionospheric storm scale is consistent with previous studies.

(2) The VTEC gradient derived from UQRG GIMs (VgUG[7]), which allow to obtain full (non-relative) values of TEC spatial gradients and temporal variations separately. Indeed the Regional VTEC spatial Gradient indices, based on UQRG (RVGU) and the Regional Ionospheric Disturbance index based on UQRG (RIDU), are proposed to estimate the regional ionospheric perturbation degree over selected regions. In addition, the spatial and temporal components of VTEC at grid points of UQRG on a global scale are also introduced. Compared with quiet ionospheric state, the VTEC spatial and temporal gradient indices are able to capture the variations of VTEC spatial and temporal gradient during the disturbed ionospheric state.



Acknowledgements:
The work has been performed within the context of MoNEWIC ESA and PITHIA-NRF European Commission activities.



References:

1. Nishioka M, Tsugawa T, Jin H, et al. A new ionospheric storm scale based on TEC and foF2 statistics[J]. Space Weather, 2017, 15(1): 228-239.
2. Jakowski N, Hoque M M. Estimation of spatial gradients and temporal variations of the total electron content using ground-based GNSS measurements[J]. Space Weather, 2019, 17(2): 339-356.
3. Hernández-Pajares M, Juan J M, Sanz J. New approaches in global ionospheric determination using ground GPS data[J]. Journal of Atmospheric and Solar-Terrestrial Physics, 1999, 61(16): 1237-1247.
4. Hernández-Pajares, M., Roma-Dollase, D., Krankowski, A., García-Rigo, A., & Orús-Pérez, R. (2017). Methodology and consistency of slant and vertical assessments for ionospheric electron content models. Journal of Geodesy, 91(12), 1405-1414.
5. Roma-Dollase, D., Hernández-Pajares, M., Krankowski, A., Kotulak, K., Ghoddousi-Fard, R., Yuan, Y., ... & Gómez-Cama, J. M. (2018). Consistency of seven different GNSS global ionospheric mapping techniques during one solar cycle. Journal of Geodesy, 92(6), 691-706.
6. Liu, Q., Hernández-Pajares, M., Lyu, H., Nishioka, M., Yang, H., Monte-Moreno, E., Gulyaeva, T., Béniguel, Wilken, V., Olivares-Pulido, G. Orús-Pérez, R. (2021). Ionospheric storm scale index based on high time resolution UPC-IonSAT global ionospheric maps (IsUG). Space Weather, 19, e2021SW002853. https://doi.org/10.1029/2021SW002853
7. Liu, Q., Hernández-Pajares, M., Yang, H., Monte-Moreno, E., García-Rigo, A., Lyu, H., Olivares-Pulido, G., Orús-Pérez, R. (2022). A new way of estimating the spatial and temporal components of the Vertical Total Electron Content gradient based on UPC-IonSAT Global Ionosphere Maps (accepted in Space Weather).

# 1. Context

## □ Total Electron Content (TEC) extraction based on GNSS

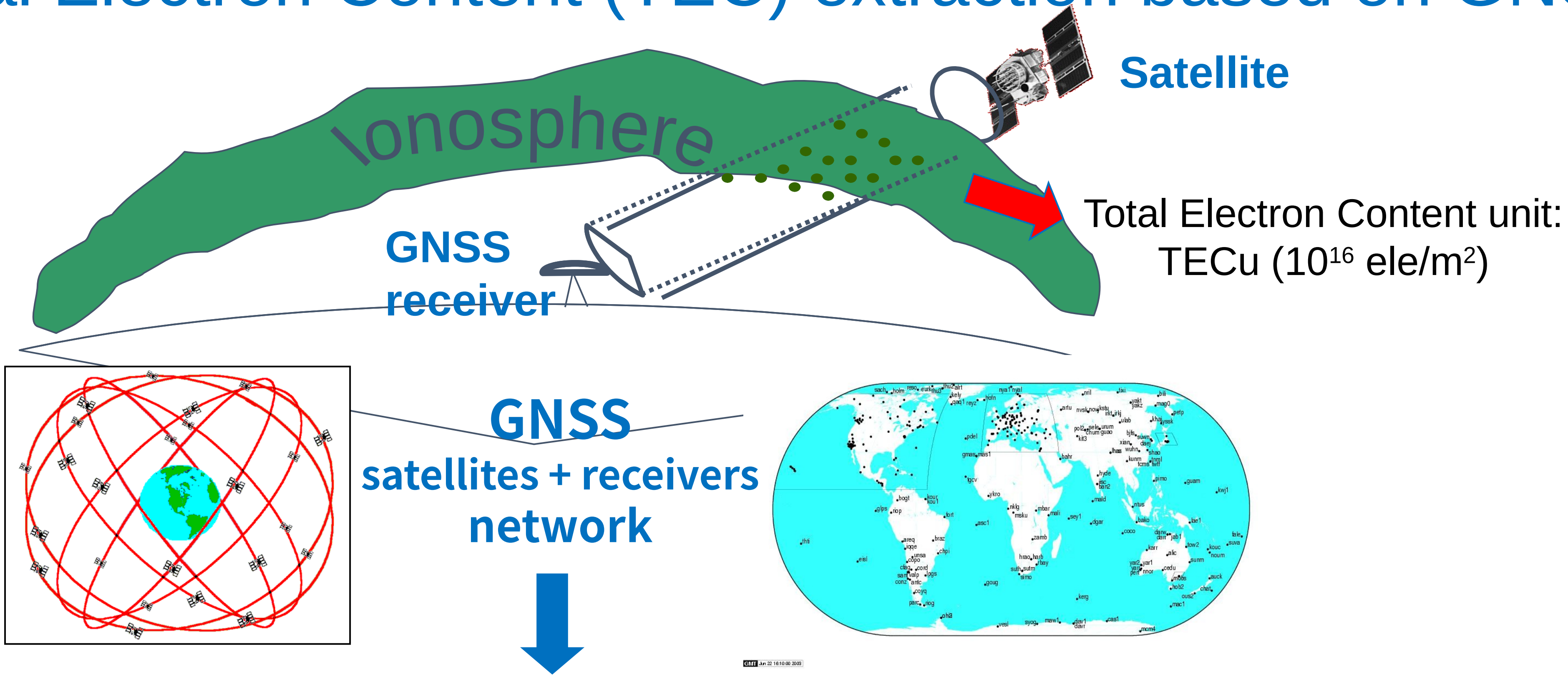


- Ionospheric error of GNSS observations is proportional to TEC and inversely proportional to signal frequency => combination of GNSS observations for extracting TEC
- Global GNSS network => Global ionospheric sounding and modeling

# 1. Motivation

## Irregular Ionosphere variation

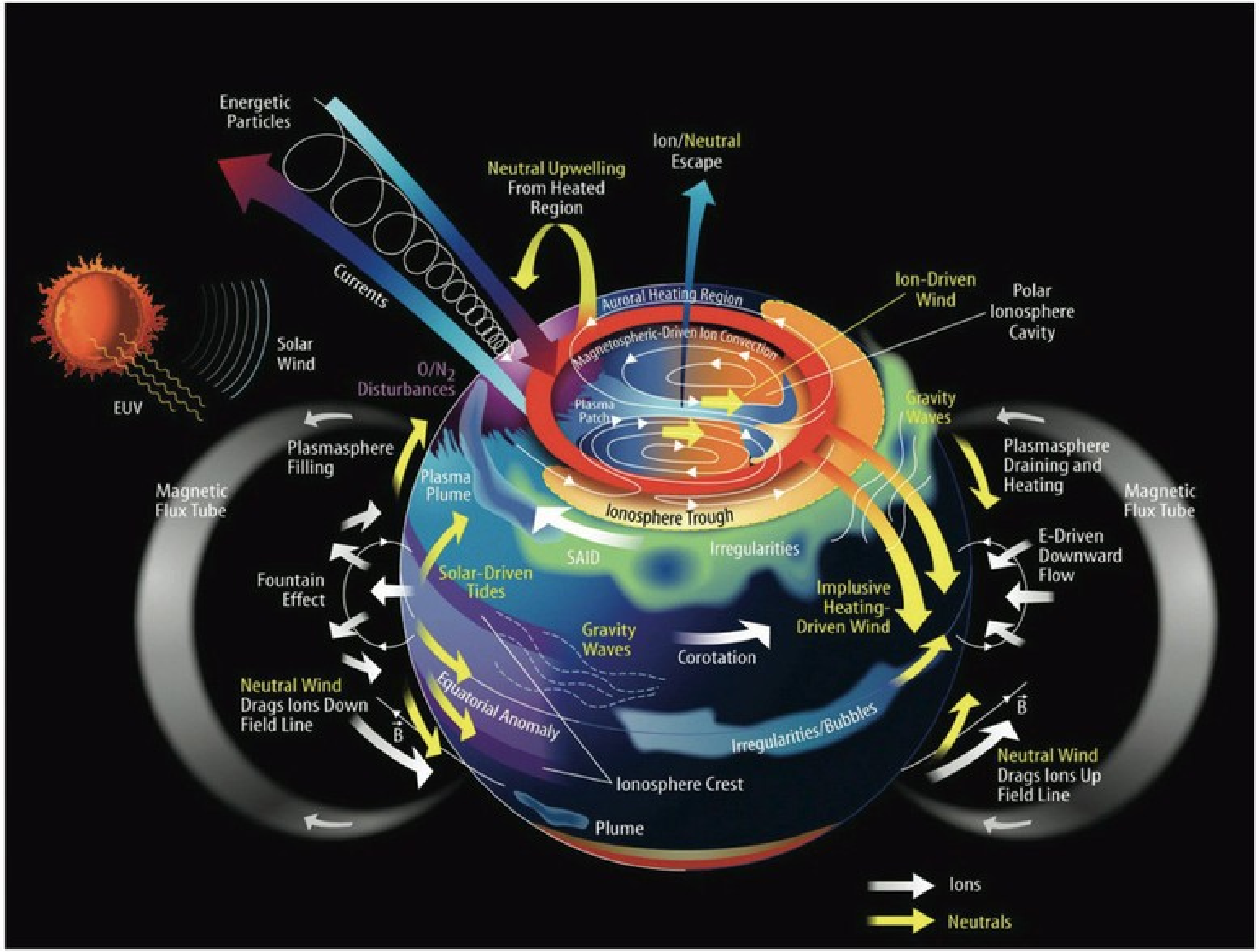


Figure from Grebowsky and Aikin, 2009

# 1. Motivation

## Space weather impacts

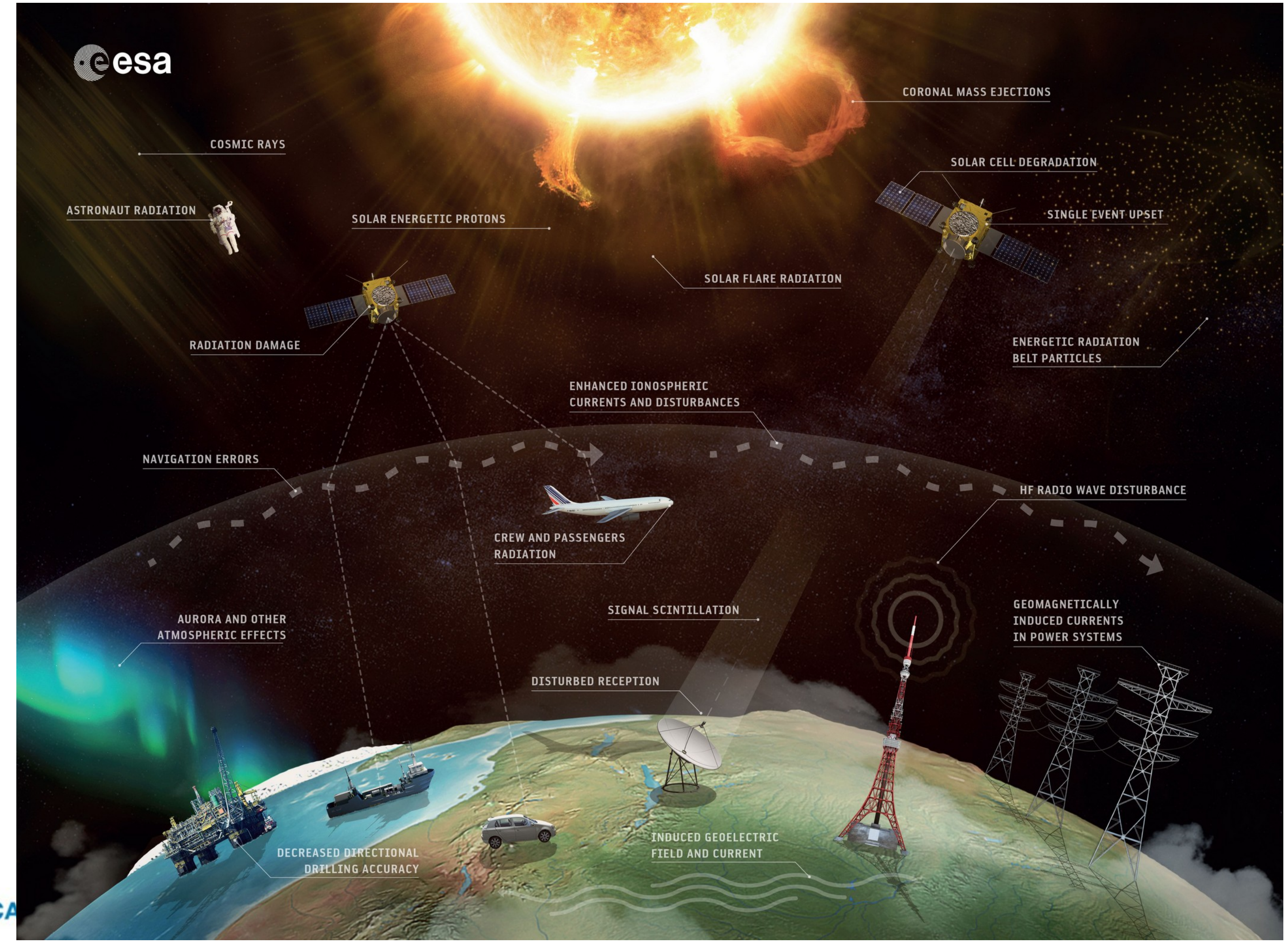


Figure from ESA/Science office, 2018

# 1. Motivation

## ☐ The impact of ionosphere on positioning

RTK

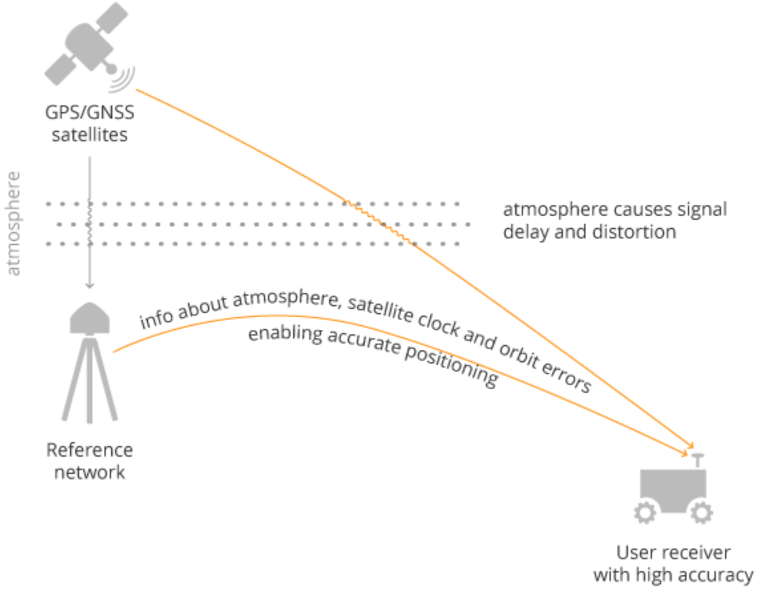


PPP

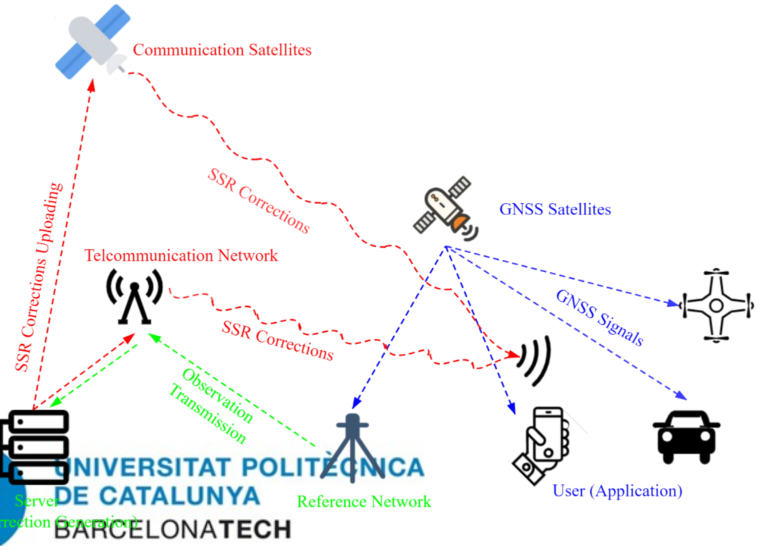


PPP-RTK

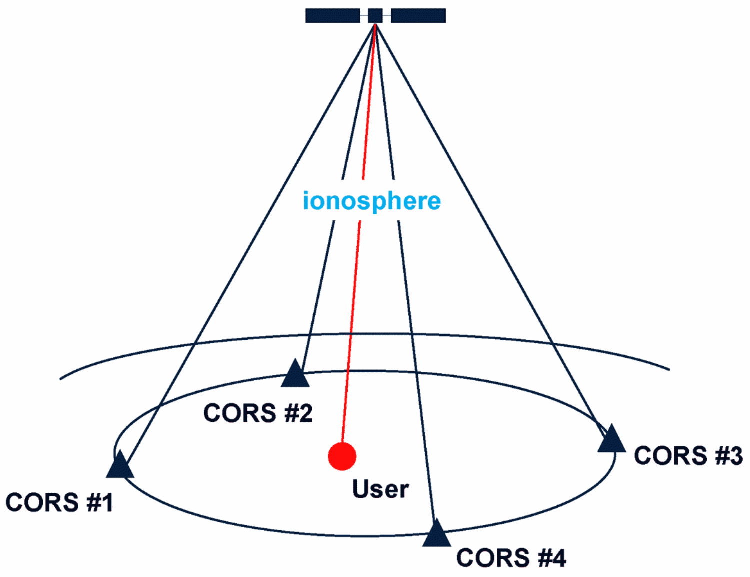


UNIVERSITAT POLITÈCNICA DE CATALUNYA
BARCELONATECH

# Solar Geomagnetic coordinates

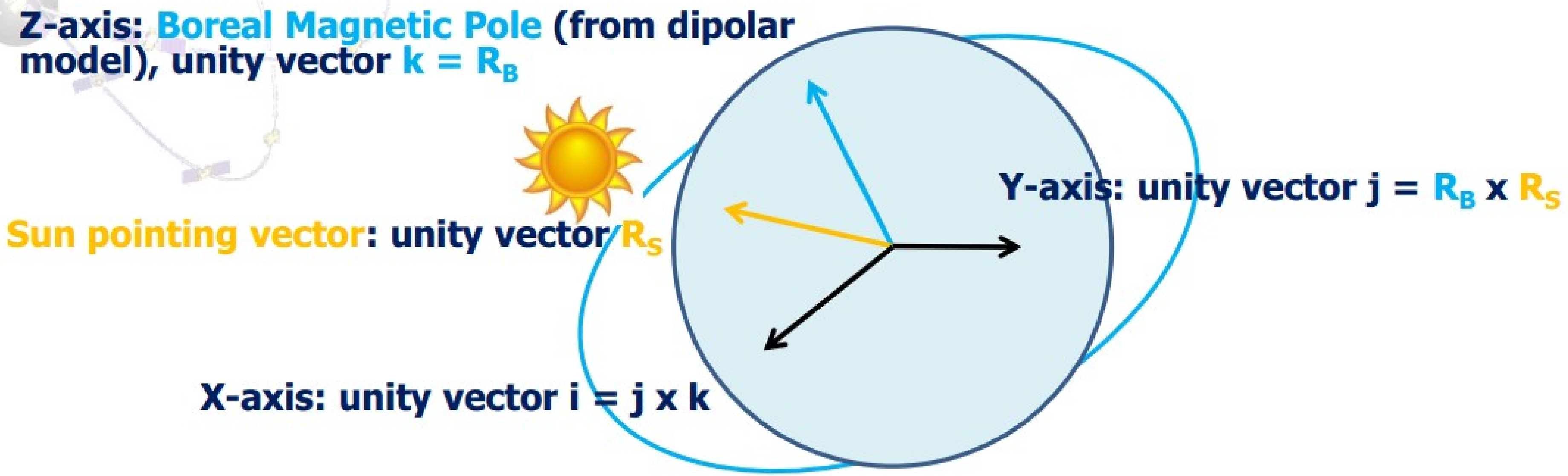


From the projection of the unity vector pointing to the ionospheric pierce point, **R**, on the new axis, **i,j,k**, we can retrieve the Solar-Magnetic Local Time (SMLT) and Magnetic Latitude, MLAT:

**R·k** = sin (MLAT)
**R·j** = cos (MLAT) * sin (SMLT)
**R·i =** cos (MLAT) * cos (SMLT)

# Tomographic implementation

GNSS satellite orbits & clocks, GNSS measurements

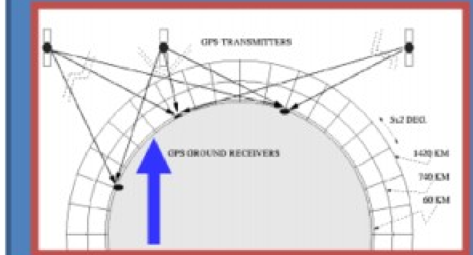


Compute the length of each ray intersection with each illuminated voxel, Δs

$$L_I = STEC + B_I = \int_{REC}^{SAT} N_e \, dl + B_I = \sum_i \sum_j \sum_k (N_e)_{i,j,k} \Delta s_{i,j,k} + B_I$$

Estimating X = (Ne…,Bi,…) in a forward Kalman filter solving Y = A X, with covariance matrices P:
Ne for each voxel-time (random-walk) and pair receiver-satellite cont. Arch (random variable)

Initialization

$\hat{X}(0)$, $P_{\hat{X}(0)}$

Prediction

$$\hat{X}^-(n) = \Phi \hat{X}(n-1)$$
$$P_{\hat{X}^-(n)} = \Phi P_{\hat{X}(n-1)} \Phi^t + Q$$

$\hat{X}^-(n)$, $P_{\hat{X}^-(n)}$

Measurements

$Y(n)$, $P_{Y(n)}$

Estimation

$$\hat{X}(n) = P_{\hat{X}(n)} \cdot \left[ A^t P^{-1}_{Y(n)} Y(n) + P^{-1}_{\hat{X}^-(n)} \hat{X}^-(n) \right]$$
$$P_{\hat{X}(n)} = \left[ A^t P^{-1}_{Y(n)} A + P^{-1}_{\hat{X}^-(n)} \right]^{-1}$$

$\hat{X}(n)$, $P_{\hat{X}(n)}$

# How?: RT-TOMION computing global VTEC maps based on GNSS data

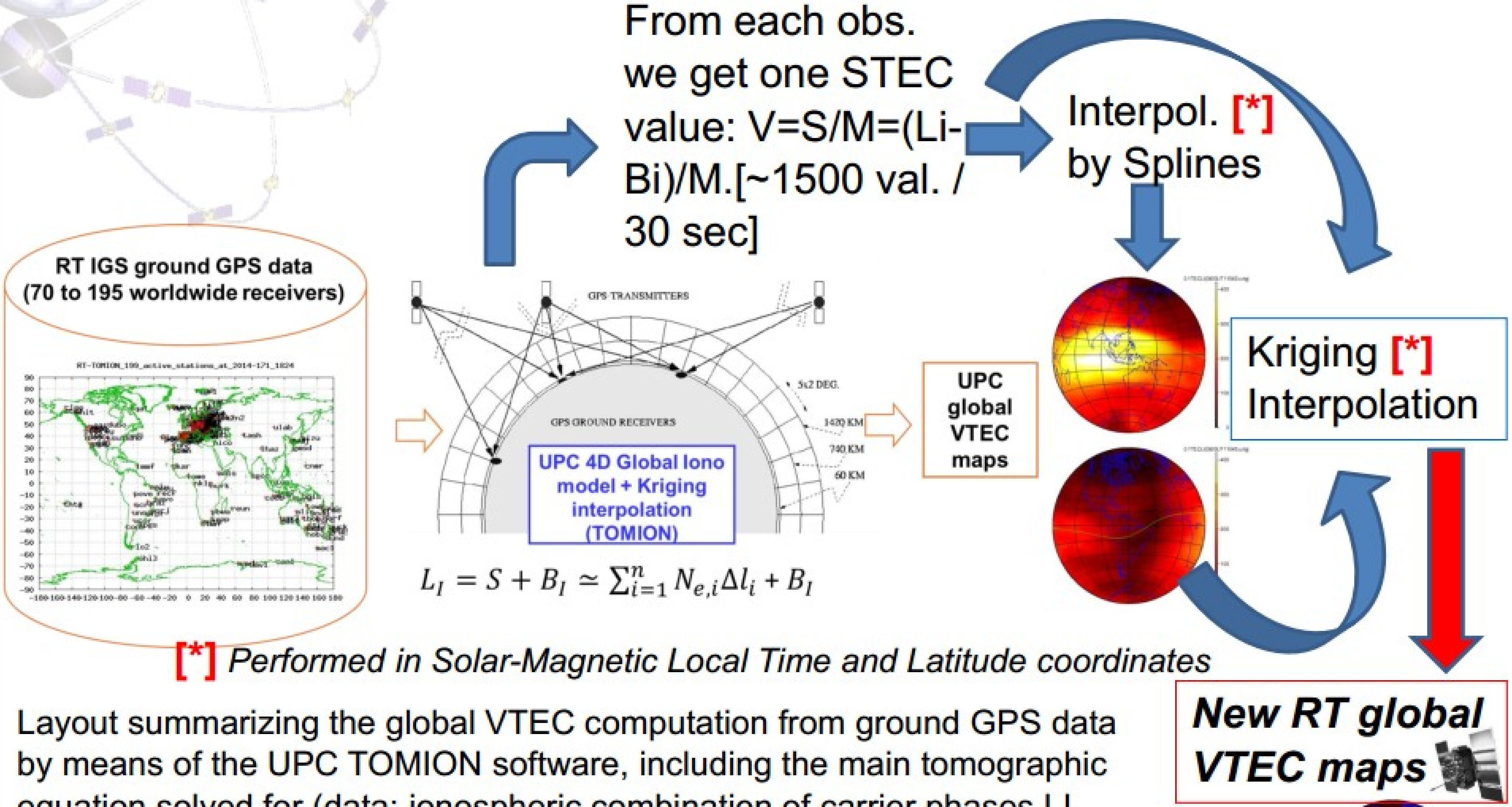


[*] *Performed in Solar-Magnetic Local Time and Latitude coordinates*

Layout summarizing the global VTEC computation from ground GPS data by means of the UPC TOMION software, including the main tomographic equation solved for (data: ionospheric combination of carrier phases LI , and length intersection within each voxel, Δli; unknowns: its ambiguity BI, the STEC, S, which includes the mean electron density within each given voxel, Ne,i).

# 2.1 Spatial and temporal components of VTEC gradient

## ☐ Evolution of Regional VTEC spatial Gradient indices

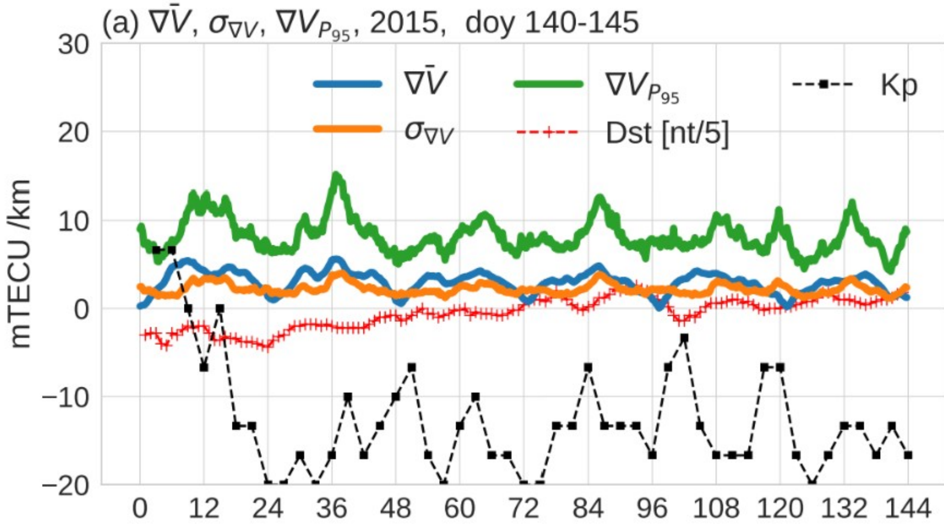


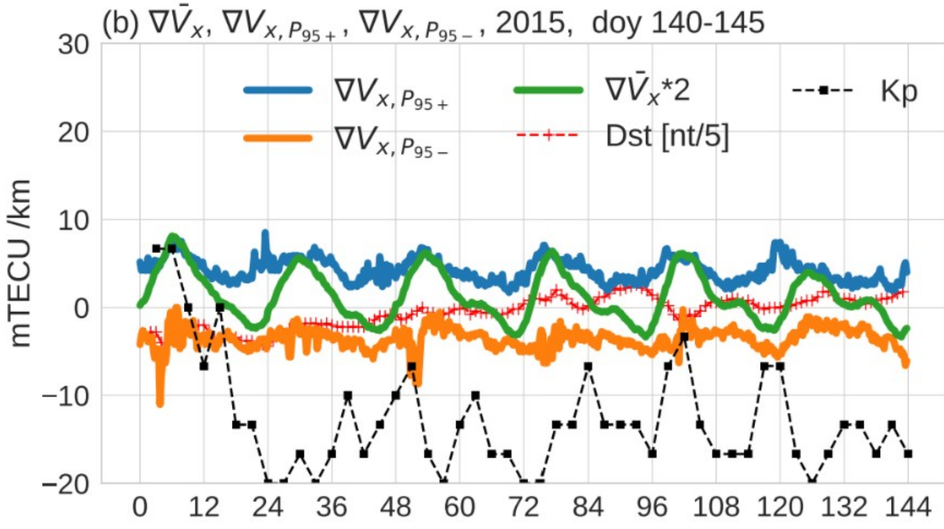


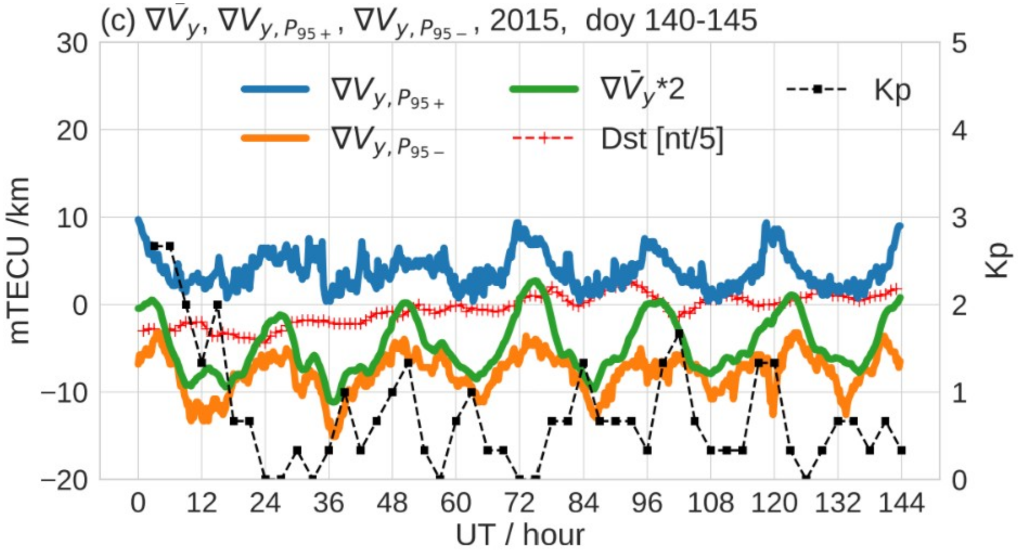


Quiet

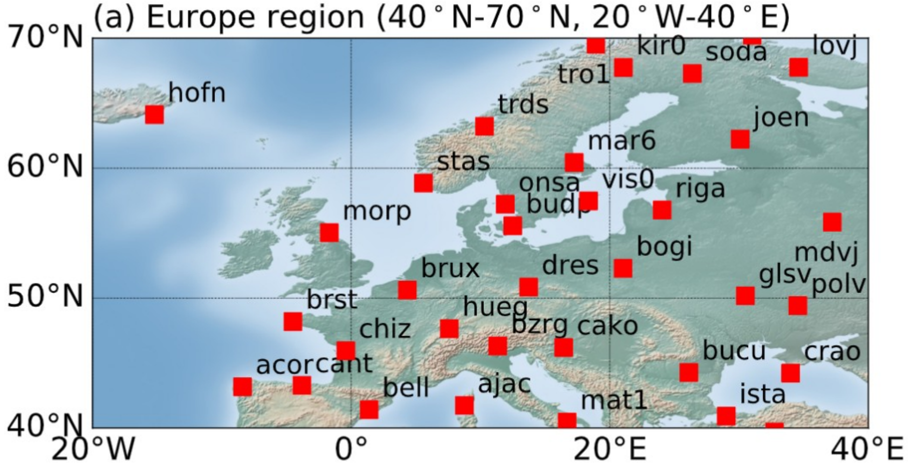

# 2.1 Spatial and temporal components of VTEC gradient

## □ Evolution of Regional VTEC spatial Gradient indices

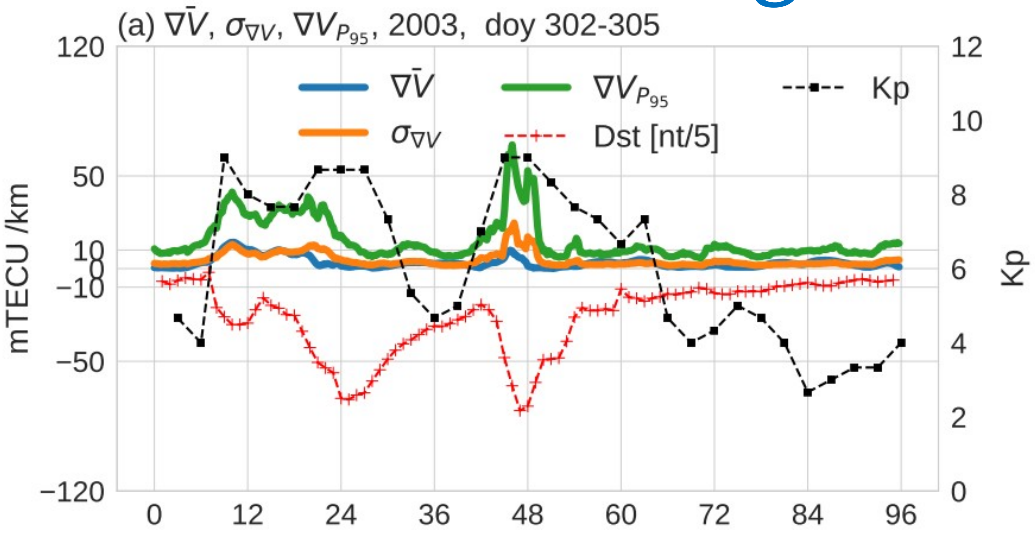


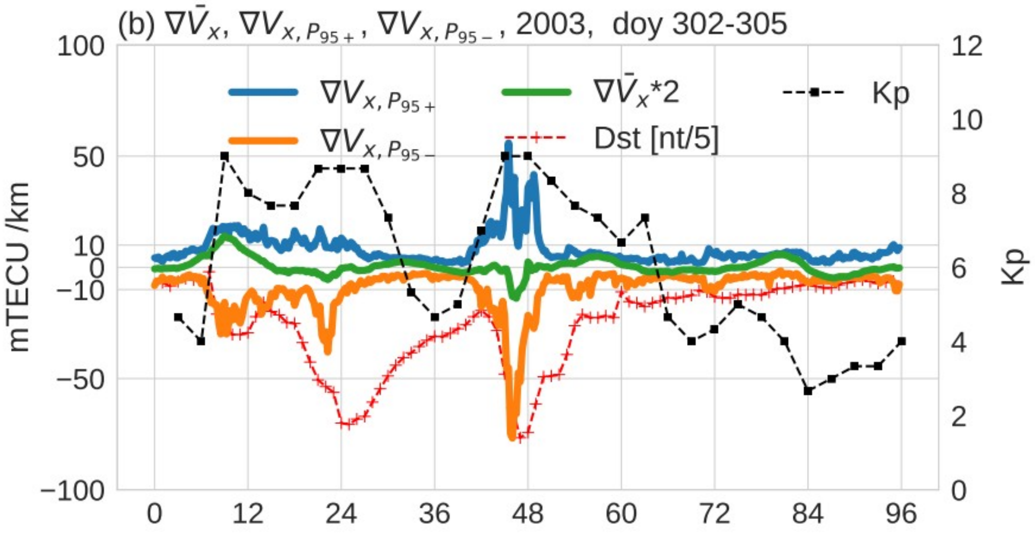


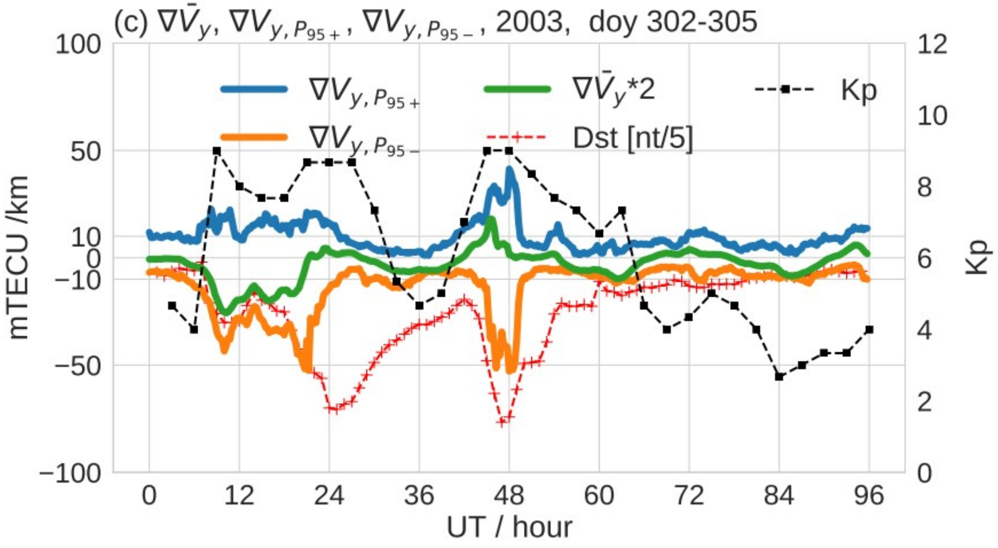


Halloween Storms of 2003

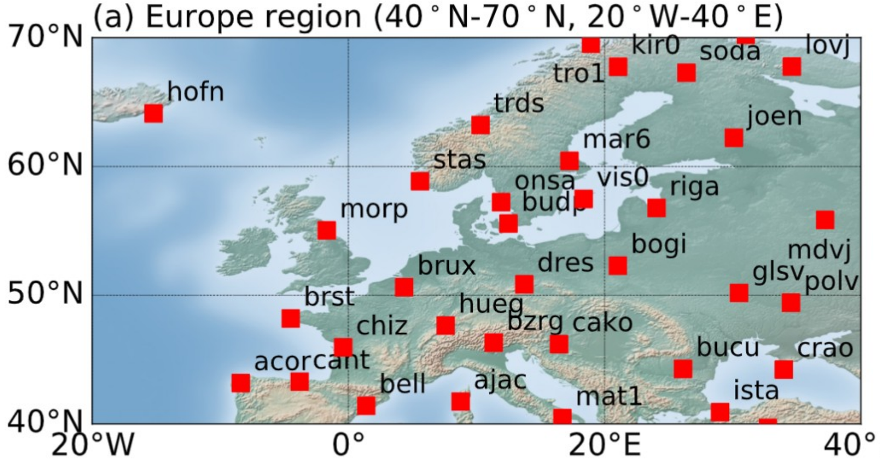

# 2.1 Spatial and temporal components of VTEC gradient

- boxplot of VTEC spatial gradient

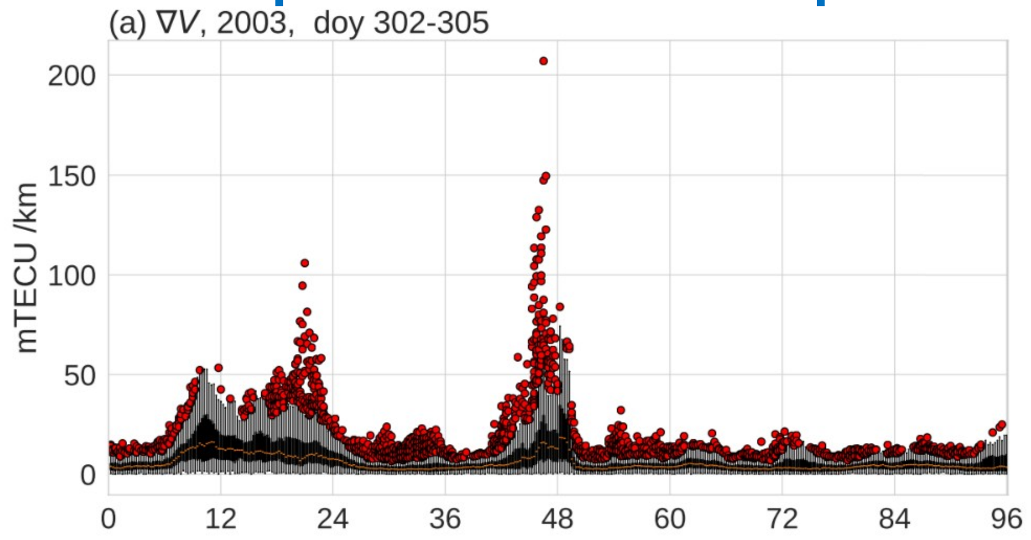


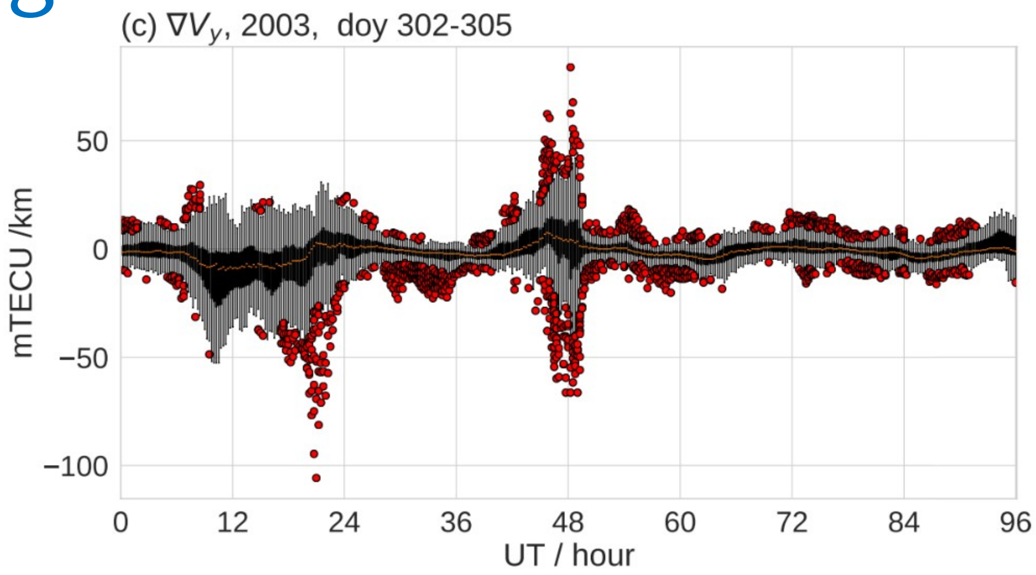


Storm

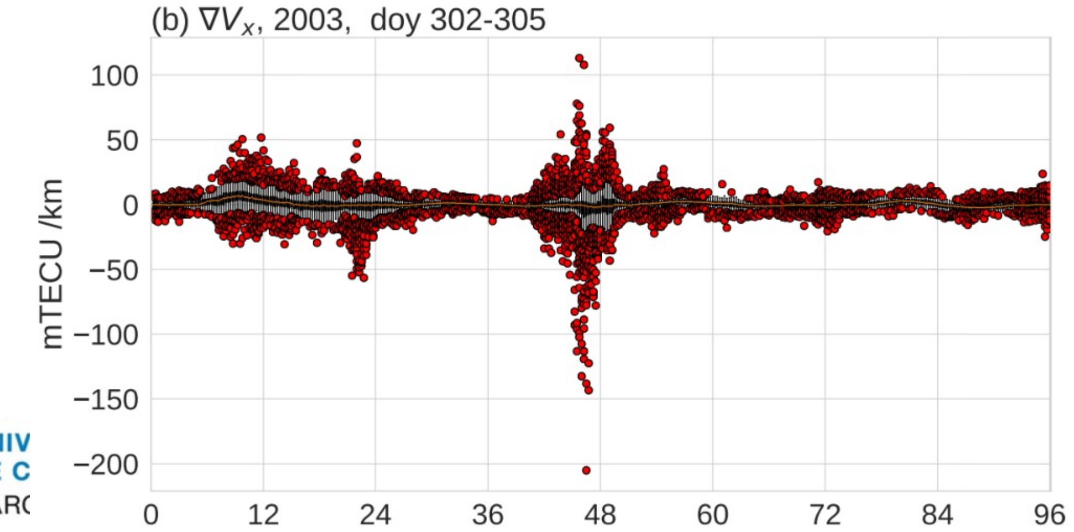


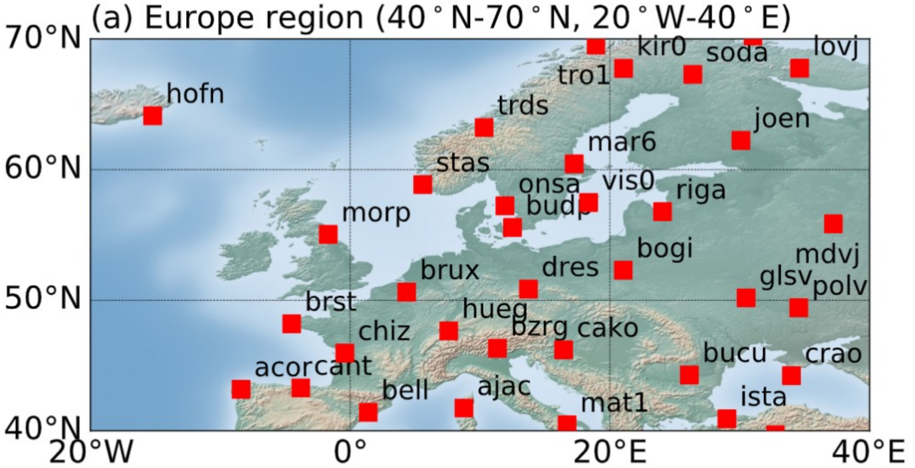

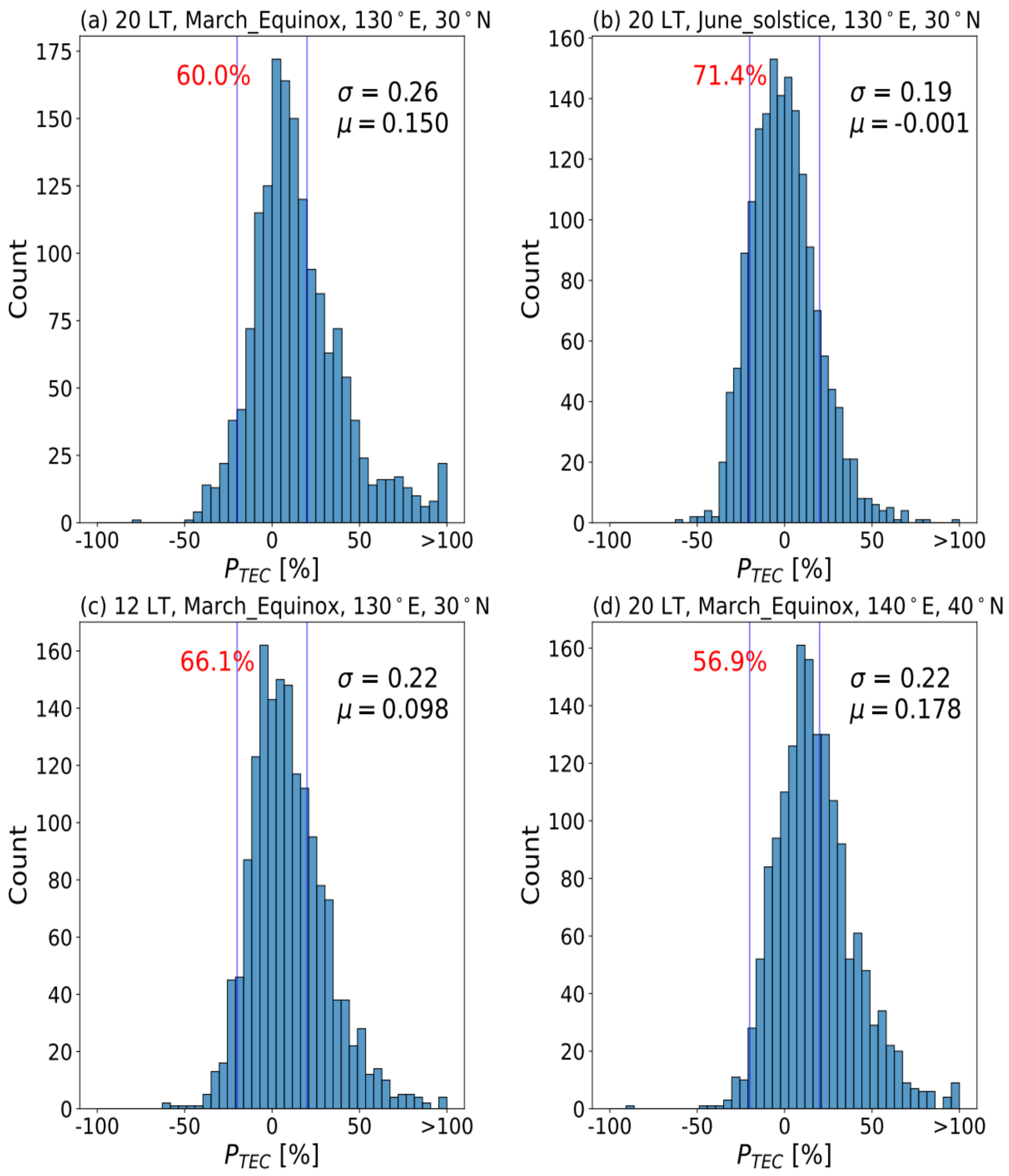
(a) 20 LT, March_Equinox, 130 ° E, 30 ° N
60.0%
σ = 0.26
μ = 0.150
(b) 20 LT, June_solstice, 130 ° E, 30 ° N
71.4%
σ = 0.19
μ = -0.001
(c) 12 LT, March_Equinox, 130 ° E, 30 ° N
66.1%
σ = 0.22
μ = 0.098
(d) 20 LT, March_Equinox, 140 ° E, 40 ° N
56.9%
σ = 0.22
μ = 0.178
Count
-100
-50
0
50
>100
P_TEC [%]

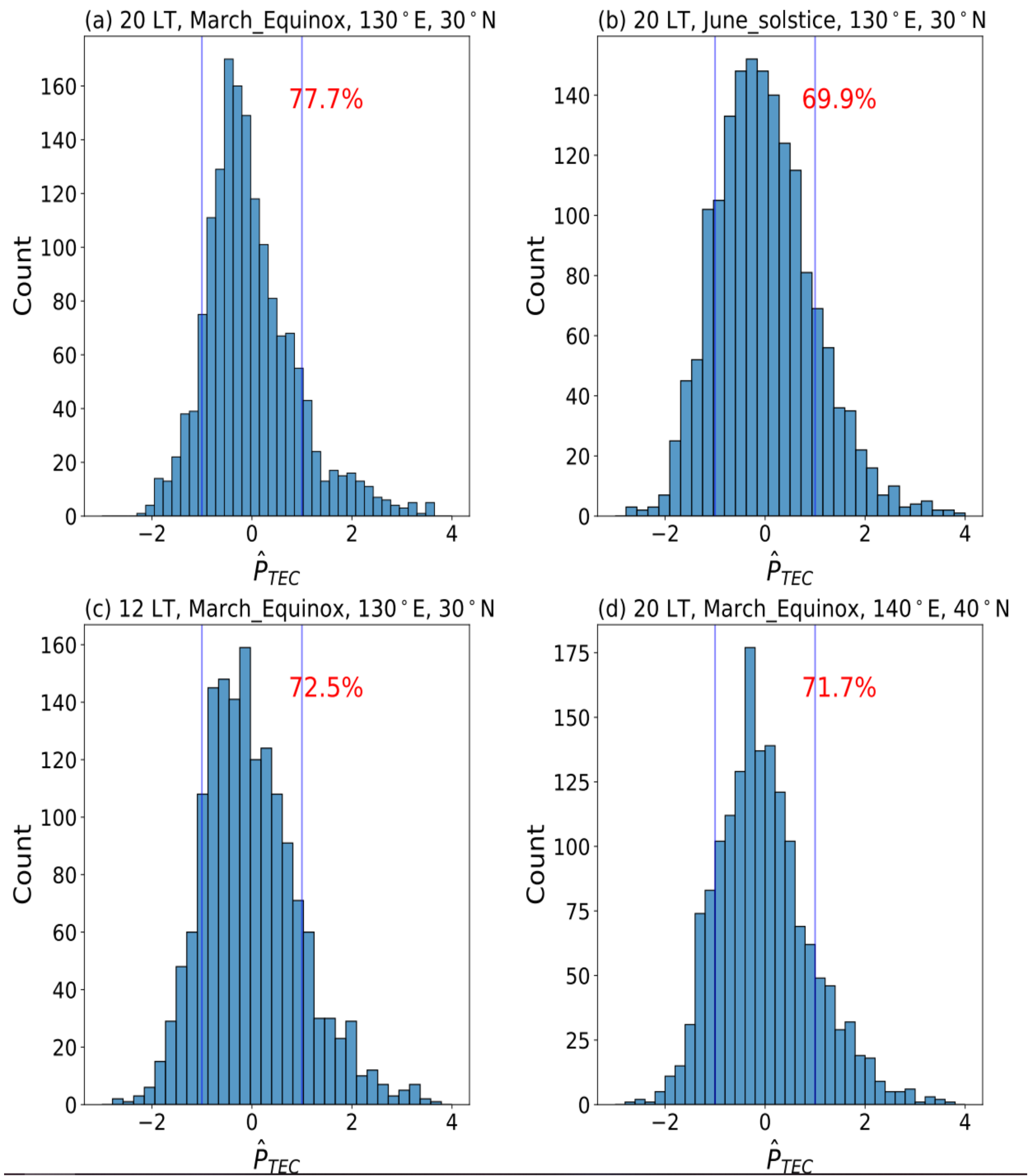
(a) 20 LT, March_Equinox, 130 ° E, 30 ° N
77.7%
(b) 20 LT, June_solstice, 130 ° E, 30 ° N
69.9%
(c) 12 LT, March_Equinox, 130 ° E, 30 ° N
72.5%
(d) 20 LT, March_Equinox, 140 ° E, 40 ° N
71.7%
Count
−2
0
2
4
P̂_TEC

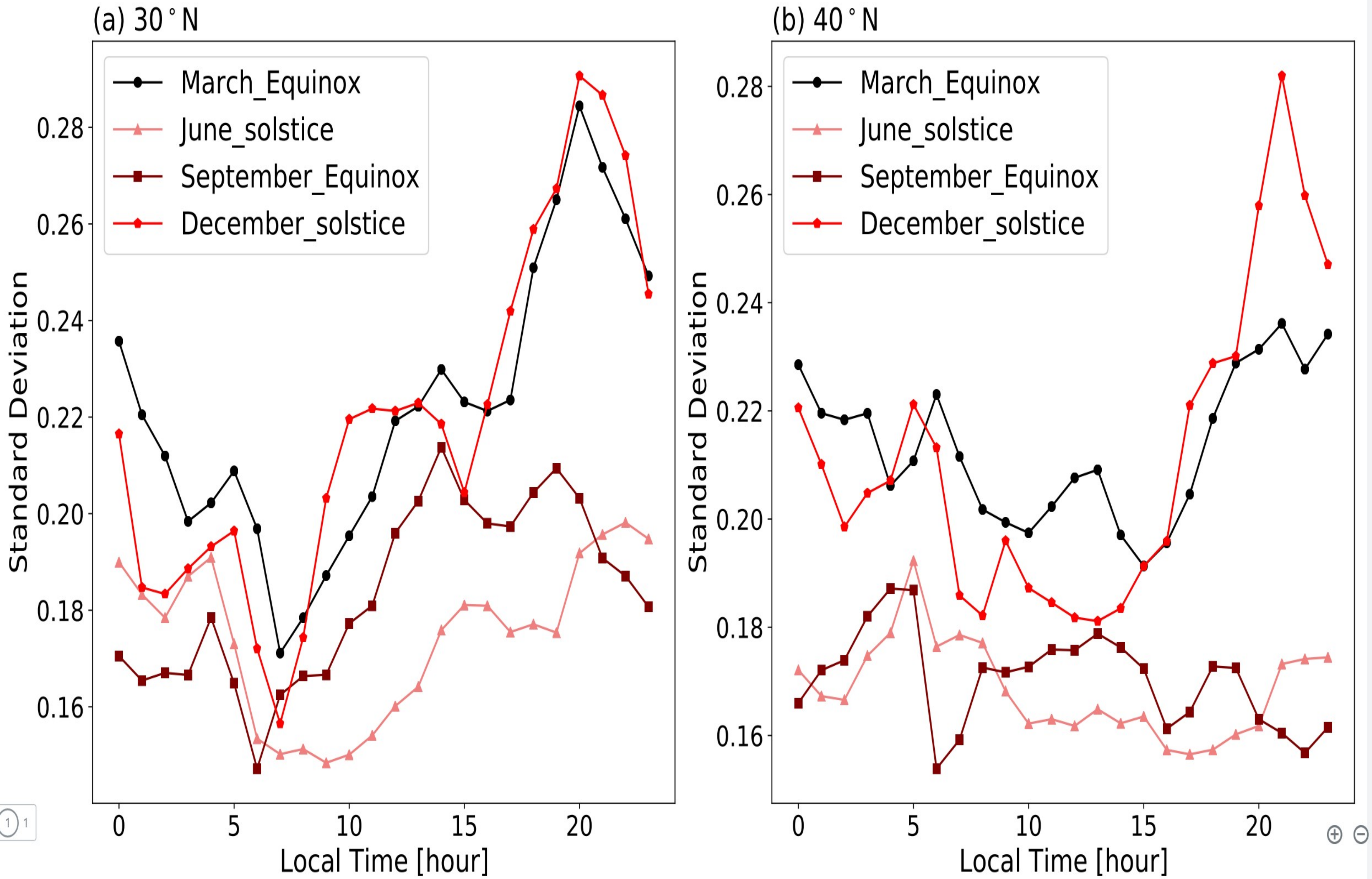

(a) 30 ° N
(b) 40 ° N
March_Equinox
June_solstice
September_Equinox
December_solstice
Standard Deviation
Local Time [hour]
0.16
0.18
0.20
0.22
0.24
0.26
0.28
0
5
10
15
20

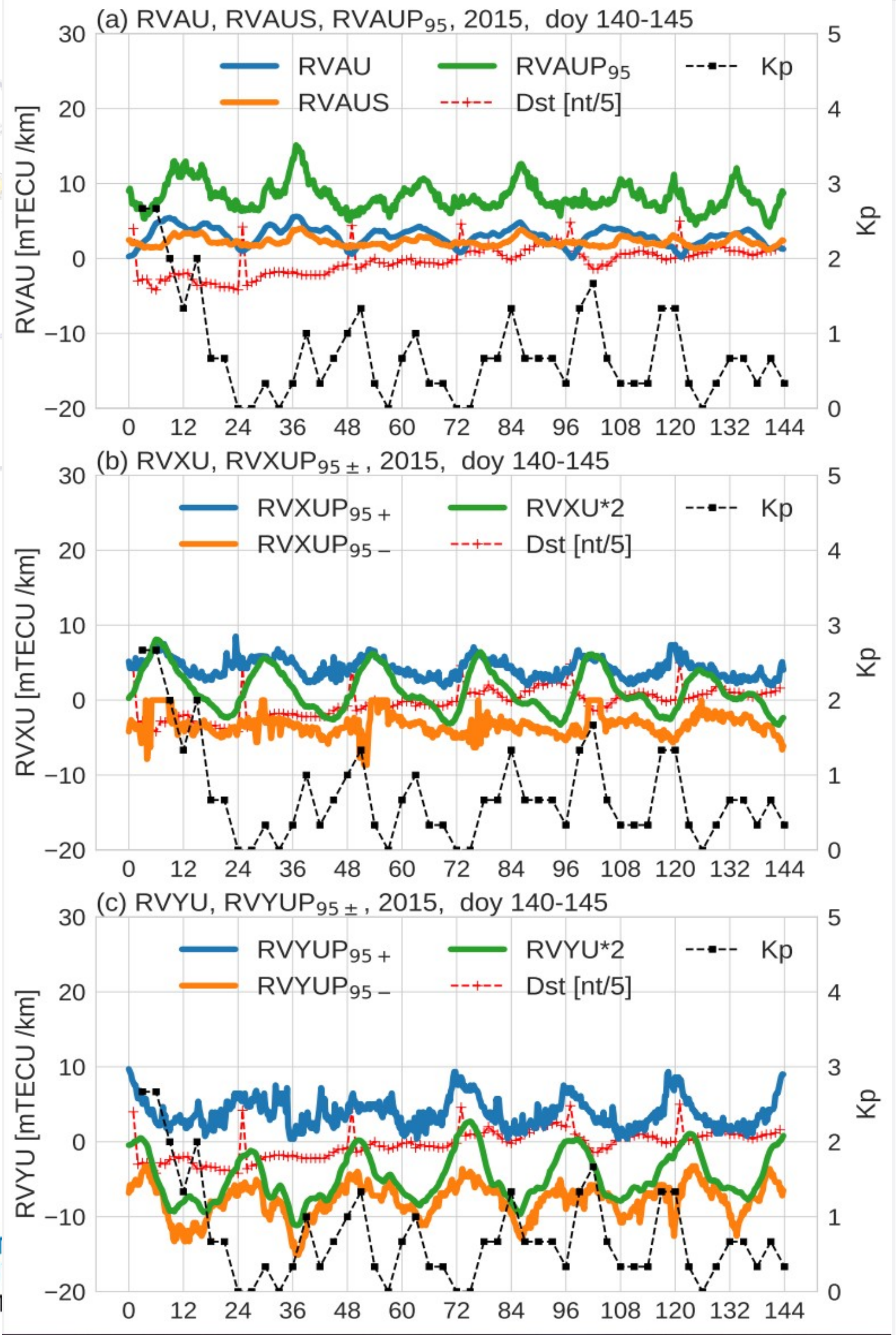


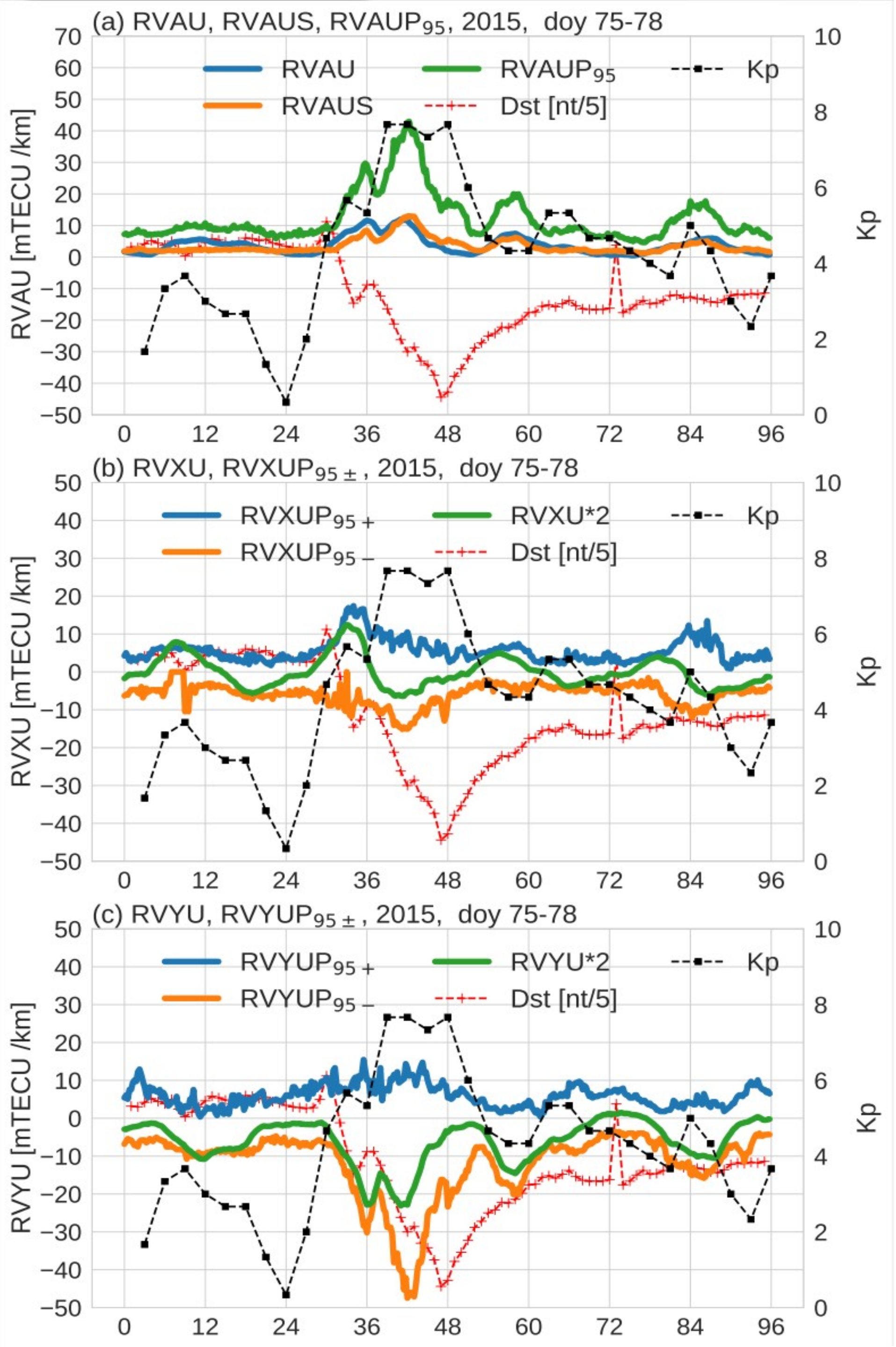


UNIVERSITAT
DE CATALUN
BARCELONAT

# 2.2 Ionospheric storm scale index

## Ionospheric storm

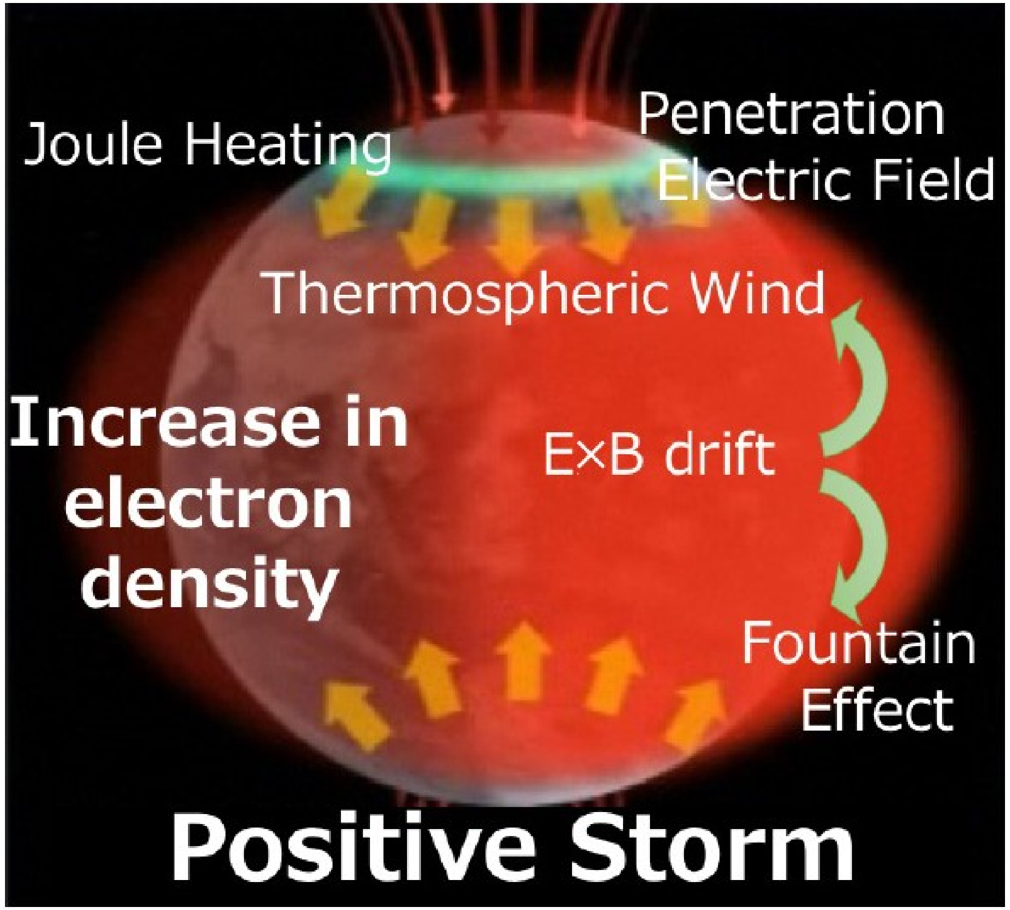


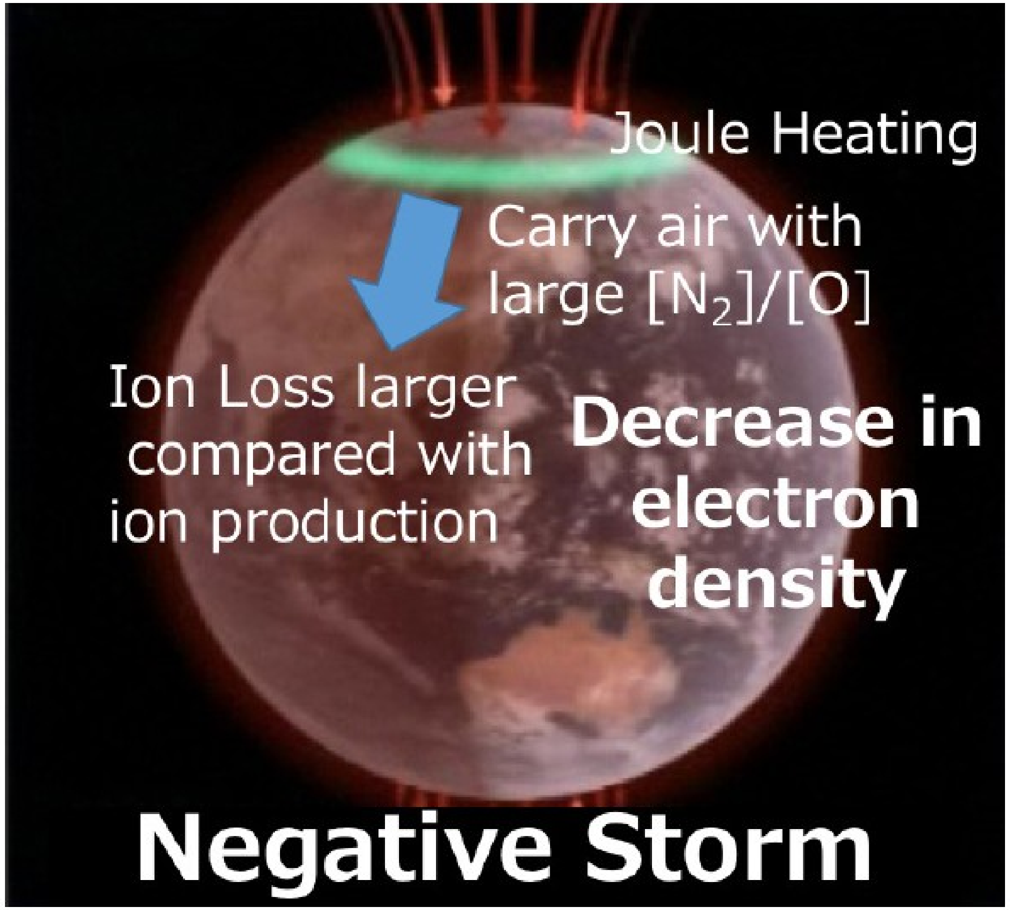


Figure from https://swc.nict.go.jp/en/knowledge/ionosphere.html

Users know the receiver-satellites geometry and can compute bounds on the horizontal and vertical position errors.

These bounds are called Protection Levels (HPL and VPL). They provide good confidence ($10^{-7}$/hour probability) that the true position is within a the corresponding cylinder/ellipsoid around the computed position.

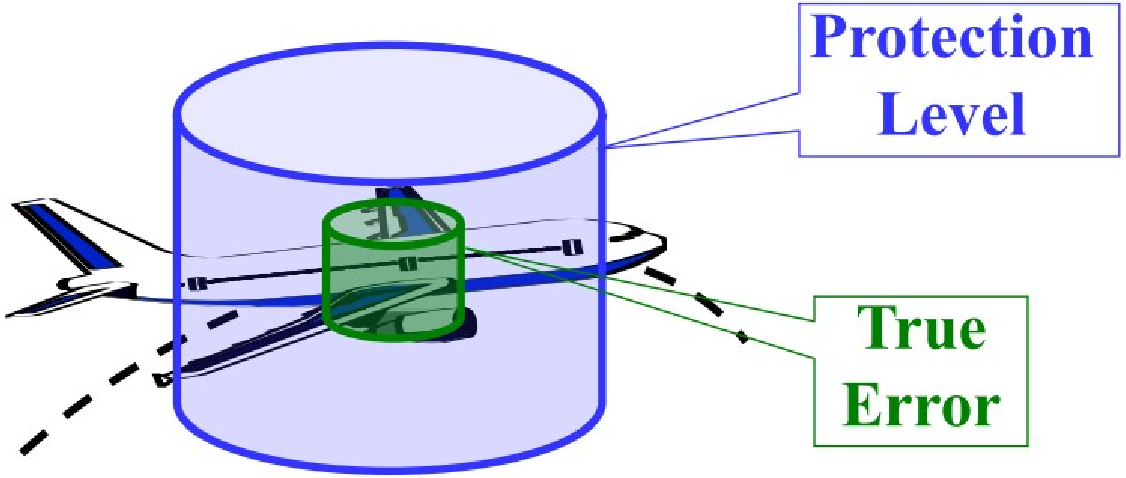


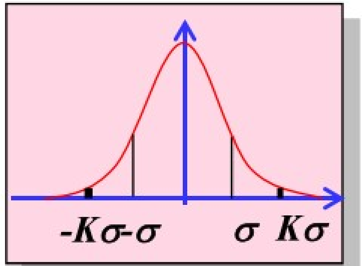


Tail area Probability

P(VPE>VPL) < $10^{-7}$ /sample

$$VPL = K_V \sqrt{\sum_{i=1}^{N} s_{V_i}^2 \sigma_i^2}$$

$$\sigma_i^2 = \sigma_{i,flt}^2 + \sigma_{i,UIRE}^2 + \sigma_{i,air}^2 + \sigma_{i,tropo}^2$$

GEOMETRY

UNIVERSITAT POLITÈCNICA DE CATALUNYA BARCELONATECH